106
21

Removal of Soluble Iron and Manganese from Groundwater by Chemical Oxidation and Oxide-Coated Multi-Media Filtration

by

Bradley M. Coffey

Thesis submitted to the Faculty of
the Virginia Polytechnic Institute and State University
in partial fulfillment of the requirements for the degree of

MASTER OF SCIENCE

in

ENVIRONMENTAL ENGINEERING

APPROVED:

W R Knocke
W. R. Knocke, Chairman

R. C. Hoehn
R. C. Hoehn

D. L. Gallagher
D. L. Gallagher

August, 1990

Blacksburg, Virginia

REMOVAL OF SOLUBLE IRON AND MANGANESE FROM GROUNDWATER BY CHEMICAL OXIDATION AND OXIDE-COATED MULTI-MEDIA FILTRATION

by

Bradley M. Coffey

Committee Chairman: William R. Knocke
Environmental Engineering

(ABSTRACT)

This study evaluated alternatives to continuously regenerated greensand for iron and manganese removal. Specific objectives were (1) to investigate the applicability for removing soluble manganese by adsorption and oxidation onto the surface of manganese oxide-coated media, and (2) to develop mathematical models to predict the removal of soluble manganese both in the presence and absence of free chlorine.

Results from a pilot-scale experiment in Columbus, Indiana, showed that when the filters were operated in a conventional oxidant addition mode (i.e., with the addition of HOCl and $KMnO_4$) the anthracite-sand and anthracite-sand-garnet configurations both provided efficient treatment because of the reduced rate of head loss. Further experiments, without the use of $KMnO_4$ or greensand, equally removed manganese by adsorption and oxidation onto oxide-coated media; however, the treatment process resulted in reduced head loss and oxidant costs.

Results from this study and other previous research demonstrated that manganese removal by oxide coatings is an efficient and functional treatment mechanism. However, little quantitative information was available to predict these processes. Therefore, mathematical models were developed to help

predict design and operational conditions needed to implement oxide-coated media as a treatment process. Two separate models were developed to predict (1) the continuous removal of soluble manganese in the presence of free chlorine (continuous regeneration model), and (2) the eventual breakthrough of soluble manganese without oxidant addition (intermittent regeneration model). Each model was derived from chemical reaction, mass balance, or isotherm equations and was further developed by a sensitivity analysis and parameter estimation. The two models were then verified by predicting manganese removal from independent research.

The continuous regeneration model can help predict the removal of soluble manganese by adsorption and oxidation on the surface of oxide-coated media and is useful in the design of filters for continuous Mn(II) removal. The intermittent regeneration model effectively predicts the performance of filters without the addition of an oxidant and is useful for treatment plants which cannot apply chlorine continuously to their filter applied water.

ACKNOWLEDGEMENTS

I sincerely thank Dr. Knocke for serving as my major advisor. His insight, advice, prodding, and patience allowed this thesis to reflect not only my efforts, but also the effort of many others. I also thank Dr. Gallagher and Dr. Hoehn for serving on my committee. In particular, Dr. Gallagher offered insight into the mathematics and modeling of the adsorption process and Dr. Hoehn provided an excellent background on the limnological cycle of manganese.

Dr. Toshi Umezawa contributed greatly to my research through an excellent translation of a Japanese paper. The translation was pivotal in the modeling effort.

I thank Columbus City Utilities in Columbus, Indiana, for their support of the pilot-plant study. The management, operators, maintenance personnel, and quality control technicians offered invaluable help during my three months in Indiana. Thanks also to my cousin, Bill Coffey, for washing hundreds of bottles and mopping up my many spills.

Upon leaving Blacksburg, I must acknowledge the help of my parents away from home, Cliff and Phyllis Randall. For eight years, they opened their home and dinner table to me and offered sanctuary from the university. Sasha and Leslie Jogi, also, offered home and hearth frequently. The times spent with the Randalls and the Jogis will always be remembered.

Finally, I thank my parents for their unconditional love and support through my many years of college. As a boy, their reading to me every night and answering countless questions instilled in me a love of learning that continues today.

TABLE OF CONTENTS

LIST OF TABLES

LIST OF FIGURES

CHAPTER 1

INTRODUCTION

Iron and manganese are often found in groundwaters and hypolimnetic regions of reservoirs in concentrations exceeding secondary maximum contaminant levels. Iron is typically removed by chemical oxidation followed by solid-liquid separation. Manganese is also removed by this method, with the addition of stronger oxidants such as potassium permanganate, or by adsorption/oxidation onto manganese greensand. Generally, greensand filters are operated in a continuous regeneration mode with potassium permanganate added to the unfiltered water. This method allows the greensand to act as an oxidation buffer, alternatively removing excess soluble manganese or permanganate.

Knocke *et al.* (1988) showed efficient manganese removal with only the addition of free chlorine by filtration through naturally oxide-coated anthracite and sand from full-scale treatment facilities. They concluded that this "natural greensand" effect is a viable treatment mechanism for soluble manganese removal. This treatment method includes potential benefits over either greensand or strong oxidant addition because of reduced head loss buildup from using larger media than greensand, reduced oxidant costs because of the elimination of potassium permanganate, and reduced solids loading due to the elimination of $MnO_{x(s)}$ formed by the reduction of permanganate and the oxidation of soluble Mn(II).

This thesis study evaluated alternatives to continuously regenerated greensand for iron and manganese removal. Studies were conducted both on

a laboratory-scale and at a full-scale treatment plant in Columbus, Indiana. Specific objectives were:

1. to evaluate alternative media configurations for particulate iron and manganese removal that would increase the volume of water treated before metals breakthrough and decrease the rate of head loss accumulation;

2. to investigate the applicability of removing soluble manganese [Mn(II)] by adsorption and oxidation onto the surface of oxide-coated media; and,

3. to develop a mathematical model to predict (a) the removal of soluble manganese by adsorption/oxidation onto the surface of oxide coated media in the presence of free chlorine and (b) the exhaustion of the manganese adsorption capacity in the absence of free chlorine.

CHAPTER 2

LITERATURE REVIEW

Water Quality Concerns with Iron and Manganese

The presence of iron and manganese negatively impacts the water quality of roughly 40 percent of the public water supplies in the United States (Stiles, 1979). Iron and manganese concentrations above the secondary maximum contaminant levels of 0.3 mg Fe/L and 0.05 mg Mn/L cause aesthetic problems such as discolored water, turbidity, stained laundry and plumbing fixtures, and an astringent or bitter taste. In addition, these metals may accelerate biological growth in the distribution system, further contributing to taste-and-odor problems (Trace Inorganic Substances Committee, 1987).

Iron and manganese may occur at high concentrations in groundwater and hypolimnetic regions of reservoirs. They are often present in groundwaters in concentrations exceeding the secondary maximum contaminant levels from the dissolution of iron and manganese from mineral sediments under conditions of low redox potential (anaerobic) and low pH. Iron and manganese are present also in the hypolimnetic regions of reservoirs for these same reasons; however, microbial and metal-organic interactions contribute significantly to their presence (Stumm and Morgan, 1981; Stone and Morgan, 1984). In rare cases, iron and manganese can be present at high concentrations in streams and rivers impacted by industrial wastes or acid mine drainage (Griffin, 1960).

Iron and Manganese Chemistry and Removal

Presence of Iron and Manganese

Iron occurs in natural waters primarily in two oxidation states (II and III). The solubility of Fe(II) in water is usually controlled by the presence of carbonate (CO_3^{2-}) and the formation of ferrous carbonate ($FeCO_{3(s)}$). Occasionally in waters with very low alkalinity, the solubility of Fe(II) is controlled by ferrous hydroxide ($Fe(OH)_{2(s)}$) (Stumm and Morgan, 1981). The concentration of iron in solution is also affected by the presence of metal-organic complexes; when large quantities of humic or tannic acids are present, the solubility of iron may be many times greater than predicted by the solubility product of ferrous hydroxide or ferrous carbonate (Theis and Singer, 1974; Waite *et al.*, 1988)

Manganese also occurs in two primary oxidation states in natural waters (II and IV), and the solubility of Mn(II) is controlled by the presence of carbonate (Morgan, 1967). Potassium permanganate, with a manganese oxidation state of VII, is frequently added to oxidize soluble manganese; therefore, its chemistry must be considered also. Similar to iron, manganese precipitates can be affected by the formation of metal-organic complexes (Montgomery, 1985).

Oxidation of Iron and Manganese

Most traditional methods for controlling iron and manganese include the oxidation of soluble Fe(II) and Mn(II) into their much less soluble forms, Fe(III) and Mn(IV). These forms readily precipitate and then are removed by standard solid-liquid separation techniques such as coagulation, sedimentation, and

filtration. In general, manganese is more difficult to remove from water than iron because of its slower oxidation rate (Stumm and Morgan, 1981) and its tendency to form colloidal solids when rapidly oxidized (Morgan and Stumm, 1964). These colloidal solids may not be removed satisfactorily by filtration without coagulation. Many researchers have investigated the oxidation of Fe(II) and Mn(II) and some of their observations are summarized in Table 1 and 2.

Soluble Manganese Removal Using Greensand

Another common method for removing iron and manganese from raw water supplies is filtration through manganese greensand. Manganese greensand is produced from the mineral glauconite by repeated treatments of manganous sulfate and potassium permanganate (Griffin, 1960). After it is processed, greensand contains significant amounts of $MnO_{x(s)}$ on the surface [3 - 4 mg Mn/g media; Hungate (1988)]. This manganese oxide coating can then sorb soluble manganese (Wilmarth, 1968). In addition, the greensand operates as a conventional filter medium, removing particulate iron and manganese. However, since greensand has a small effective size (≈0.3 mm), head loss may be rapid.

Without the continuous addition of an oxidant to regenerate the $MnO_{x(s)}$ adsorption sites, soluble manganese eventually breaks through, and the filter becomes exhausted. The normal capacity of a greensand filter is about 0.09 lb of soluble manganese per cubic foot of filter media (Wilmarth, 1968). Once the filter is exhausted, it must be regenerated by the addition of a strong oxidant. This addition oxidizes the sorbed manganese, further increasing the total oxide coating present. The oxidant is added either continuously (continuous

Table 1. Summary of Iron Oxidation Methods

Oxidant Used	Oxidation Reaction	Stoichiometry	Comments	References
oxygen $O_{2(aq)}$	$2\ Fe^{2+} + {}^1/_2\ O_2 + 5\ H_2O \leftrightarrow 2\ Fe(OH)_{3(s)} + 4H^+$	$0.14\ \frac{mg\ O_{2(aq)}}{mg\ Fe(II)}$	• rapid oxidation above pH 7.0 • reduced reaction rate in presence of organics	• Stumm and Lee (1961) • Jobin and Ghosh (1972) • Robinson *et al.* (1968)
free chlorine HOCl	$2\ Fe^{2+} + HOCl + 5\ H_20 \leftrightarrow 2\ Fe(OH)_{3(s)} + Cl^- + 5\ H^+$	$0.47\ \frac{mg\ HOCl}{mg\ Fe(II)}$	• rapid oxidation above pH 5.0	• Nordell (1961) • Knocke *et al.* (1990)
potassium permanganate $KMnO_4$	$3\ Fe^{2+} + MnO_4^- + 7\ H_2O \leftrightarrow 3Fe(OH)_{3(s)} + MnO_{2(s)} + 5H^+$	$0.94\ \frac{mg\ KMnO_4}{mg\ Fe(II)}$	• very rapid oxidation rate above pH 5.0	• Nordell (1961) • Knocke *et al.* (1990)

Table 2. Summary of Manganese Oxidation Methods

Oxidant Used	Oxidation Reaction	Stoichiometry	Comments	References
oxygen $O_{2(aq)}$	a: $Mn^{2+} + 1/2O_2 + H_2O \leftrightarrow MnO_{2(s)} + 2H^+$ b: $Mn^{2+} + MnO_{2(s)} \leftrightarrow \{Mn^{2+} \bullet MnO_{2(s)}\}$ c: $\{Mn^{2+} \bullet MnO_{2(s)}\} + 1/2O_2 + H_2O \rightarrow 2\ MnO_{2(s)} + 2H^+$	none (autocatalytic reaction)	• Autocatalytic reaction (i.e., reaction rate increases with time because the reaction creates its own catalyst, $MnO_{2(s)}$) • very slow reaction rate below pH 9.5	• Morgan (1964) • Morgan and Stumm (1964) • Kessick and Morgan (1975) • O'Conner (1971)
free chlorine HOCl	$Mn^{2+} + HOCl + H_2O \leftrightarrow MnO_{2(s)} + Cl^- + 3\ H^+$	$0.95 \frac{\text{mg HOCl}}{\text{mg Mn(II)}}$	• slow reaction rate below pH 8 • reaction catalyzed in presence of $MnO_{2(s)}$ • THM formation concern with long HOCl contact times	• Edwards and McCall (1946) • Wong (1984) • Knocke *et al.* (1988) • Cleasby (1975)
potassium permanganate $KMnO_4$	$3Mn^{2+} + 2\ MnO_4^- + 2H_20 \leftrightarrow 5\ MnO_{2(s)} + 4\ H^+$	$1.92 \frac{\text{mg KMnO}_4}{\text{mg Mn(II)}}$	• rapid oxidation rate between pH 5.5-9.0 • forms additional $MnO_{2(s)}$ which contributes to solids loading to filter	• Knocke *et al.* (1987) • Adams (1968) • O'Conner (1971)

regeneration) or periodically (intermittent regeneration). Usually, either potassium permanganate or free chlorine is used for the regeneration of the greensand (Sayell and Davis, 1975; Wong, 1984). Detailed discussions of the regeneration process are provided by Hungate (1988) and Occiano (1988).

In summary, greensand filters contain a moderate amount of $MnO_{x(s)}$ surface coating, and this coating can then adsorb Mn(II). Eventually, the sorbed Mn(II) must be oxidized or the removal capacity of the filter is exhausted. The following section describes the sorption process in more detail .

Ion Exchange/Sorption of Soluble Manganese

In contrast to the stoichiometric oxygenation of iron, Morgan (1964) concluded that a different mechanism controlled the oxygenation of soluble manganese. He suggested the following sequence of reactions to describe the process:

$$Mn^{2+} + {}^1/_2\, O_2 + H_2O \xrightarrow{\text{slow}} MnO_{2(s)} + 2\, H^+ \qquad (1)$$

$$Mn^{2+} + MnO_{2(s)} \xrightarrow{\text{fast}} Mn^{2+}{\bullet}MnO_{2(s)} \qquad (2)$$

$$Mn^{2+}{\bullet}MnO_{2(s)} + {}^1/_2\, O_2 + H_2O \xrightarrow{\text{very slow}} 2\, MnO_{2(s)} + 2\, H^+ \qquad (3)$$

This set of reactions includes sorption of soluble manganese directly onto $MnO_{2(s)}$ (Eq. 2) and the slow oxidation of that sorbed Mn(II) (Eq. 3). Since the oxygenation of sorbed manganese was extremely slow, more manganese was removed from solution than could be accounted for by oxidation alone. Therefore, the manganese oxidation was considered nonstoichiometric.

Morgan (1964) proposed the following model to describe the overall removal of manganese:

$$-\frac{d[Mn^{2+}]}{dt} = k_1 [Mn^{2+}] + k_2 [Mn^{2+}][MnO_{2(s)}] \quad (4)$$

where k_1 and k_2 represented, respectively, the oxidation and adsorption removal rate constants. The reaction was termed "autocatalytic" because the Mn(II) removal rate increased as the reaction progressed. This increase resulted from the formation of $MnO_{2(s)}$ which could then remove more Mn(II).

Morgan's (1964) research provided a foundation for additional research into the removal of Mn(II) from solution. His later research demonstrated this phenomenon in more detail (Morgan and Stumm, 1964; Morgan, 1967; Kessick and Morgan, 1975; Pankow and Morgan, 1981). However, during this research, he only considered batch adsorption of Mn(II) onto colloidal $MnO_{2(s)}$ in a heterogeneous solution. Later, others began to attribute Mn(II) removal to sorption onto $MnO_{2(s)}$ which was coated on the surface of water treatment plant filter media (Nakanishi, 1967; Cleasby, 1975; Hem, 1980; Lloyd *et al.*, 1983; Trace Inorganic Substances Committee, 1987; Knocke *et al.*, 1988; Hungate, 1988; and Occiano, 1988).

The coupling of Morgan's research to practical observations at water treatment plants was pivotal in the understanding of manganese removal by oxide-coated filter media. For example, Edwards and McCall (1946) noted that manganese oxide coatings on sand filters catalyzed the removal of manganese in the filter bed, especially with the addition of chlorine. Others also noted the importance of a "seasoning" or "aging" of the filter media for manganese

removal (Griffin, 1960; Weng *et al.*, 1986); however, no quantitative information on the effect of the $MnO_{2(s)}$ coating was proposed.

Nakanishi (1967) was probably the first researcher to incorporate Morgan's results to characterize and predict soluble manganese removal through a filter bed coated with $MnO_{2(s)}$. Unfortunately, his results were not well known until this present thesis study because they were not previously translated from Japanese. Knocke *et al.* (1988) studied the "natural greensand" effect of oxide-coated media and determined it was an efficient Mn(II) removal mechanism. He showed that the removal efficiency was affected by the surface $MnO_{x(s)}$ concentration, its oxidation state, and the applied water pH.

Although $MnO_{2(s)}$ was shown to have a large sorption capacity for Mn(II) [approximately 0.5 mole Mn(II) sorbed per mole $MnO_{2(s)}$ at pH 7.5; Morgan (1964)] in Eq. 3, the oxidation of the sorbed Mn(II) was very slow; therefore, the total adsorption capacity of the $MnO_{2(s)}$ was quickly exhausted. Several researchers noted, however, that free chlorine could oxidize the sorbed Mn(II) much more quickly than oxygen (Nakanishi, 1967; Knocke *et al.*, 1988; Hungate, 1988; Occiano, 1988). Knocke *et al.* (1988) demonstrated the utility of using free chlorine to regenerate the sorption sites filled by Mn(II). The oxidation of the sorbed Mn(II) was so rapid, in fact, that continuous regeneration of the sites was possible with continuous chlorine addition in a bed of $MnO_{2(s)}$-coated filter media.

Modeling of Manganese Adsorption/Oxidation:

Very little previous research modeled the removal of manganese in oxide-coated filter media. The original model for manganese oxidation was

proposed by Morgan (1964) but applied only to batch experiments with colloidal $MnO_{x(s)}$ in a heterogeneous suspension. Nakanishi (1967) provided the first known model for manganese removal through a filter bed with the continuous addition of free chlorine to regenerate the adsorption sites. Hungate (1988) proposed a model to predict the breakthrough of soluble manganese without media regeneration. Hungate's model, unfortunately, could not predict the expanding wavefront for Mn(II) removal seen in his experiments.

CHAPTER 3

THEORETICAL MODEL DEVELOPMENT

For the design and operation of soluble manganese removal plants, one must understand the quantitative relationships between the Mn(II) concentration in the unfiltered water, oxidant concentration, total adsorption capacity of the media, hydraulic loading rate (HLR), and effluent manganese concentration. If continuous regeneration of the media is not possible, the Mn(II) breakthrough pattern must be understood to determine the required media regeneration frequency. This chapter describes the development of two separate models to address these design and operation criteria.

Continuous Regeneration Model

Knocke *et al.* (1988), Hungate (1988), Occiano (1988), and Nakanishi (1967) investigated continuous removal of soluble manganese from raw water. Nakanishi developed a Mn(II) removal technique using manganese oxide-coated sand in Japan as a modification of conventional treatment methods such as greensand. Nakanishi's method used a $MnO_{2(s)}$-coated sand bed with free chlorine as the regenerant. Nakanishi's work was translated from Japanese for this thesis study and a modified version of his model derivation follows.

Development of Equations

First, consider a plug-flow filter bed containing a manganese oxide-coated media. If a portion of the $MnO_{2(s)}$ coating on the filter media reacts with

the OH^- ion and becomes $MnO(OH)_{2(s)}$, its reaction with Mn(II) can be expressed as follows:

$$Mn^{2+} + MnO(OH)_{2(s)} \underset{k_2}{\overset{k_1}{\Leftrightarrow}} MnO_2MnO_{(s)} + 2H^+ \quad (5)$$

Alternatively, oxidation of the sorbed Mn(II) by HOCl is:

$$MnO_2MnO_{(s)} + HOCl \underset{k_4}{\overset{k_3}{\Leftrightarrow}} 2\,MnO_{2(s)} + H^+ + Cl^- \quad (6)$$

A mass balance of Mn(II) in the filter bed gives:

$$-u\frac{\partial [Mn^{2+}]}{\partial z} = \frac{\partial s}{\partial t} + \varepsilon\frac{\partial [Mn^{2+}]}{\partial t} \quad (7)$$

where:

Mn^{2+} = Mn(II) concentration ($^{mol}/L$) at depth z and time t

s = amount of Mn(II) per liter of media adsorbed at depth z accumulated until time t ($^{mol}/L$-bed volume)

u = apparent filtration velocity = hydraulic loading rate/porosity ($^{in}/min$)

ε = media porosity

z = bed depth (in)

t = time (min)

Solution of Equations

Adsorption of Mn(II) onto oxide-coated media and the oxidation of the sorbed manganese are heterogeneous reactions between the solid phase and solution. The reactions occur only on the media surface. If this surface reaction

limits the entire reaction, the rate of Mn(II) sorption onto coated media, $\partial s/\partial t$, can be expressed as follows:

$$\frac{\partial s}{\partial t} = k_1 [Mn^{2+}] (s_o - s') - k_2 s' [H^+]^2 \quad (8)$$

where:

s_o = total Mn(II) adsorption capacity of oxide-coated media (^{mol}/L-bed volume)

s' = amount of manganese-manganite ($MnO_2MnO_{(s)}$) in one liter of oxide-coated media at depth z and time t (^{mol}/L-bed volume)

k_1, k_2 = rate constants (L/mol*min and L^2/mol^2*min, respectively)

In the presence of an oxidant, the reduction of $MnO_{2(s)}$ does not occur (i.e., k_4 = 0 in Eq. 6) and the oxidation by free chlorine is irreversible. The total mass transfer of $MnO_2MnO_{(s)}$ can then be expressed by three terms: (1) the addition due to sorption onto $MnO(OH)_2$, $k_1 [Mn^{2+}] (s_o - s')$; (2) the removal due to desorption from $MnO_2MnO_{(s)}$, $-k_2 s' [H^+]^2$; and (3) the removal due to oxidation by free chlorine, $-k_3 s' [HOCl]$. Therefore, Eq. 9 is obtained.

$$\frac{\partial s'}{\partial t} = k_1 [Mn^{2+}] (s_o - s') - k_2 s' [H^+]^2 - k_3 s' [HOCl] \quad (9)$$

where:

H^+ = concentration of H^+ at depth z and time t (^{mol}/L)

HOCl = free chlorine concentration (as Cl_2) at depth z and time t (^{mol}/L)

In the case of steady state (i.e., $\partial s'/\partial t = 0$) Eq. 10 is derived from Eq. 9 by algebraic manipulation:

$$s' = \frac{k_1\ [Mn^{2+}]\ s_o}{k_1\ [Mn^{2+}] + k_2\ [H^+]^2 + k_3\ [HOCl]} \tag{10}$$

When Eq. 10 is substituted into Eq. 8, Eq. 11 is obtained.

$$\frac{ds}{dt} = \frac{k_1\ k_3\ [Mn^{2+}]\ [HOCl]\ s_o}{k_1\ [Mn^{2+}] + k_2\ [H^+]^2 + k_3\ [HOCl]} \tag{11}$$

The pH negligibly changes within the bed. Accordingly, $k_2\ [H^+]^2$ is a constant. The chlorine concentration remaining at any depth can be stoichiometrically calculated based on Eq. 12 from the amount of Mn(II) oxidized between depth 0 and depth z.

$$[HOCl] = [HOCl]_o - \{\ [Mn^{2+}{}_o] - [Mn^{2+}]\ \} \tag{12}$$

where:

$[HOCl]_o$ = free chlorine (as Cl_2) in the unfiltered water ($^{mol}/L$)

$[Mn^{2+}]_o$ = Mn(II) in the unfiltered water ($^{mol}/L$)

By the substitution of Eq. 12, Eq. 11 becomes a function of only one variable, $[Mn^{2+}]$, in Eq. 13:

$$\frac{ds}{dt} = \frac{\{k_1\ k_3\ [Mn^{2+}]\ \{[HOCl]_o - [Mn^{2+}]_o\} + k_1\ k_3\ [Mn^{2+}]^2\}\ s_o}{[k_1 + k_3]\ [Mn^{2+}] + k_2\ [H^+]^2 + k_3\ \{\ [HOCl]_o - [Mn^{2+}]_o\}} \tag{13}$$

In the case of steady state ($\partial[Mn^{2+}]/\partial t = 0$), Eq. 7 gives Eq. 14:

$$-\ u\ \frac{d[Mn^{2+}]}{dz} = \frac{ds}{dt} \tag{14}$$

Eq. 14 is solved by substituting Eq. 13 and integrating using the boundary condition $[Mn^{2+}] = [Mn^{2+}]_o$ at $z = 0$. This provides the solution for the two kinetic equations (Eq. 5 and Eq. 6) and the mass balance equation (Eq. 7). The solution is:

$$\frac{z\,s_o}{u} = \frac{1}{k_1} \ln \frac{[Mn^{2+}]_o}{[Mn^{2+}]} + \frac{1}{k_3} \ln \frac{[HOCl]_o}{[HOCl]_o - \{[Mn^{2+}]_o - [Mn^{2+}]\}}$$

$$+ \frac{k_2 [H^+]^2}{k_1 k_3 \{[HOCl]_o - [Mn^{2+}]_o\}} \left\{ \ln \frac{[Mn^{2+}]_o}{[Mn^{2+}]} - \ln \frac{[HOCl]_o}{[HOCl]_o - \{[Mn^{2+}]_o - [Mn^{2+}]\}} \right\} \quad (15)$$

Eq. 15 shows a relationship between the Mn(II) concentrations in the water before and after filtration in relation to the hydraulic loading rate (HLR), media depth, total adsorption capacity of the oxide-coated media, free chlorine concentration in the unfiltered water, and pH.

Comparison of Nakanishi Theory to Results from Morgan and Stumm

The ion exchange reaction (Eq. 5) provided the basis for Nakanishi's model. The equation, repeated below, shows that two moles of hydrogen ions are liberated with every mole of manganese adsorbed onto the $MnO(OH)_{2(s)}$:

$$Mn^{2+} + MnO(OH)_{2(s)} \underset{k_2}{\overset{k_1}{\leftrightarrow}} MnO_2MnO_{(s)} + 2\,H^+ \quad (5)$$

Experimental results from Morgan and Stumm (1964), however, indicated that the reaction does not occur to this extent. In fact, they stated:

> "It is apparent that a simple exchange in equivalent proportions, i.e., 2 moles of H^+ per more of Mn^{2+}, does not take place under the conditions of the experiments. This results partially because other cations in the system (Na^+, K^+) can also be exchanged for Mn^{2+}."

Morgan and Stumm (1964) suggested a reaction order with respect to pH of less than two. For batch experiments in the presence of 43 $^{mg}/_{L}$ $MnO_{2(s)}$, only 1.3 moles of hydrogen ions were released per mole of Mn(II) sorbed;

therefore, the exponent on the hydrogen ion in Eq. 15 would be 1.3 instead of 2.0. Correspondingly, the reaction rate constants k_1 and k_2 would differ from Nakanishi's in both units and magnitude.

The significance of the differences in Nakanishi's and Morgan's theories should be considered in the implementation and application of the model. In Chapter 5, a sensitivity analysis of the Nakanishi model provides further insight into the effect of pH variations. In addition, the comparison of model predictions to experimental results obtained by Occiano (1988) and Hungate (1988) show effects of pH on the removal of manganese.

The pH effects on the continuous adsorption model were consolidated into one term of Eq. 15. As a result, Nakanishi defined the total adsorption capacity functionally as follows: A solution with a Mn(II) concentration of 100 mg/L at pH 7.5 was continuously circulated through a column containing one liter of oxide-coated media. When the solution concentration stabilized, the amount of manganese removed was expressed as mol per liter of media, thus giving the total capacity. Therefore, no change in the total adsorption capacity was attributed to a change in pH. Nakanishi approached the concept of total adsorption capacity differently than other researchers and the distinction must be noted.

The impact of pH on the system of reactions is seen in Eq. 5. As the pH increases, the reaction shifts to the right, and more Mn(II) sorbs onto the oxide-coated media; as the pH decreases, less Mn(II) sorbs onto the media. This effect was noted by other researchers. For example, Figure 1 from Morgan (1964), showed an increasing amount of Mn(II) adsorbed onto colloidal $MnO_{2(s)}$ as the solution pH increases. Hungate (1988) also showed that manganese

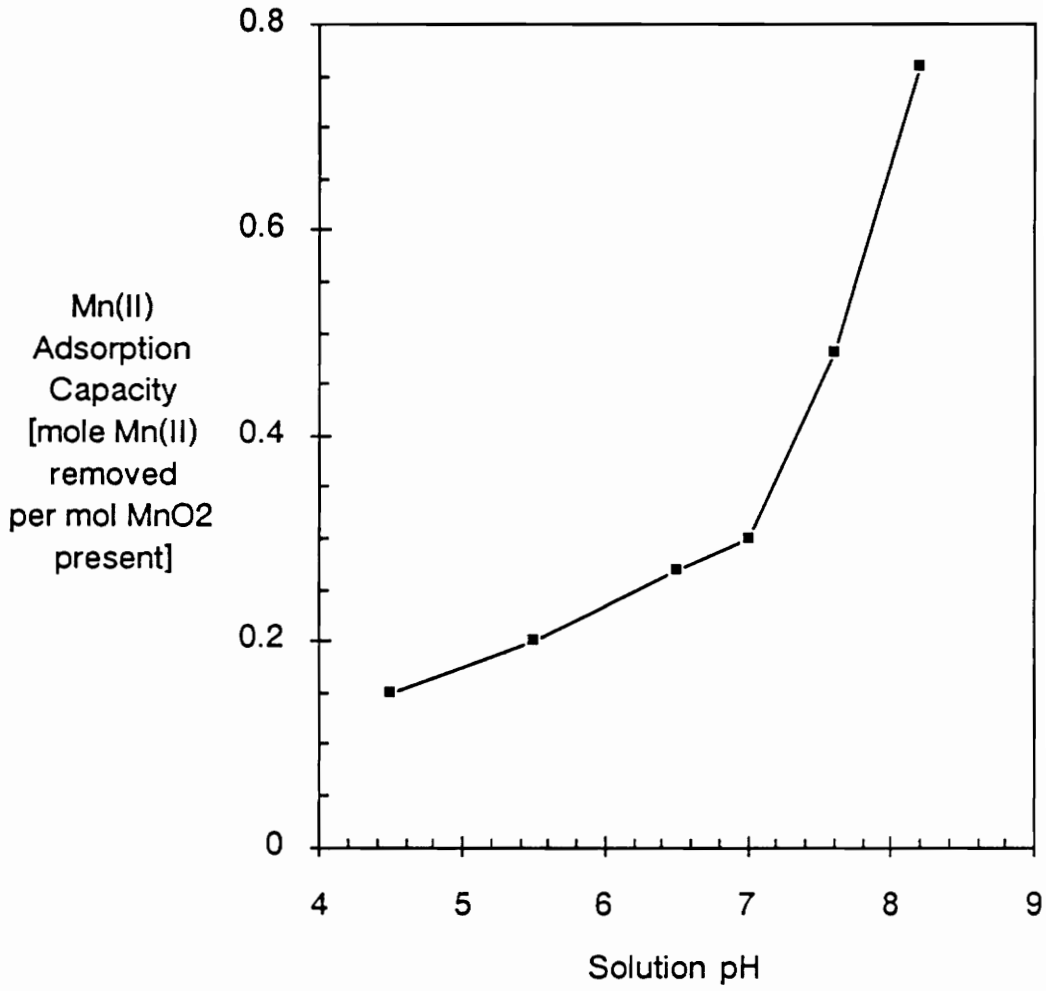

Figure 1. Influence of pH on Sorption of Mn(II) onto MnO_2 at 25° C (from Morgan (1964))

oxide coatings on filtration plant media responded similarly to changes in pH of the filter applied water.

Intermittent Regeneration Model

Hungate (1988) investigated the removal of soluble manganese without the continuous addition of free chlorine (intermittent regeneration). He achieved limited success in adapting a model for the adsorption of soluble manganese onto oxide-coated anthracite. Hungate's model assumed a constant pattern behavior (favorable isotherm) for the adsorption process, and, as a result, it could not be used to predict a broadening of the mass transfer zone for manganese removal. The favorable isotherm assumption is widely used in the simulation and design of adsorption models, particularly the adsorption of organic compounds onto activated carbon. In order to model the adsorption of Mn(II) onto oxide-coated media, therefore, a semi-empirical model incorporating a linear isotherm was chosen from Ruthven (1984). The solution to the linear isotherm equations was solved by Thomas (1944) and is known as the Thomas solution.

Development of Equations

The linear adsorption model is based on a mass balance of manganese in the filter:

$$u\frac{\partial [Mn^{2+}]}{\partial z} + \frac{\partial [Mn^{2+}]}{\partial t} + \frac{1-\varepsilon}{\varepsilon}\frac{\partial q}{\partial t} = 0 \qquad (16)$$

where:

$\partial q/\partial t$ = mass transfer rate between solution and media (mol/(L*min))

z = depth (m)

u = hydraulic loading rate (m/min)

ε = porosity

In addition to a mass balance equation, the linear adsorption isotherm is represented by:

$$\frac{\partial q}{\partial t} = k\ K\ ([Mn^{2+}] - [Mn^{*}]) \tag{17}$$

where:

k = rate constant (1/min)

K = constant (dimensionless)

$[Mn^{2+}]$ = Mn(II) concentration in solution (mol/L)

$[Mn^{*}]$ = Mn(II) concentration in sorbed phase (mol/L)

This model is subject to the following boundary values and initial conditions:

(1) constant Mn(II) concentration ($[Mn^{2+}]_o$) for all time at $z = 0$

(2) no Mn(II) in sorbed phase ($[Mn^{*}] = 0$) for all depth at $t = 0$

Solution of Equations

The solution of the mass balance and linear isotherm equations are:

$$\frac{[Mn^{2+}]}{[Mn^{2+}]_o} = \frac{1}{2}\ \text{erfc}\left(\sqrt{\xi} - \sqrt{\tau} - \frac{1}{8}\sqrt{\xi} - \frac{1}{8}\sqrt{\tau}\ \right) \tag{18}$$

where:

$$\xi = \frac{k K z}{u}\left(\frac{1-\varepsilon}{\varepsilon}\right) \tag{19}$$

and:

$$\tau = k\left(t - \frac{z}{u}\right) \tag{20}$$

This model is useful for predicting the breakthrough of Mn(II) during adsorption onto oxide-coated media. Note that pH does not appear explicitly in this model. Instead, the model incorporates the effects of pH into the parameters k and K; therefore, the parameters k and K must be estimated from a bench- or pilot-scale experiment conducted at pH conditions similar to those to be found in the scale-up process.

CHAPTER 4

EXPERIMENTAL METHODS AND MATERIALS

Experimental Design

The experimental portion of this thesis contains two major sections. First, several media configurations were tested to determine which provided the best quality effluent with respect to soluble and particulate iron and manganese while the rate of head loss was minimized. (These are referred to as the "media configuration" experiments.) Second, the removal of manganese by adsorption and oxidation onto the surface of oxide-coated filter media was investigated as an alternative manganese control strategy. (These studies are referred to as the "adsorption/oxidation" experiments.)

A continuous-flow, pilot-scale filtration apparatus was constructed to investigate these issues. A sketch of the experimental setup is shown in Figure 2. Three main components comprised the system: the detention tank, the reaction chamber, and the filters. The Plexiglas detention tank provided a constant-head feed for the experiment and held 16.8 gallons; this volume corresponded to a detention time between 4.25 and 17 minutes, depending upon the system flow rate. The hydraulic loading applied to each filter ranged from 2 to 6 gpm/ft^2. The raw water entered the detention tank below the water surface to minimize oxygen transfer into the raw water. As a result, an average of less than 1 percent of the manganese and 2.3 percent of the iron in the raw water oxidized in the detention tank.

The reaction chamber (Figure 3) design was similar to that of Columbus City Utilities Water Plant No. 1. The design incorporated five baffles with

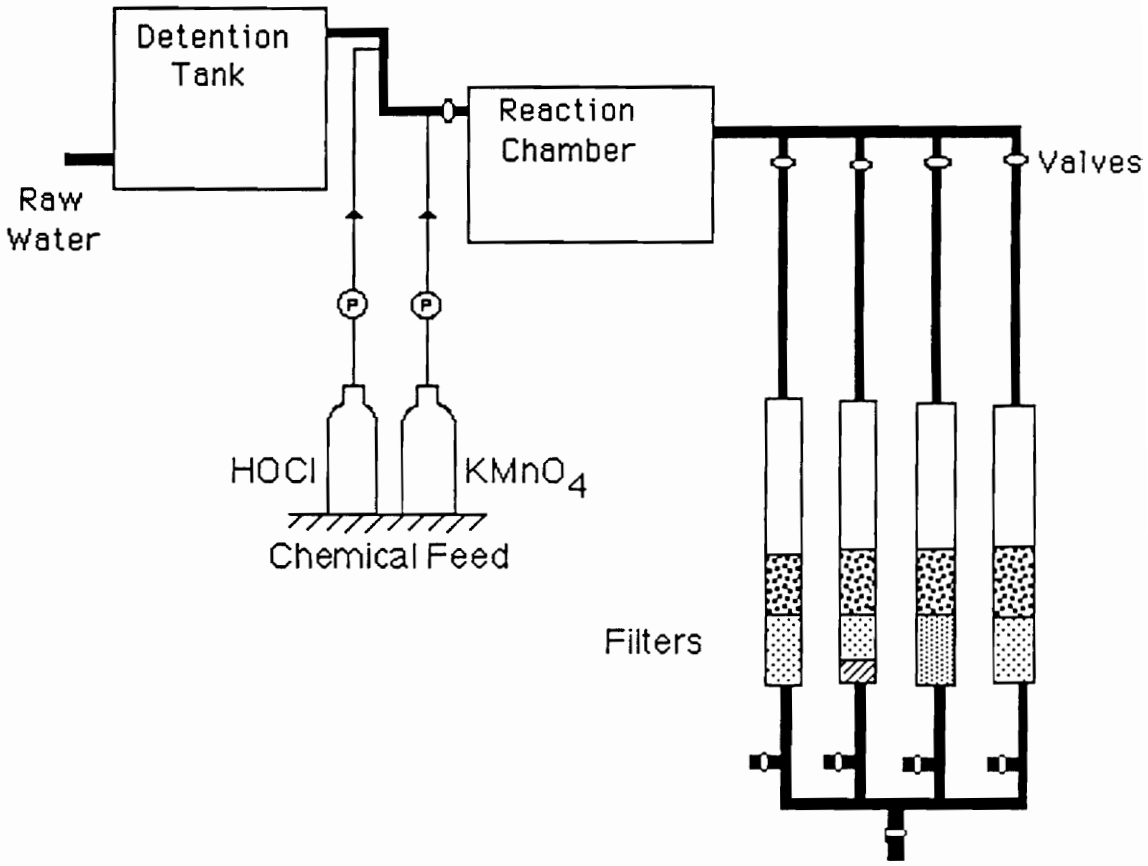

Figure 2. Schematic of pilot-plant

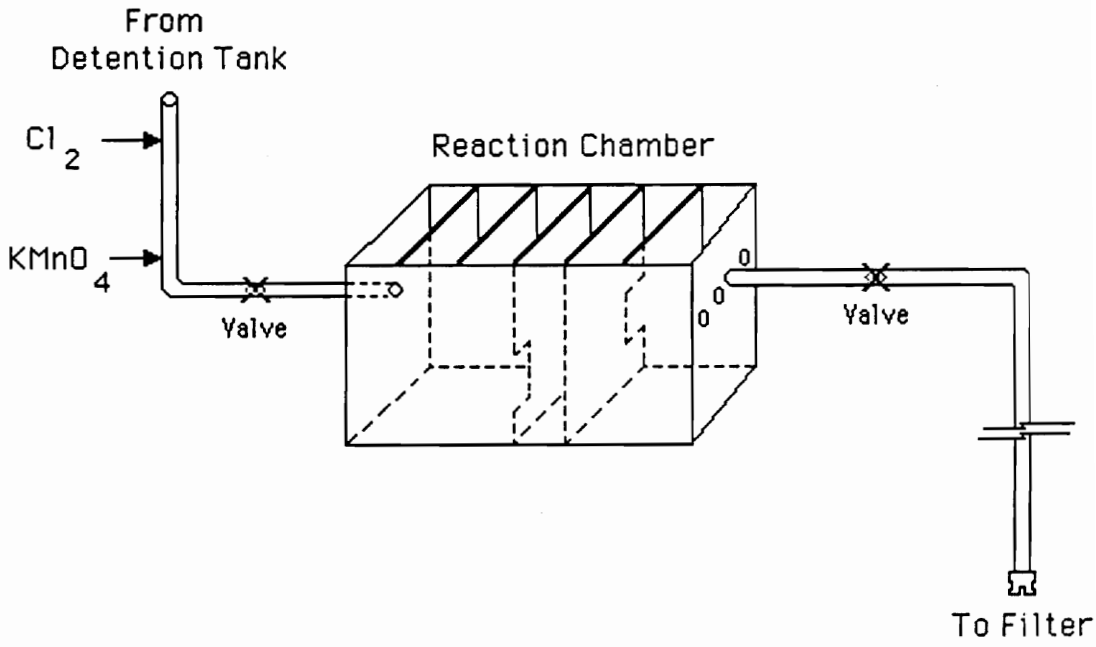

Figure 3. Reaction chamber design

openings on alternating sides. The baffles reduced short circuiting within the reaction chamber. The reaction chamber held 11.2 gallons; this volume corresponded to a detention time between 2.8 and 11.3 minutes depending upon the system flow rate. This detention time allowed complete oxidation of Fe^{2+} and Mn^{2+} in the presence of both chlorine and $KMnO_4$.

The reaction chamber then fed four filters. Four outlets mounted at the same height on the reaction chamber promoted equal flow to the filters. Valves on each of the filter feed-lines provided fine-tuning control of the flow to the filters. The filters were constructed of 5.5-inch (inside diameter) clear, Plexiglas tubes with $^1/_4$-inch wall thickness. The nominal filter height was 9 feet. A valve on the effluent line of each filter individually controlled the flow. To maintain consistency with the filter design at Water Plant No. 1, the filter effluent lines were not raised above the filter media level. This design did not prevent the possibility of air entrapment in the filters, but during the course of the study air-binding was never encountered. Figure 4 shows a more detailed view of a filter. Brass nipple fittings were mounted every six inches along the entire filter length. These openings allowed both the determination of head loss (by use of a manometer board) and the collection of water samples throughout the media depth. Typically, three head loss measurements were recorded throughout the depth of the filter. The head loss was calculated as the difference between the pressure head (height of water in the manometer column) at a port in the media and the pressure head of the standing water in the filter.

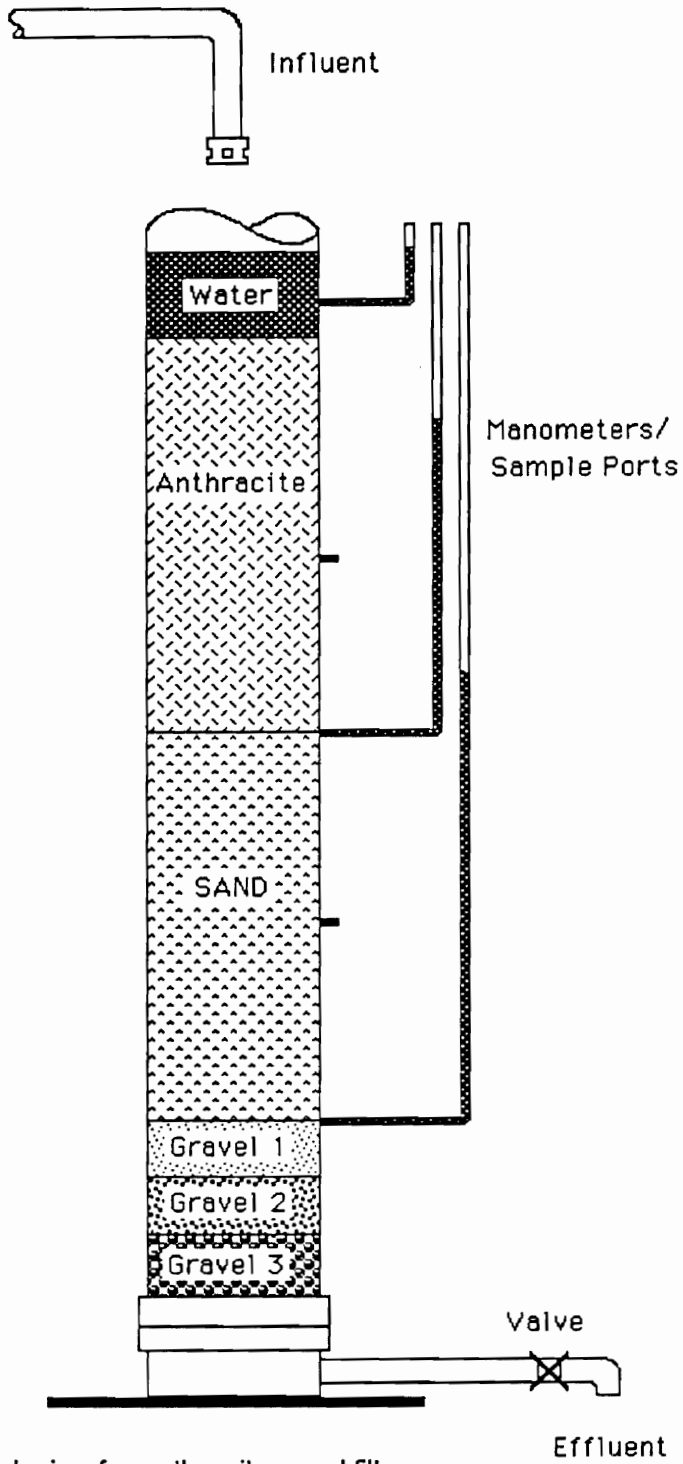

Figure 4. Filter design for anthracite-sand filter

Media Configuration and Characterization

Media depths were selected to be representative of traditional iron- and manganese-removal systems. The media configurations in each filter are listed in Table 3, and a sketch of the filters is shown in Figure 5. Even though only four filters were constructed, five different media configurations were investigated by changing the media in one filter partway through the study. Table 3 also shows the effective size and uniformity coefficient for the media. The effective size is defined as the particle size for which 10 percent of the media (by weight) is smaller. The uniformity coefficient is defined as the ratio of the 60 percent particle size to the 10 percent particle size. The effective size and uniformity coefficient were determined by Seico Engineers of Columbus, Indiana.

At the bottom of each filter, three, two-inch layers of gravel were placed to support the media. The layered gravel sizes were $^1/_2$ - $^1/_4$ inch, $^1/_4$ - $^1/_8$ inch and $^1/_8$ inch - #12 mesh. The Unifilt Corporation of Zelienople, Pennsylvania supplied the gravel.

The following media were used in selected filters: (1) virgin [new] anthracite, (2) virgin sand, (3) greensand, (4) garnet, (5) oxide pre-coated sand, (6) oxide pre-coated anthracite, and (7) a mixture of sand and anthracite from Water Plant No. 2 in Columbus, Indiana. The virgin anthracite, virgin sand, greensand, and garnet were obtained from the Unifilt Corporation. The pre-coated anthracite and pre-coated sand were obtained from the General Filter Company of Ames, Iowa. To obtain the media from Water Plant No. 2, one filter cell was drained below the media surface and about 0.5 ft^3 of media was scraped from the top few inches of the filter. Water Plant No. 2 was used as the

Table 3. Media Configurations, Effective Sizes, and Uniformity Coefficients Used in the Pilot-Plant Study

	Media Configurations (inches)				
Filter No.	Gravel	Garnet	Greensand	Sand	Anthracite
I (anthracite-sand)	6	0	0	12	18
II (anthracite-greensand)	6	0	12	0	18
III (tri-media)	6	3	0	6	21
IV (precoated anthracite-sand)	6	0	0	14*	20*
V (Water Plant #2 anthracite-sand)	6	0	0	10†	24†
Effective Size (mm)	–	0.25	0.30	0.50	0.95
Uniformity Coefficient	–	2.0	1.8	1.5	1.6

Note: * = precoated media
† = media from Columbus City Utilities Water Plant No. 2

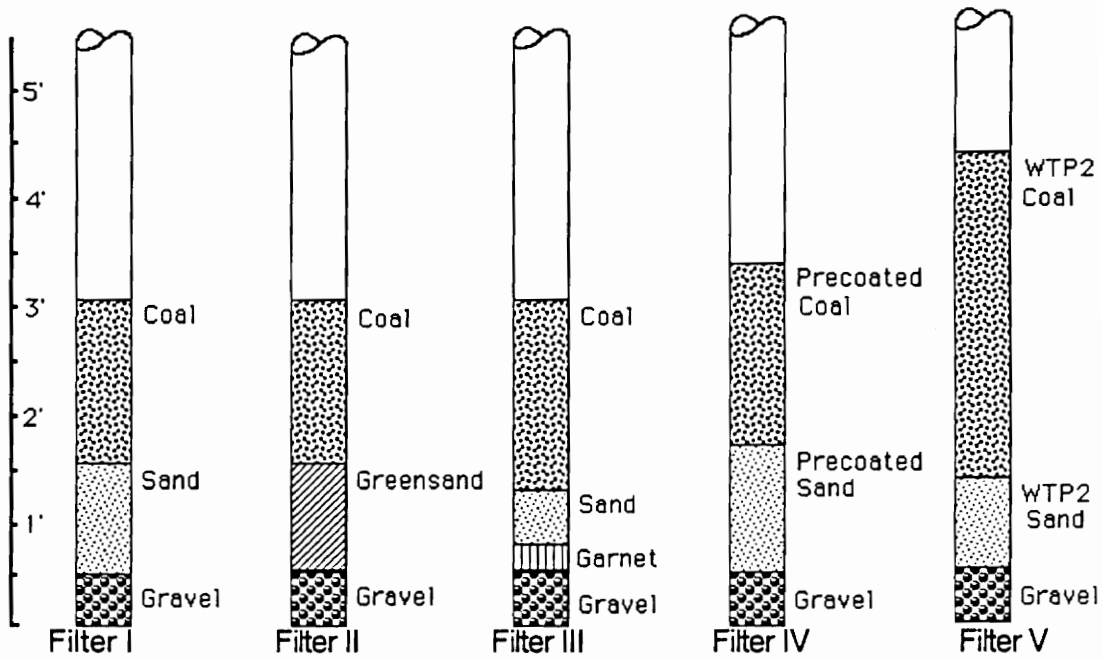

Figure 5. Filter Configurations

source because the media at Water Plant No. 1 contained predominantly greensand.

Once the media was placed in a filter, it was backwashed twice for fifteen minutes each at greater than 50 percent bed expansion. These washings removed any fines from the new filter media. Clean-bed, hydraulic-loading profiles were obtained by recording head losses at several hydraulic loadings for each filter. The hydraulic loadings ranged from 2.0 to 7.1 gpm/ft^2.

The amount of surface oxide coating on the media was quantified by application of a hydroxylamine sulfate (HAS) extraction procedure. Specific media which were extracted included samples of the pre-coated media, samples from the Water Plant No. 2 media, and a sample of anthracite coal from Filter III at the end of the pilot-plant study. The extraction procedure follows:

A 4.00 g media sample was placed into a 125 mL polyethylene bottle. A 100-mL volume of 0.5 percent HNO_3 was then added to provide the necessary acidic conditions for the extraction. An excess amount of HAS (approximately 1.0 g HAS) was then added to the bottle. The bottle was sealed and periodically shaken for two hours. The reaction between the oxide coating and the HAS reduced and dissolved the manganese on the filter media surface. After the extraction, 10 mL of the extracted liquid were filtered through a 0.2 µm Gelman membrane filter to remove any particulate matter. The filtrate manganese concentration was then analyzed with a Perkin-Elmer atomic absorption spectrophotometer.

The total amount of manganese on the media surface was determined from the following equation:

$$EMC = \frac{(V)(C)}{M_{samp}} \quad (21)$$

where:

EMC = extractable manganese concentration, $^{(mg\ Mn)}/_{(g\ media)}$

V = volume of acid added to flask, L

C = Mn concentration in acid solution after HAS addition, $^{mg}/_{L}$

M_{samp} = mass of media sample extracted, g

Chemical Addition System

Chemicals were injected between the detention tank and the reaction chamber at two locations 34 inches apart along a $^{1}/_{2}$-inch PVC pipe. Because of the short distance and small pipe diameter, virtually no lag time existed between the addition of the two chemicals. For example, the time lag was 1.3 seconds when four filters were operating at 2 $^{gpm}/_{ft^2}$.

A Cole-Palmer dual-head diaphragm pump provided a constant flow rate of chemicals from two 20-L carboys. The flow rate for each side of the pump was set at 10 $^{mL}/_{min}$ for each experiment. The pump rates were checked periodically and did not vary more than five percent. The chemical dosages during each experiment were varied by adjusting the concentration of the stock solutions within the carboys, thus eliminating the need to change the chemical-feed pump rates for each experiment.

During the media configuration experiments, the only chemicals added to the system were sodium hypochlorite and potassium permanganate. The chlorine stock solution was prepared by adding a 10.0 percent (as Cl_2) sodium hypochlorite solution to demineralized water in one of the 20-L carboys.

Demineralized water was used because hardness in the Columbus tap water formed a precipitate in the presence of high sodium hypochlorite concentrations. The potassium permanganate solution was prepared by adding a concentrated solution of free-flowing grade $KMnO_4$ to a second carboy containing tap water. Free-flowing grade $KMnO_4$ contains approximately ninety percent $KMnO_4$ and ten percent inert ingredients.

The $KMnO_4$ was added stoichiometrically to oxidize the manganese from Mn^{2+} to Mn^{4+} in a ratio of 1.92 mg $KMnO_4$ per mg Mn^{2+}. The specific equation for Mn^{2+} oxidation by $KMnO_4$ is:

$$3Mn^{2+} + 2\,MnO_4^- + 2\,H_20 \rightarrow 5\,MnO_{2(s)} + 4\,H^+ \quad (22)$$

The chlorine was added stoichiometrically to oxidize the iron from Fe^{2+} to Fe^{3+} in a ratio of 0.47 mg HOCl per mg of Fe^{2+}. The specific equation for Fe^{2+} oxidation by HOCl is:

$$2\,Fe^{2+} + HOCl + 5\,H_2O \rightarrow 2\,Fe(OH)_{3(s)} + Cl^- + 5\,H^+ \quad (23)$$

An additional amount of chlorine was added to insure a residual of 1.0 to 1.5 mg/L as Cl_2 in the filter effluent.

Raw Water Supply

For the media configuration experiments, the raw water supply was obtained by tapping into the main raw water line of Water Plant No. 1 prior to any chemical addition. To ensure a flow of fresh, raw water, the pilot-plant filtration system operated only when raw water flowed through the main. The flow was regulated and measured with two valves and a standard residential water meter. Approximately 75 ft. of $^1/_2$-inch PVC pipe brought the water from the raw water main to the pilot-plant. The raw water then flowed into the

constant-head, detention tank. Typical chemical characteristics of the raw water are summarized in Table 4.

For the adsorption/oxidation experiments, the water supply was taken from the finished water line at Water Plant No. 1. For the column exhaustion experiments, the finished water was dechlorinated by the addition of a sodium thiosulfate ($Na_2S_2O_3$) solution in a stoichiometric ratio of 4.46 mg $Na_2S_2O_3$ per mg of free chlorine. Finished water was used instead of raw water to prevent limited filter-run time due to the accumulation of iron oxide precipitates in the media. Manganese was then added from a manganous sulfate stock solution with the diaphragm pump. Typical chemical characteristics of the finished water before the addition of $Na_2S_2O_3$ and manganese are summarized in Table 4.

Filter Run Procedures: Media Configuration Experiments

The following describe the procedure for the experiments designed to investigate the optimal media configuration for iron and manganese removal:

1. Each of the filters containing greensand or oxide-coated media were fully oxidized (charged) with a concentrated solution of $KMnO_4$. Originally, the filters were charged using the manufacturer's recommendation of 2-3 oz. $KMnO_4/ft^3$ of media during a 30 minute contact time. Dry $KMnO_4$ was added to the reaction chamber where it dissolved and flowed through the filters. Later, the filters were charged with $KMnO_4$ until the influent and effluent color of the permanganate solution appeared nearly the same intensity.

Table 4. Average Suppy Water Characteristics at Columbus City Utilities Water Plant #1 (June, 1989)

Component	Units	Raw Water	Finished Water
iron	mg/L	1.39	0.15
manganese	mg/L	0.20	0.024
hardness	mg/L as $CaCO_3$	382	395
alkalinity	mg/L as $CaCO_3$	292	281
pH	–	7.4	7.4
fluoride	mg/L	–	0.87
total chlorine	mg/L as Cl_2	–	0.86

2. The filters were backwashed to at least 50 percent expansion for 10-15 minutes. The backwash flow was then slowly reduced for 3-4 minutes to allow proper settling and separation of the media.
3. The raw water feed to the filters was started without any chemical addition until equilibrium was approached in all of the filters. This often entailed fine-tuning of both the influent and effluent valves for the filters. Equilibrium was defined to be when the head losses through the filters changed very slowly relative to each other and the standing water level in all filters was nearly constant. Values of initial head loss and flow rate were then recorded for each filter.
4. Chemical addition was then started to the reaction chamber. The chemicals were previously mixed in the 20-L carboys according to the procedure in the Chemical Addition System section. The chemicals used in these experiments were HOCl and $KMnO_4$. In some experiments, only chlorine was applied so that a comparison could be made between its iron and manganese removal performance with removal by a combination of chlorine and permanganate.
5. The following parameters were measured every 1-4 hours (depending on the hydraulic loading) during the entire filter run: head loss, flow rate, detention tank Fe and Mn concentration (total and soluble), reaction chamber Fe and Mn concentration (total and soluble), filter effluent Fe and Mn (total and soluble), and effluent chlorine residual. Less frequently measured parameters included solution pH and temperature.

6. The experiments continued until iron and manganese oxides broke through the filter. The filter runs typically lasted from 8-24 hours, depending on the hydraulic loading conditions used in a particular study.

Filter Run Procedures: Adsorption/Oxidation Experiments

The adsorption/oxidation experiments were subdivided into two categories: continuous regeneration and column exhaustion. The continuous regeneration experiments determined the manganese removal profile due to adsorption and oxidation onto the filter media oxide coatings in the presence of free chlorine. The chlorine continually regenerated the manganese oxide coating on the filter media, thereby maintaining an essentially constant concentration of Mn^{2+} adsorption sites within the filter. In contrast, the column exhaustion experiments showed both the Mn^{2+} adsorption capacities without chlorine and the Mn^{2+} wavefront propagation in each filter.

Continuous Regeneration Experiments

1.-3. The first three steps of the continuous regeneration experiments were identical to the steps in the media configuration experiments.

4. Chemical addition to the reaction chamber was then started. The chemicals used in these experiments were (1) a manganous sulfate solution to provide the desired concentration of soluble manganese and (2) a chlorine solution to continuously regenerate the columns. The chlorine was added above the levels already present in the finished water. Note that no Mn(II) was oxidized by HOCl in the bulk solution.

5. Each of the following parameters was periodically measured throughout the entire filter run: total filter head loss, flow rate, reaction chamber Mn

concentration (total and soluble Mn), manganese concentrations at six-inch intervals through the filter media (total Mn) and influent and effluent chlorine residual.

6. The experiments generally continued for 30 hours.

Column Exhaustion Experiments

1.-3. The first three steps of the continuous regeneration experiments were identical to the steps in the media configuration experiments.

4. Chemical addition was then started to the reaction chamber. The chemicals used in these experiments were (1) a manganous sulfate solution to provide the desired concentration of manganese and (2) a sodium thiosulfate solution to eliminate the chlorine residual in the supply water.

5. Each of the following parameters was periodically measured throughout the entire filter run: total head loss, flow rate, reaction chamber Mn concentration (total and soluble Mn), and manganese concentrations at six-inch intervals through the filter media (total Mn). Chlorine concentrations in the reaction chamber were periodically monitored to ensure that no residual was present.

6. The experiments continued for 1-4 days, depending on the hydraulic loading and manganese concentration applied.

Analytical Methods

Throughout the experiments, samples were first collected in glass beakers from each filter port or effluent valve. A syringe-filter was used to separate the particulate and soluble fractions of the samples. In each case,

approximately 50 mL of the sample were filtered through a 0.45 µm Gelman membrane filter into 60- or 125-mL Polyethylene bottles. All of the total metals samples were immediately acidified with 0.5 mL of 10 percent HNO_3. The samples to be analyzed for soluble metals were acidified after filtration. The Fe and Mn concentrations were measured with a Perkin-Elmer Atomic Absorption Spectrophotometer.

Chlorine residuals were determined with a Wallace and Tiernan amperometric titrator according to Method 408C described in *Standard Methods* (1985). A Fisher Accumet pH meter was used to quantify influent and effluent pH values. Flow rates were calculated by the measurement of filter effluent volumes over a specified time interval (between 10 and 30 seconds).

Quality Assurance/Quality Control Methods

Quality assurance was maintained during analytical testing by the periodic measurement of standards. In addition, the AA was initialized and standardized every ten unknown samples. Three samples with known concentrations were analyzed between the restandardization points.

Some experiments were duplicated to determine if repeatable results could be obtained. Figures 6 and 7 show the comparison of total head loss and iron breakthrough for two filter runs with similar operating parameters. In Figure 6, the total head loss accumulation profiles are closely matched. Figure 7 shows the iron breakthrough patterns of the two tests. The volume of water treated before the beginning of breakthrough differs by about five percent. The breakthrough profile, however, diverges after the beginning point. These

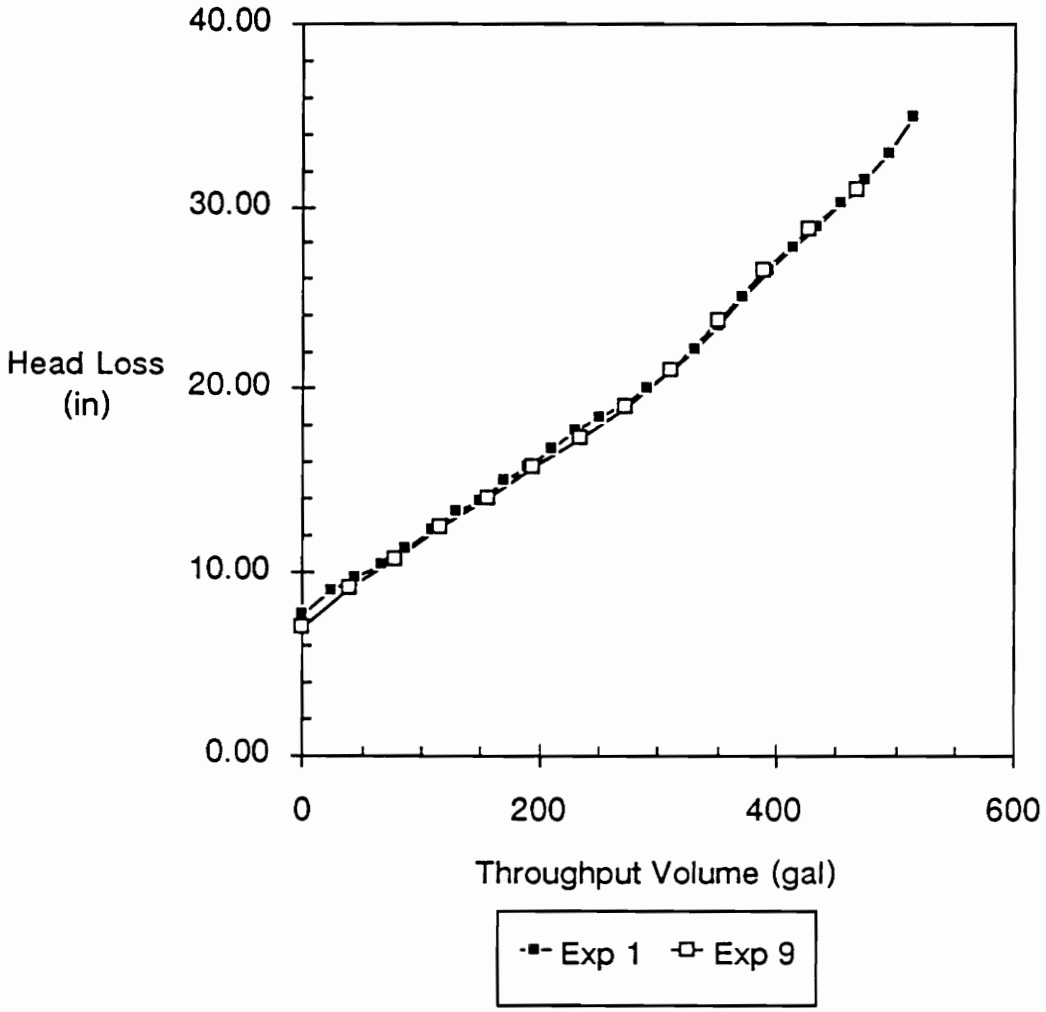

Figure 6. Head Loss Comparison for Repeated Test in Filter I (anthracite-sand) (HLR = 4 $^{gpm/ft^2}$, HOCl = 3.0 $^{mg/L}$, $KMnO_4$ = 0.5 $^{mg/L}$)

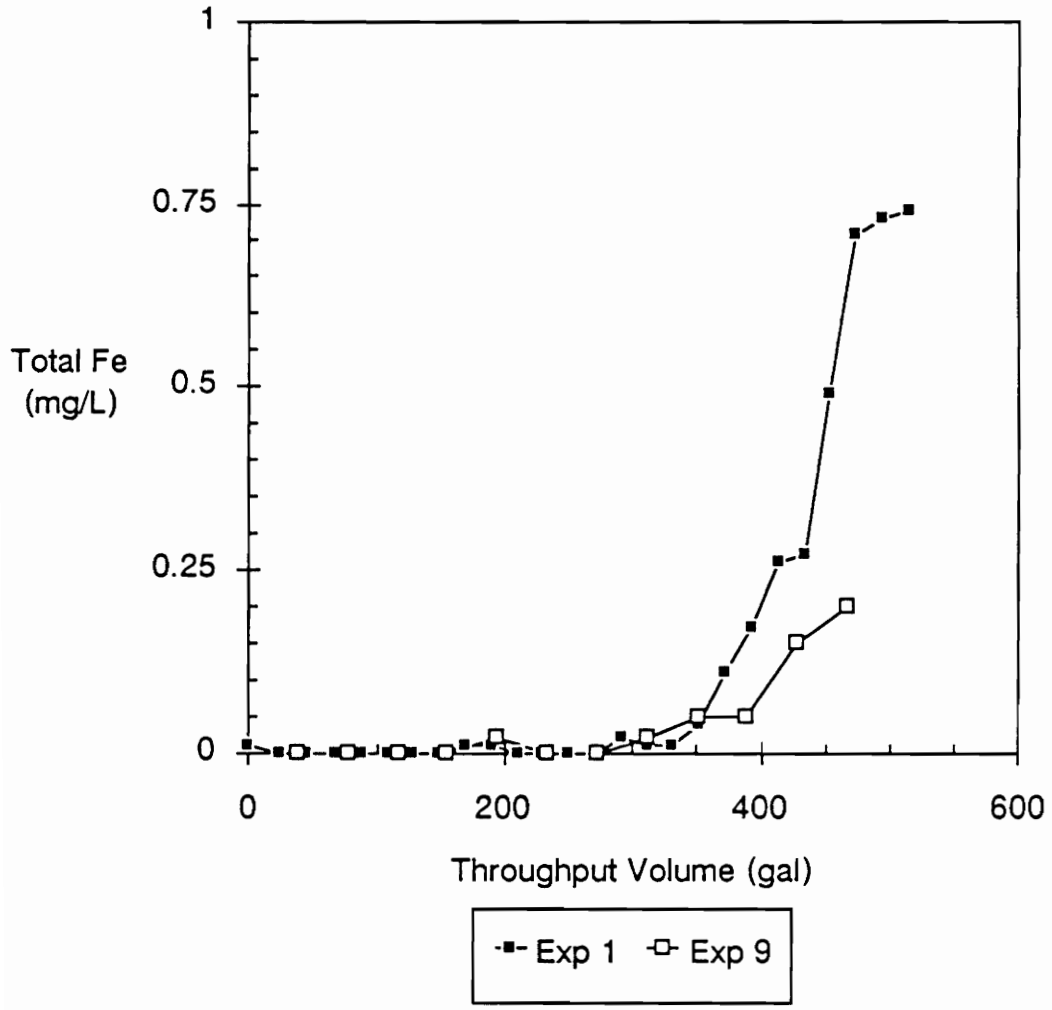

Figure 7. Iron Breakthrough Comparison for Repeated Test on Filter I (anthracite-sand) (HLR = 4 $^{gpm}/_{ft^2}$, HOCl = 3.0 $^{mg}/_{L}$, $KMnO_4$ = 0.5 $^{mg}/_{L}$)

figures show the experiments to be highly repeatable for the important operational characteristics of head loss and metals breakthrough.

Experimental Methods from Other Research

Finally, experimental data from other research (Hungate, 1988; Occiano, 1988; Pankow and Morgan, 1981; and Morgan, 1964) were used to develop mathematical models for the removal of Mn(II) from raw water supplies using either continuous regeneration of the Mn(II) removal capacity with the addition of chlorine or intermittent regeneration of the Mn(II) removal capacity with the periodic addition of a stronger oxidant. The experimental methods used by these researchers are described in their respective publications.

Data Management

The data gathered in these experiments was stored, organized, and graphed with Microsoft Excel, a spreadsheet program for the Macintosh computer.

CHAPTER 5

EXPERIMENTAL RESULTS

This chapter presents some of the data collected during the experimental pilot-plant portion of the study, a sensitivity analysis of the two manganese removal models, and a parameter estimation for both of the models. Specific subsections include the pilot-plant results (1) with chlorine and permanganate added to the unfiltered water, (2) with chlorine alone added, and (3) with no oxidants added.

Filter Media Configurations

Figure 8 shows the head loss profile during normal filter operation with the addition of both permanganate and chlorine. Most of the resulting precipitated solids became trapped in the first few inches of the filter media. During this experiment, the head loss increased 21 inches at the top port (located six inches deep into the filter media). Throughout the rest of the filter, the head loss increased only 6.5 additional inches; therefore, 76 percent of the head loss accumulated within the first six inches of the filter. While this percentage varied depending on the filter and hydraulic loadings, greater than 50 percent accumulated within six inches in virtually all of the experiments. This indicates that most solids deposition occurs within the top few inches of media.

Figures 9 - 11 show the performance of Filters I through IV with respect to iron and manganese removal and head loss buildup. Each of the filters were operated between 3.8 and 4.1 gpm/ft^2. $KMnO_4$ was added at a concentration of 0.5 mg/L whereas free chlorine was added at a concentration of 3.0 mg/L. Iron

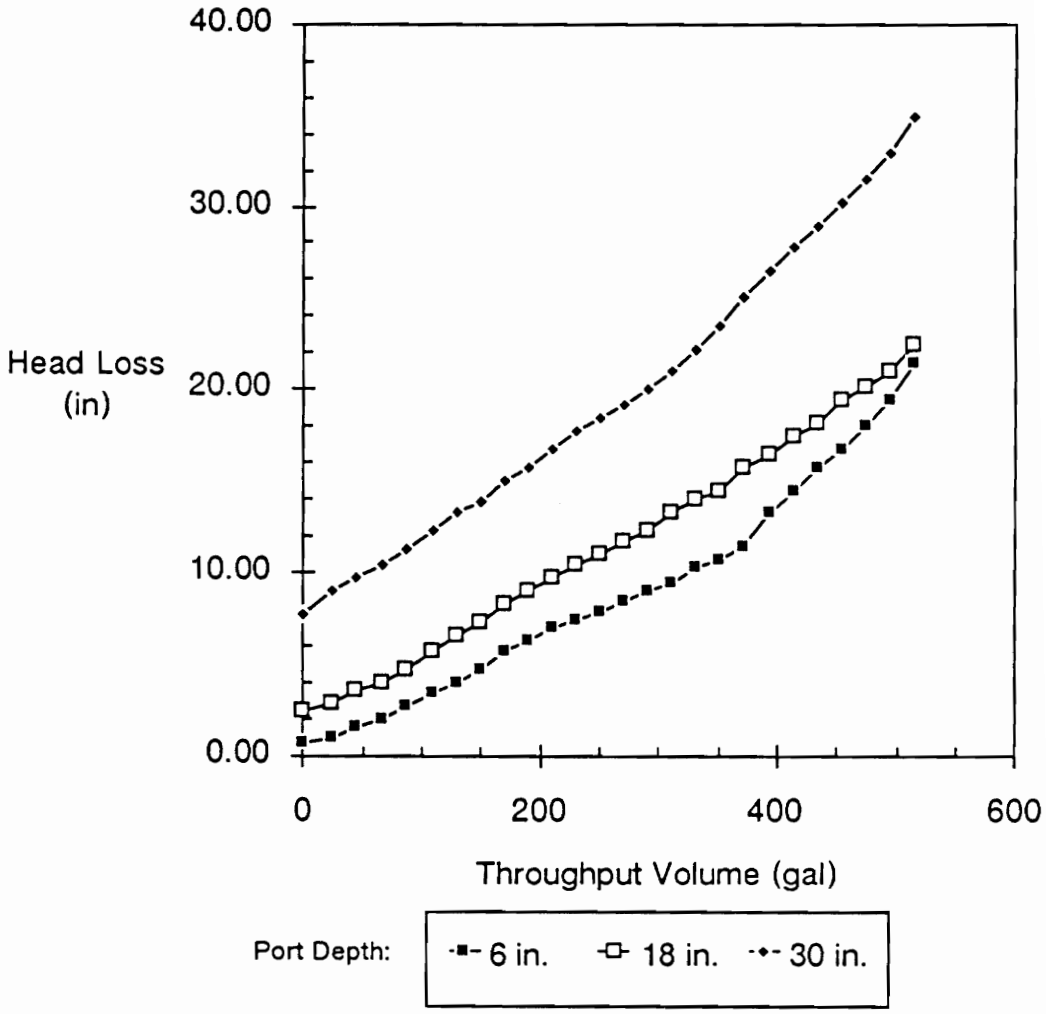

Figure 8. Head Loss Accumulation in Filter I (anthracite-sand) (HLR = 4.1 gpm/ft^2, HOCl = 3.0 mg/L, $KMnO_4$ = 0.5 mg/L)

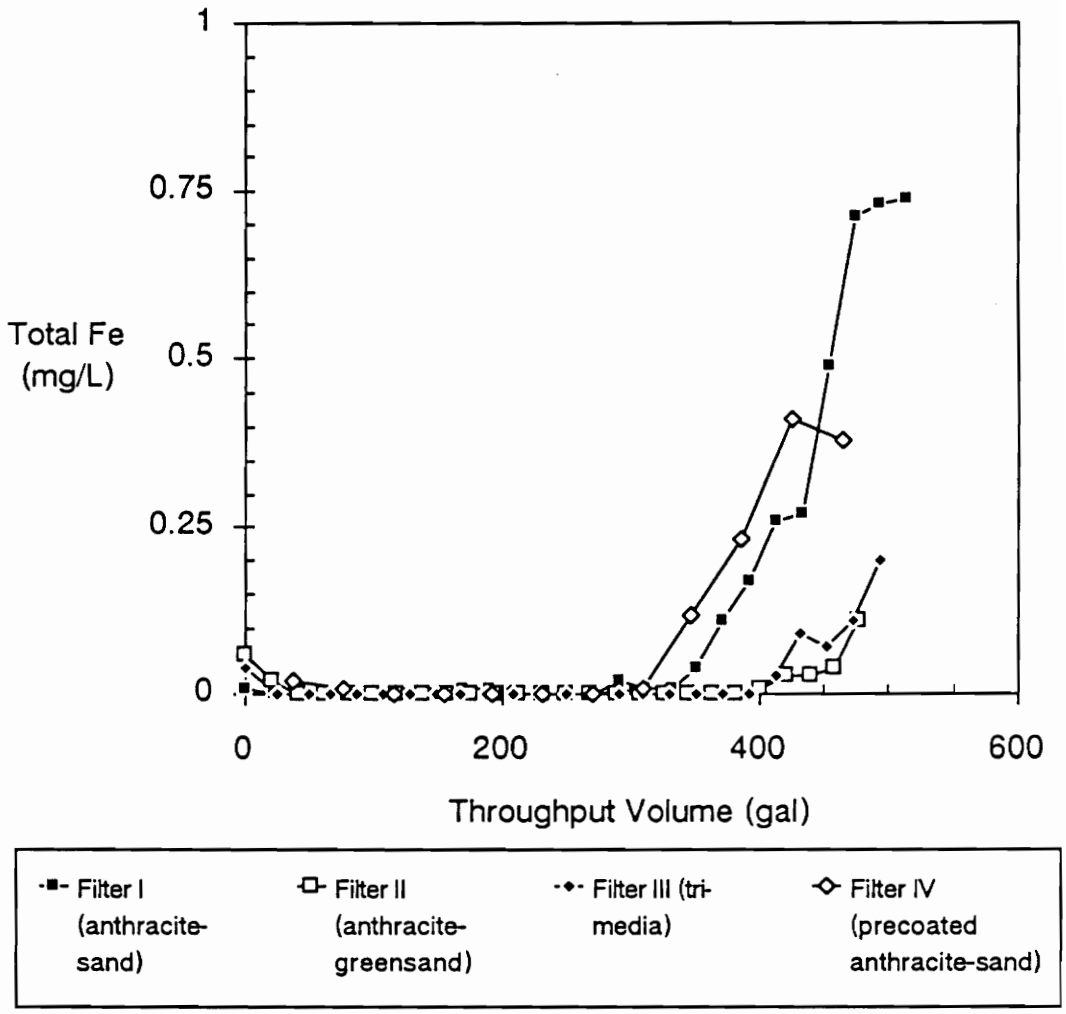

Figure 9. Iron Breakthrough in Filters I - IV (HLR = 4 $^{gpm}/_{ft^2}$, HOCl = 3.0 $^{mg}/_{L}$, $KMnO_4$ = 0.5 $^{mg}/_{L}$)

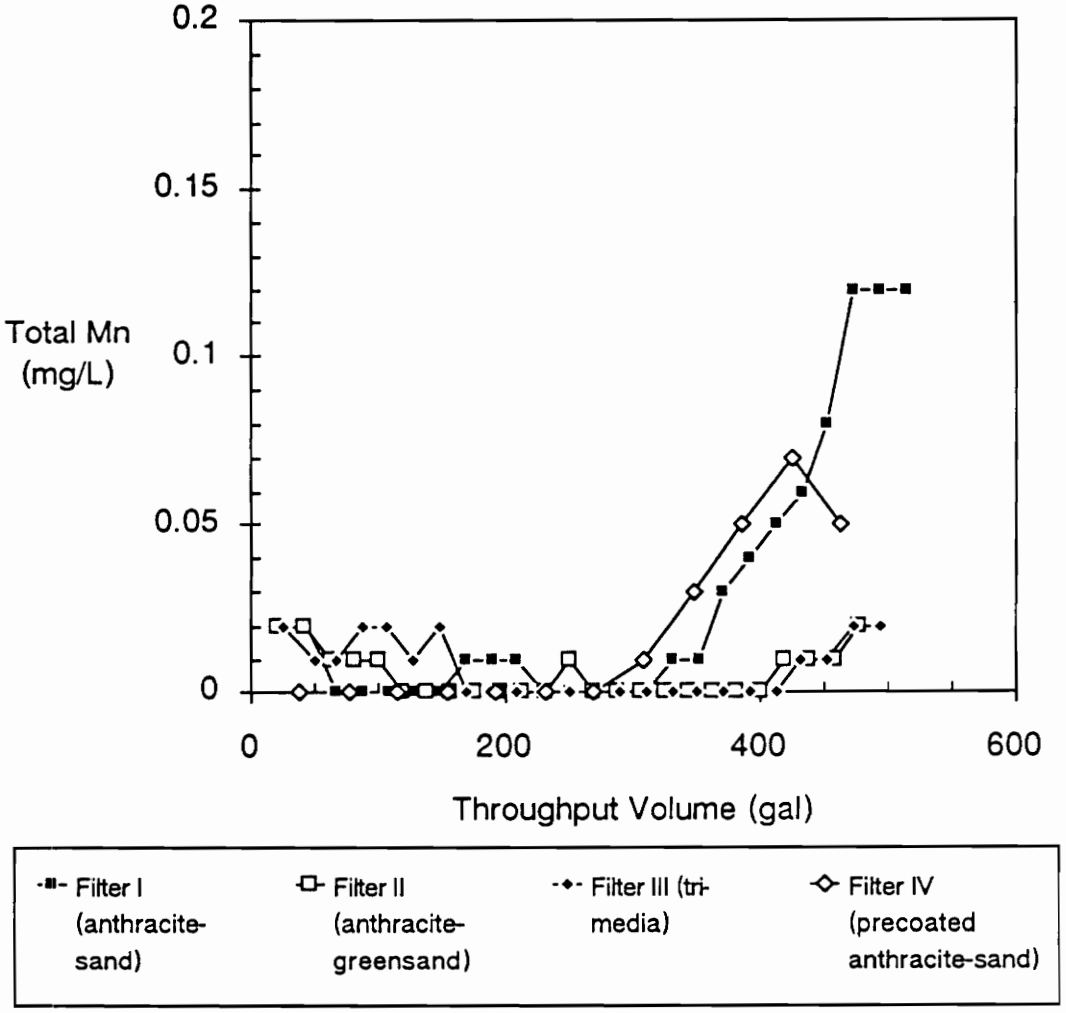

Figure 10. Manganese Breakthrough in Filters I - IV (HLR = 4 $^{gpm}/_{ft^2}$, HOCl = 3.0 $^{mg}/_{L}$, $KMnO_4$ = 0.5 $^{mg}/_{L}$)

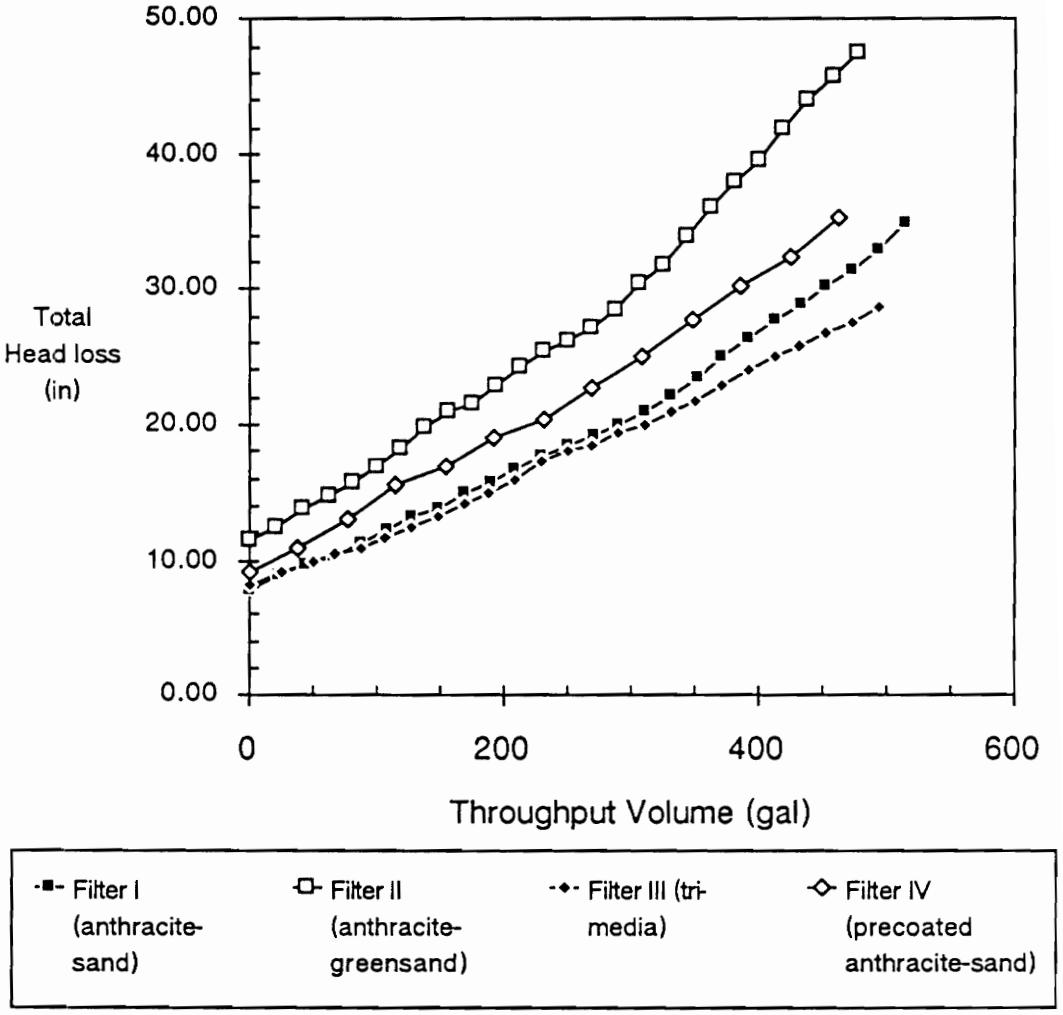

Figure 11. Total Head Loss Accumulation in Filters I - IV (HLR = 4 $^{gpm}/_{ft^2}$, HOCl = 3.0 mg/L, $KMnO_4$ = 0.5 mg/L)

and manganese breakthrough began at a throughput volume of 300 gal for Filter IV (precoated anthracite-sand), 350 gal for Filter I (anthracite-sand), and 400 gal for Filters II (anthracite-greensand) and III (tri-media). Therefore, the volume of water treated before metals breakthrough differed by as much as thirty-three percent. In each individual filter, both iron and manganese breakthrough occurred at the same total volume of water treated.

Clean bed head loss profiles describe the frictional losses within the media and not the accumulation of solids in the filter. Figure 12 shows the total clean bed head loss profile for Filters I through IV as a function of hydraulic loading. As expected, Filter II (anthracite-greensand) develops higher head loss than the other filters regardless of any solids accumulation. Also, in Filter III (tri-media) the addition of a small layer of garnet did not significantly alter the clean bed head loss profile.

Combined Adsorption/Oxidation

Media Surface Oxide Coatings

Data presented in Table 5 summarize the extractable amounts of manganese present on the filter media tested. The surface oxide coating on the Filter III media developed during a few weeks of operation. This same amount of coating was assumed present on the Filter II anthracite also. The surface oxide coating on the pre-coated sand and anthracite media (Filter IV media) was tested on the media before its installation into the filter. The Water Plant No. 2 surface oxide coating was also measured before placement into Filter V.

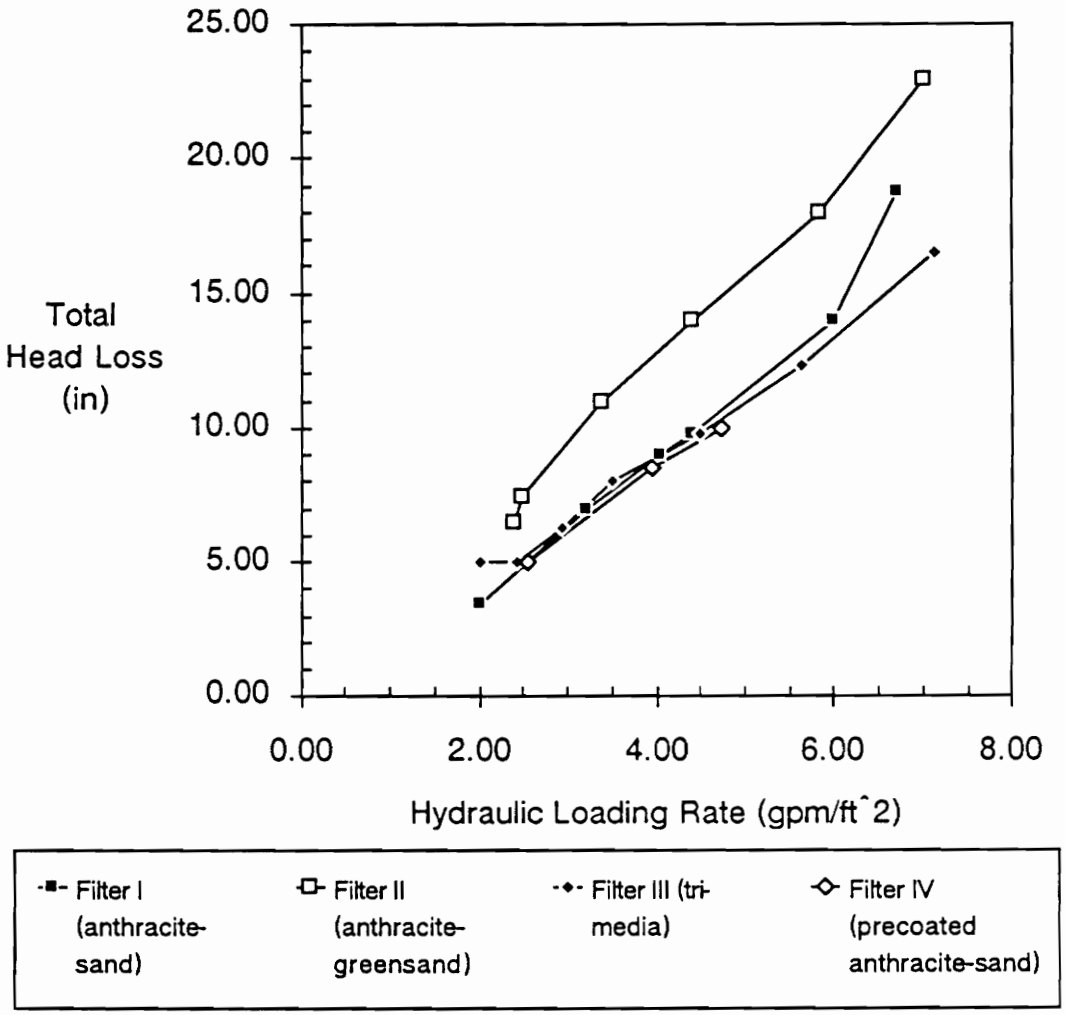

Figure 12. Clean Bed Head Loss Profile for Filters I - IV

Table 5. Extractable Surface Manganese Concentrations

Media	Extractable Mn Concentration mg Mn/g media
Water Plant 2 Sample (sand + anthracite)	16
Greensand (as provided by manufacturer)	3.0
Precoated Sand (as provided by manufacturer)	0.28
Precoated Anthracite (as provided by manufacturer)	0.071
Filter III Anthracite (at end of Filter III experiments)	0.064

Removal of Mn^{2+} in the Absence of an Applied Oxidant

Figures 13 - 15 show the manganese removal capacities of Filters II, IV, and V during 26 hours of operation at 4 gpm/ft^2. An influent manganese concentration of 1.0 mg/L was used to demonstrate the large capacity of the media for manganese uptake. Though the concentrations were measured as total manganese, tests indicated that essentially all of the manganese was in the reduced, soluble Mn(II) state.

Figure 13 shows the manganese removal in the anthracite-greensand filter. The top 18 inches of the filter media depth contained anthracite and the bottom 12 inches greensand. Virgin anthracite was placed in the filter at the beginning of the study and any oxide coating developed during only a few weeks of operation. Three hours into the experiment, however, the anthracite continued to remove more than ninety-nine percent of the applied manganese. Eventually, the removal capacity of the anthracite was exhausted and the greensand became the primary exchange surface for soluble manganese removal.

Figure 14 shows the manganese removal in the filter containing the pre-coated media. During the first hours of operation, the filter performed similarly to the greensand filter. However, the manganese removal capacity was quickly reduced and by nineteen hours of operation, the removal capacity was exhausted. In contrast, Figure 15 shows a tremendous amount of manganese removal capacity using Filter V, the filter containing Water Plant No. 2 media. Even after twenty-six hours of operation, the manganese concentration was reduced to below 0.05 mg/L within the top twenty inches of the filter.

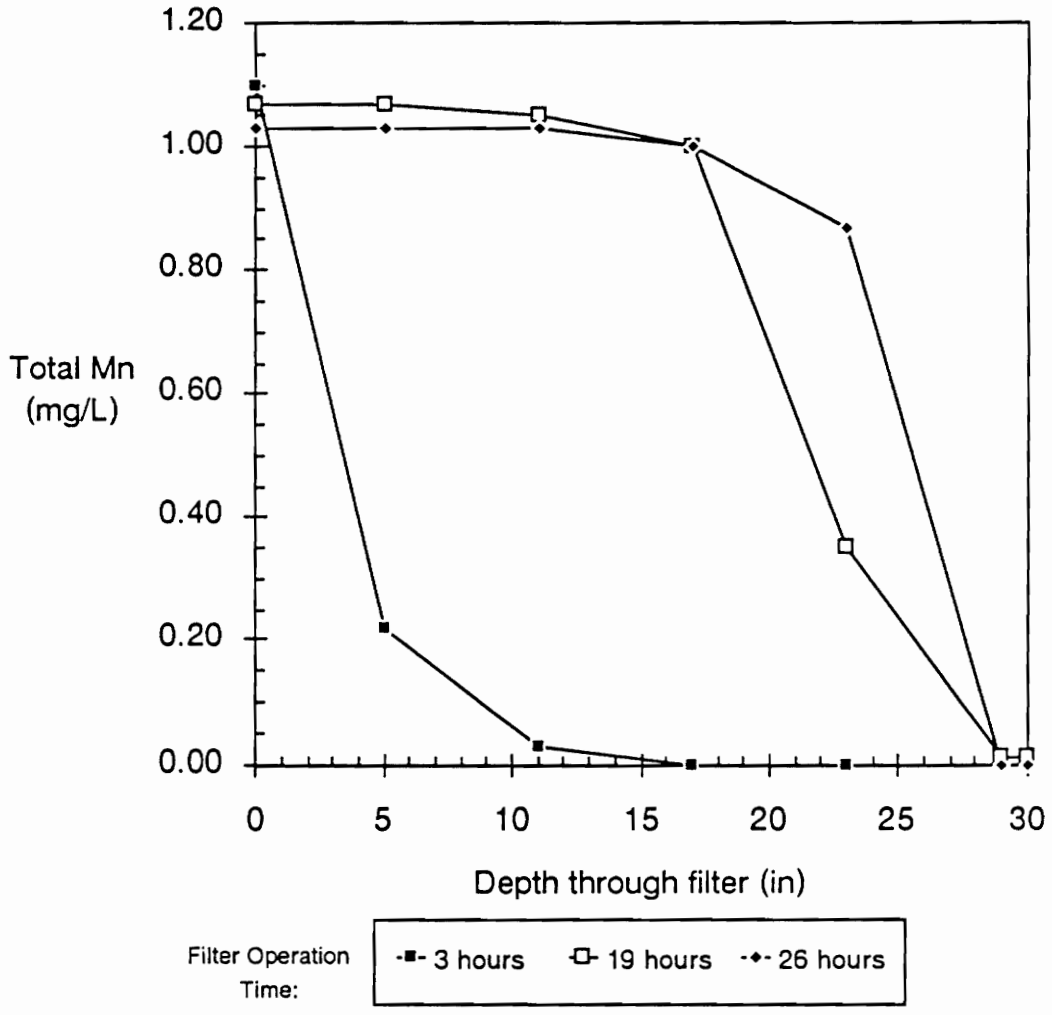

Figure 13. Manganese Uptake in Filter II (anthracite-greensand) (no oxidant addition, HLR = 4 gpm/ft^2, influent Mn(II)=1.0 mg/L)

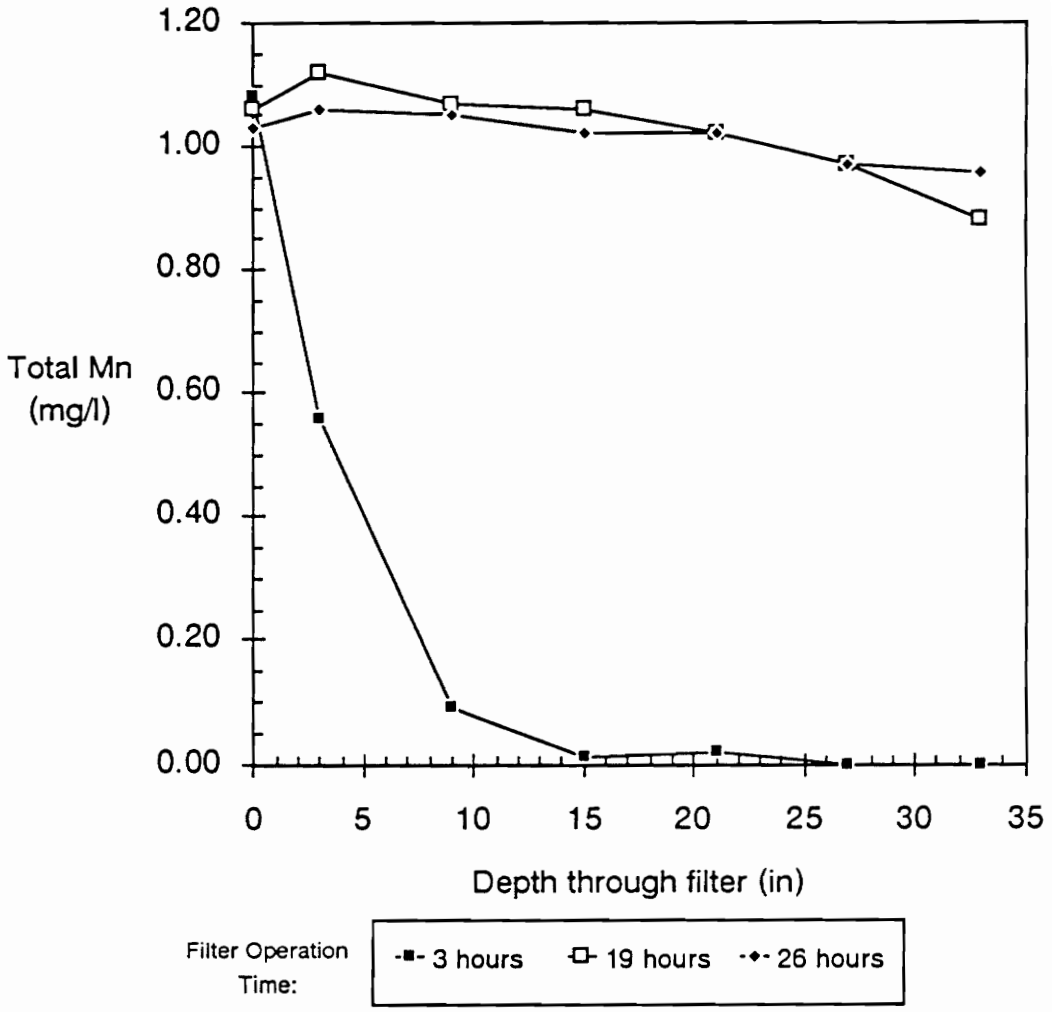

Figure 14. Manganese Uptake in Filter IV (precoated anthracite-sand) (no oxidant addition, HLR = 4 gpm/ft^2, influent Mn(II) = 1.0 mg/L)

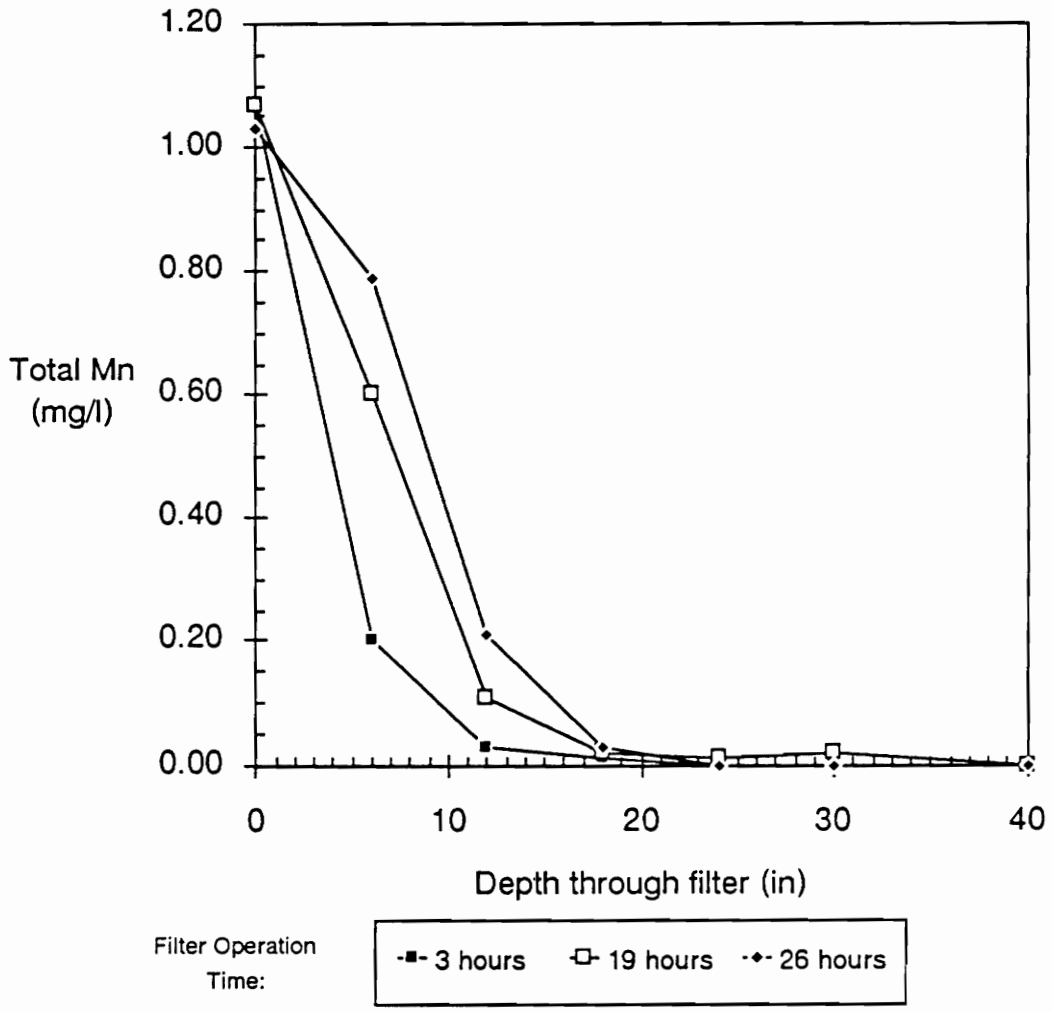

Figure 15. Manganese Uptake in Filter V (Water Plant #2 anthracite-sand) (no oxidant addition, HLR = 4 gpm/ft^2, influent Mn(II) = 1.0 mg/L)

Effect of Oxidant Addition on Mn^{2+} Removal

Figures 16 - 18 indicate that efficient manganese removal occurred in the filters with chlorine addition. An influent soluble manganese concentration of approximately 0.25 mg/L was used to simulate the manganese loadings of the Columbus raw water. Chlorine was added to the raw water to a concentration of approximately 2.5 mg/L and the hydraulic loading rate was approximately 4 gpm/ft^2. During this experiment, the manganese removal was rapid, with the soluble manganese concentration reduced to below 0.05 mg/L in the top ten inches of the filter.

Model Sensitivity Analysis

The previous sections demonstrate that manganese removal using oxide-coated media is an efficient and functional treatment mechanism. Models for these processes were developed to help predict design and operational conditions needed for implementing oxide-coated media as a treatment process. However, for the models to accurately represent the processes, their parameters must be established from similar operating conditions. The sensitivity analysis, presented below, is a helpful tool for the parameter estimation since it provides qualitative information on how changes in the parameters affect the model response.

Continuous Regeneration Model

A qualitative sensitivity analysis was completed for the major parameters of the continuous regeneration model. The initial parameters represent typical operating conditions for soluble manganese removal and are shown in Table 6.

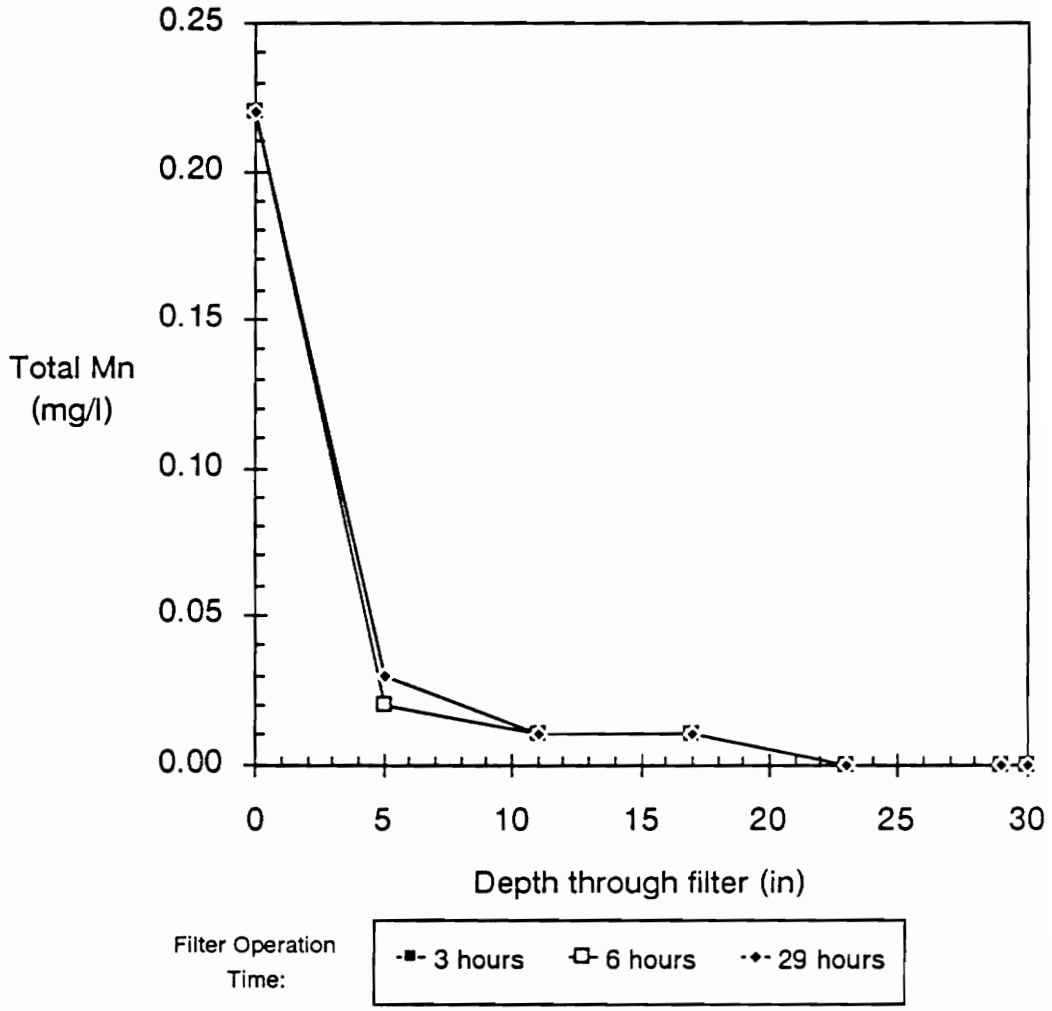

Figure 16. Manganese Removal in Filter II (anthracite-greensand) with Chlorine Addition (HOCl = 2.5 mg/L, HLR = 4 gpm/ft^2)

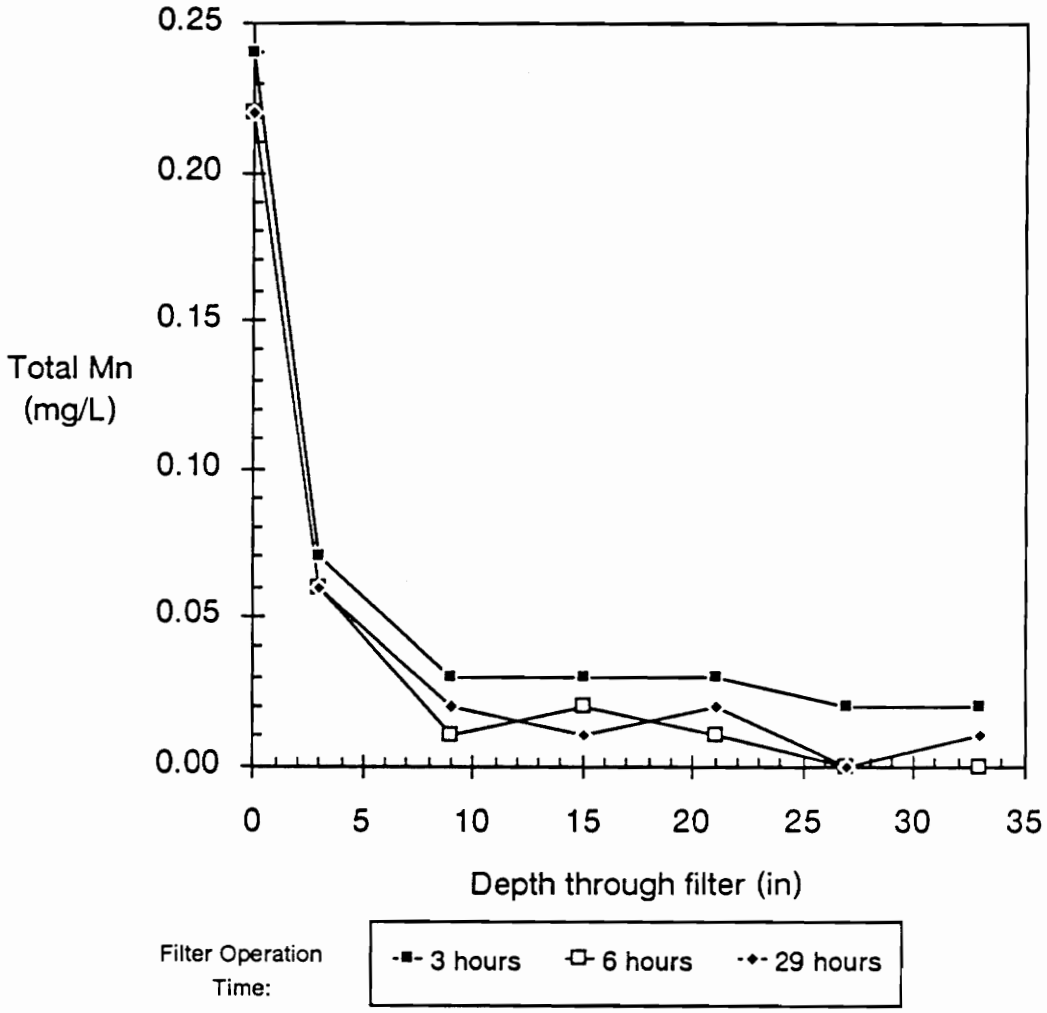

Figure 17. Manganese Removal in Filter IV (precoated anthracite-sand) with Chlorine Addition (HOCl = 2.5 mg/L, HLR = 4 gpm/ft^2)

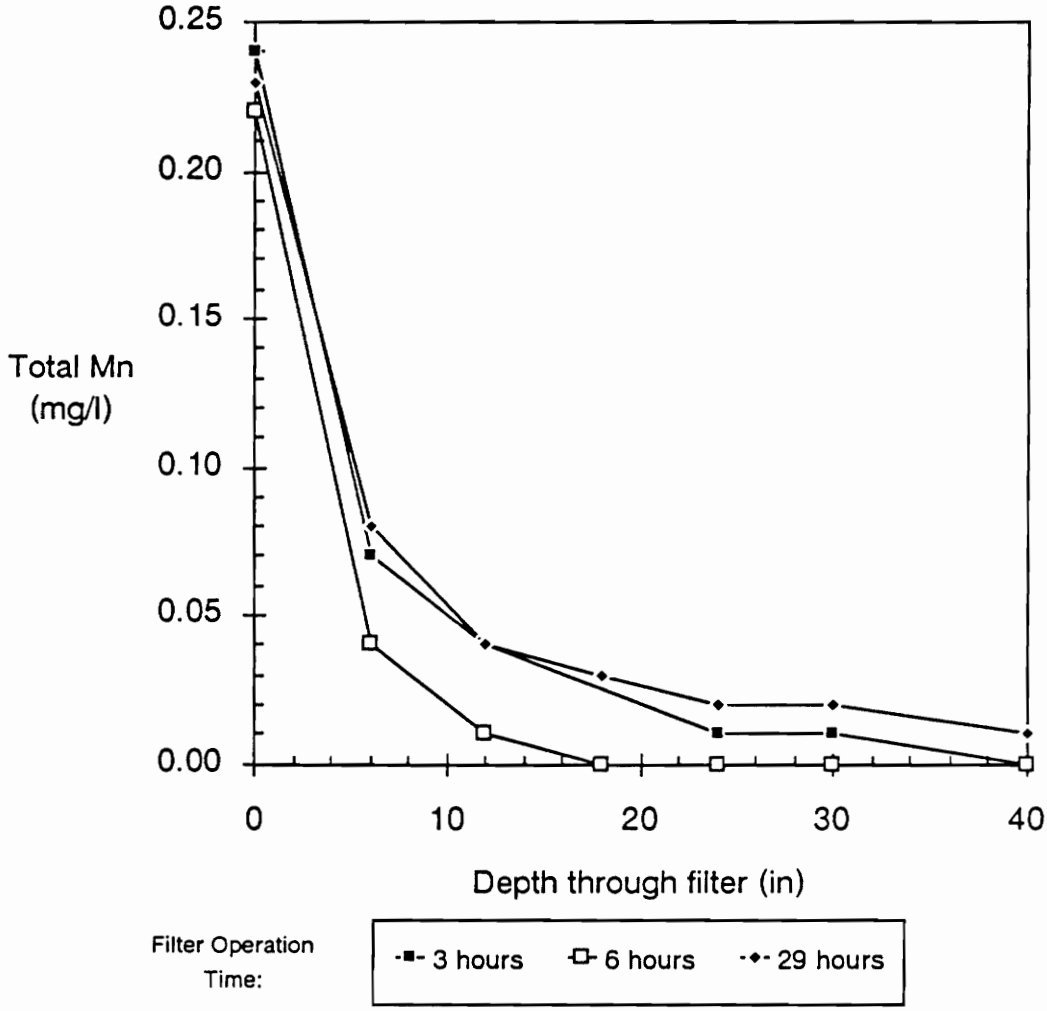

Figure 18. Manganese Removal in Filter V (Water Plant #2 anthracite-sand) with Chlorine Addition (HOCl = 2.5 mg/L, HLR = 4 gpm/ft^2)

Table 6. Operating conditions and parameters for continuous regeneration sensitivity model.

Operating Conditions and Parameters	Value
hydraulic loading rate	3.8 gpm/ft^2
Mn(II) adsortion capacity	0.09 mol/L-bed
surface oxide coating	11.8 $mg\ Mn/g$ media
porosity	0.42
pH	7.4
Influent Mn(II) conc.	1.0 mg/L
Influent Cl_2 conc.	10.0 mg/L
k_1	110 $L/(mol*min)$
k_2	5.84E9 $L^2/(mol^2*min)$
k_3	62.6 $L/(mol*min)$

Figures 19 - 23 show the effect of pH, total adsorption capacity, and reaction rates k_1, k_2, and k_3 on the manganese removal profile.

Figure 19 shows that the theoretical manganese removal depends strongly on pH when the pH is less than about 6.0. At pH values greater than approximately 7.0, the model essentially predicts no change in the manganese removal profile. Note the pH does not alter the total adsorption capacity of the media, which is defined functionally by Nakanishi at pH 7.5.

Both the total adsorption capacity, s_o, and the reaction rate constant k_1 moderately effect the manganese removal profile. Figures 20 and 21 show the effects of changing each of the parameters by a factor of 1.5 above and below the original value. These qualitative sensitivity results show that high accuracy for these two parameters is not essential for modeling of manganese removal by continuous adsorption and oxidation. In addition, an equal percent change in these parameters creates a similar change in the manganese removal pattern. Therefore, one of these parameters does not exert a greater influence on the model than the other.

Large changes in the reaction rate constants k_2 and k_3 negligibly affect the manganese removal profile as seen in Figures 22 and 23. As above, the reaction rates were altered by a factor of 1.5 above and below the initial value. In addition, changes in these parameters affect the manganese removal profile much less than similar percent changes in the total adsorption capacity or the reaction rate constant k_1. Therefore, these parameters can be more roughly estimated than k_1 or s_o.

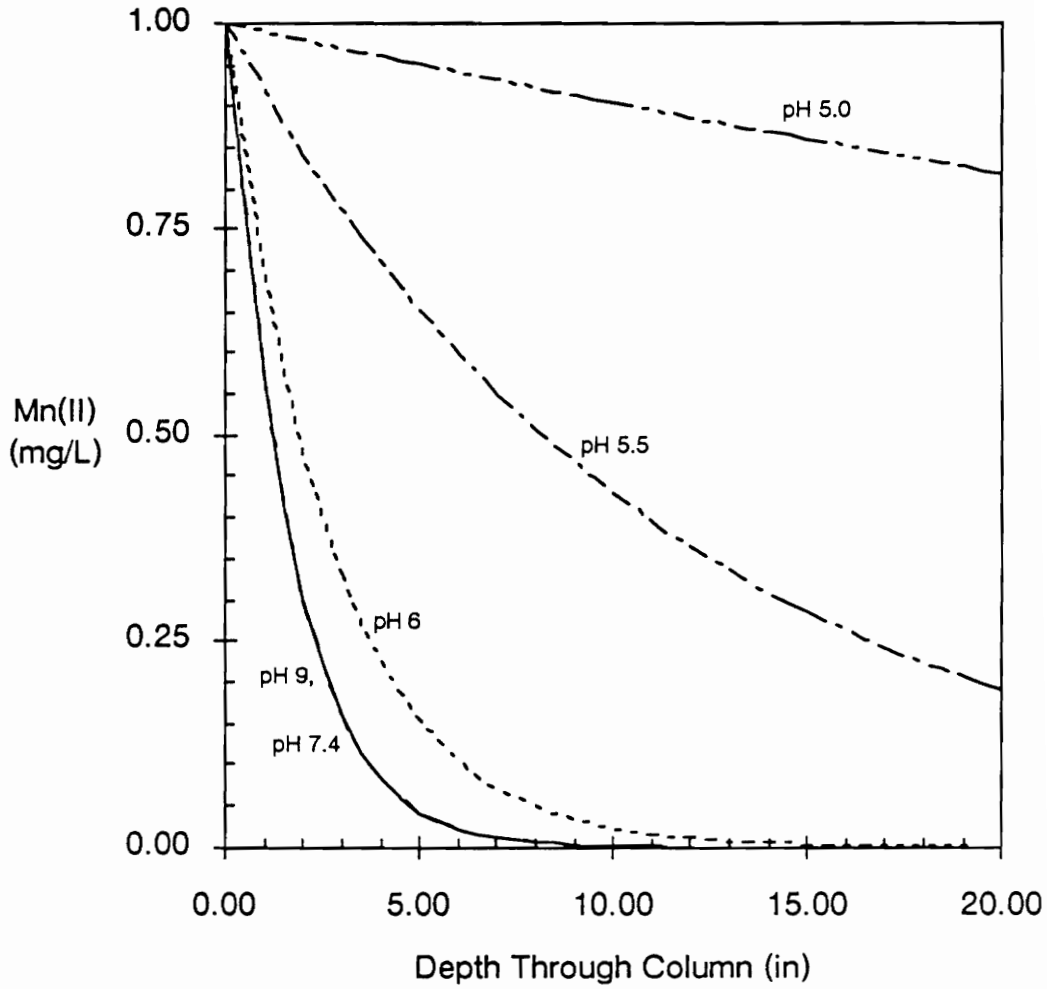

Figure 19. Effect of pH on Theoretical Manganese Removal (HOCl = 10 mg/L, HLR = 3.8 gpm/ft^2, surface oxide coating = 12 mg Mn/g media, total adsorption capacity = 0.09 mol/L-bed)

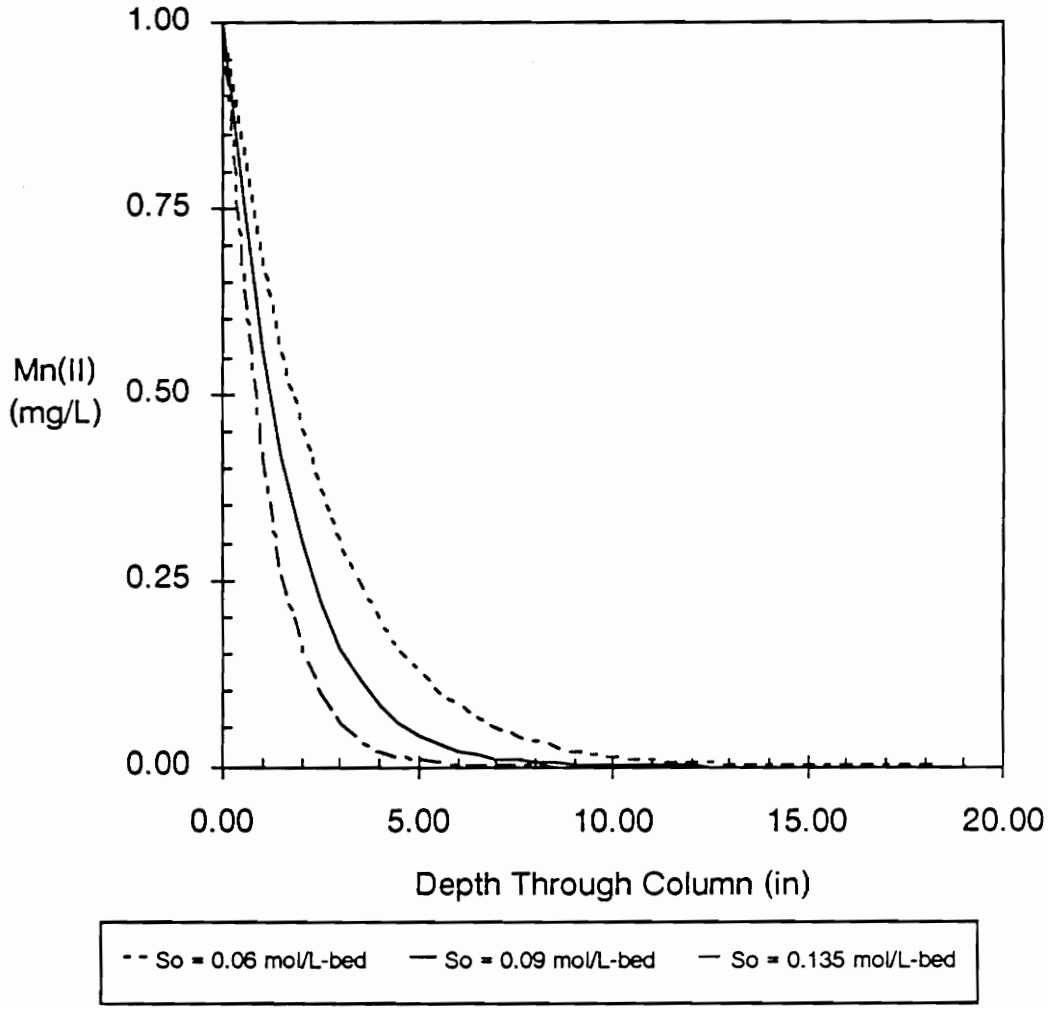

Figure 20. Effect of Total Adsorption Capacity, S_o, on Theoretical Manganese Removal (HOCl = 10 mg/L, influent Mn(II) = 1.0 mg/L, HLR = 3.8 gpm/ft^2)

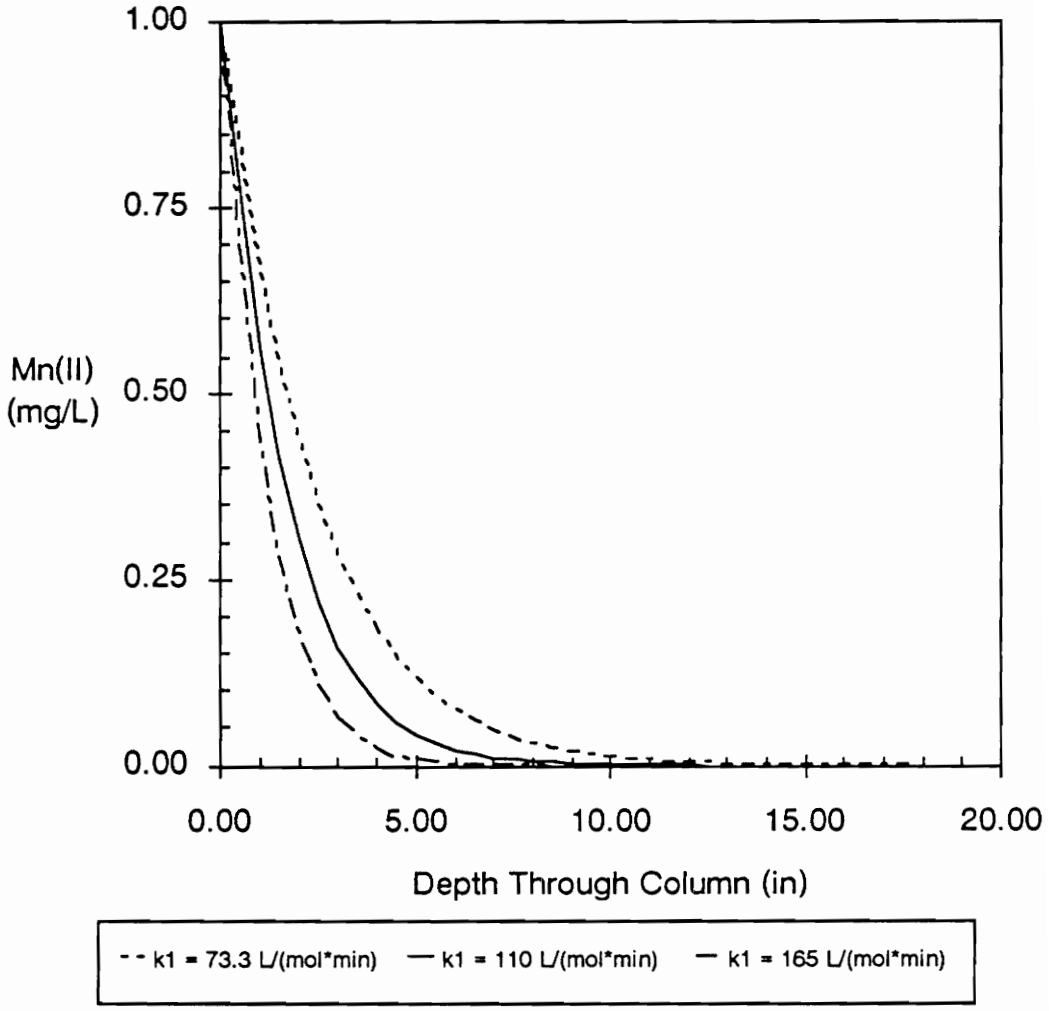

Figure 21. Effect of Reaction Constant k_1 on Theoretical Manganese Removal (HOCl = 10 mg/L, influent Mn(II) = 1.0 mg/L, HLR = 3.8 gpm/ft^2, surface oxide coating = 12 mg Mn/g media, total adsorption capacity = 0.09 mol/L-bed)

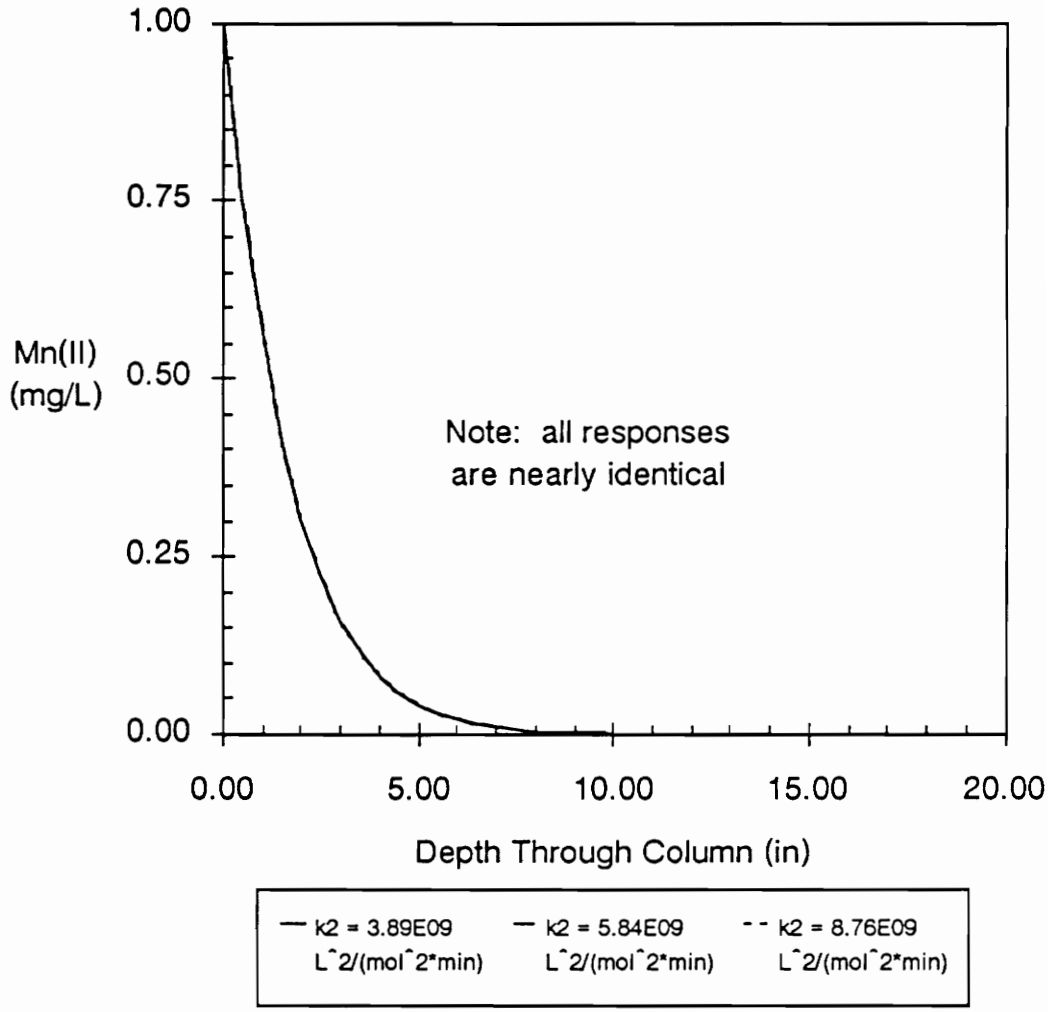

Figure 22. Effect of Reaction Constant k_2 on Theoretical Manganese Removal (HOCl = 10 mg/L, influent Mn(II) = 1.0 mg/L, HLR = 3.8 gpm/ft^2, surface oxide coating = 12 mg Mn/g media, total adsorption capacity = 0.09 mol/L-bed)

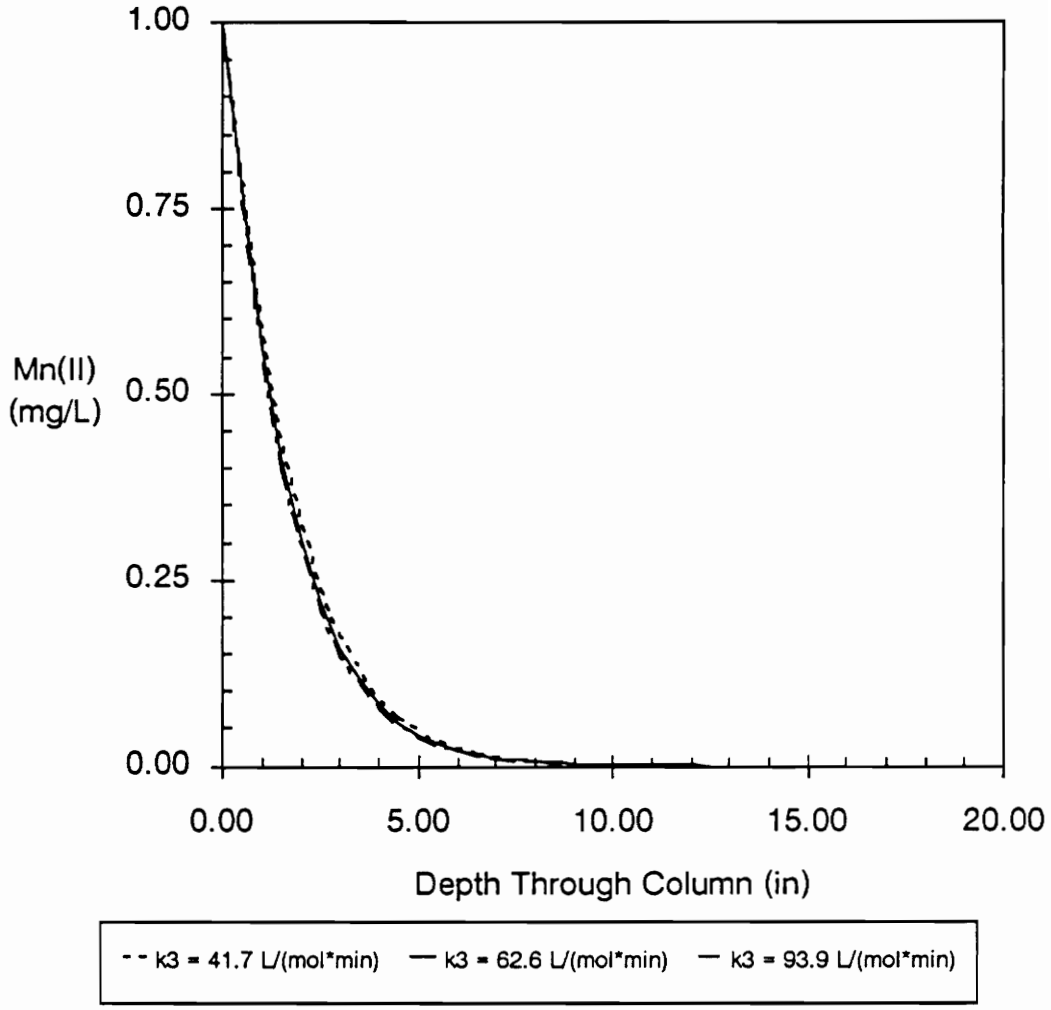

Figure 23. Effect of Reaction Constant k_3 on Theoretical Manganese Removal (HOCl = 10 mg/L, influent Mn(II) = 1.0 mg/L, HLR = 3.8 gpm/ft^2, surface oxide coating = 12 mg Mn/g media, total adsorption capacity = 0.09 mol/L-bed)

Intermittent Regeneration Model

Fewer parameters influence the manganese removal profiles or the manganese breakthrough patterns in the intermittent regeneration model than in the continuous regeneration model. For the intermittent regeneration model, only the parameters k and K affect the profiles. Since more effects are incorporated into the two parameters, a consequence is that the model becomes more sensitive to them.

For each parameter altered, two qualitative sensitivities were investigated: one relatively shallow in the column and one significantly deeper. Since the intermittent regeneration model incorporates a linear isotherm, the manganese wavefront expands through the depth of the filter. Therefore, the effects of a small change in the parameters might become accentuated deeper in the column. Figures 24 - 27 show the effect of changing the parameters k and K by a factor of 1.5 from their initial values. The initial parameter values and operating conditions are shown in Table 7.

Figures 24 and 25 show the effect of changing the parameter k. Changes in this parameter did not greatly alter the manganese breakthrough profile. Also, the effect of the parameter did not significantly change through the depth of the column (from 5.75 inches to 23 inches).

Changes in the parameter K, however, exerted a much greater influence on the intermittent regeneration model. Figures 26 and 27 show the effect of changes in this parameter. At a shallow depth through the filter, the parameter K affected the model moderately more than the parameter k. However, deeper in the filter, the influence was even more marked.

Table 7. Operating conditions and parameters for intermittent regeneration sensitivity model.

Operating Conditions and Parameters	Value
hydraulic loading rate	3.0 gpm/ft^2
porosity	0.42
pH	7.0
Influent Mn(II) conc.	0.5 mg/L
Influent Cl_2 conc.	0.0 mg/L
Depth of each column	5.75 in
Number of columns	4
k	0.0040 min^{-1}
K	800

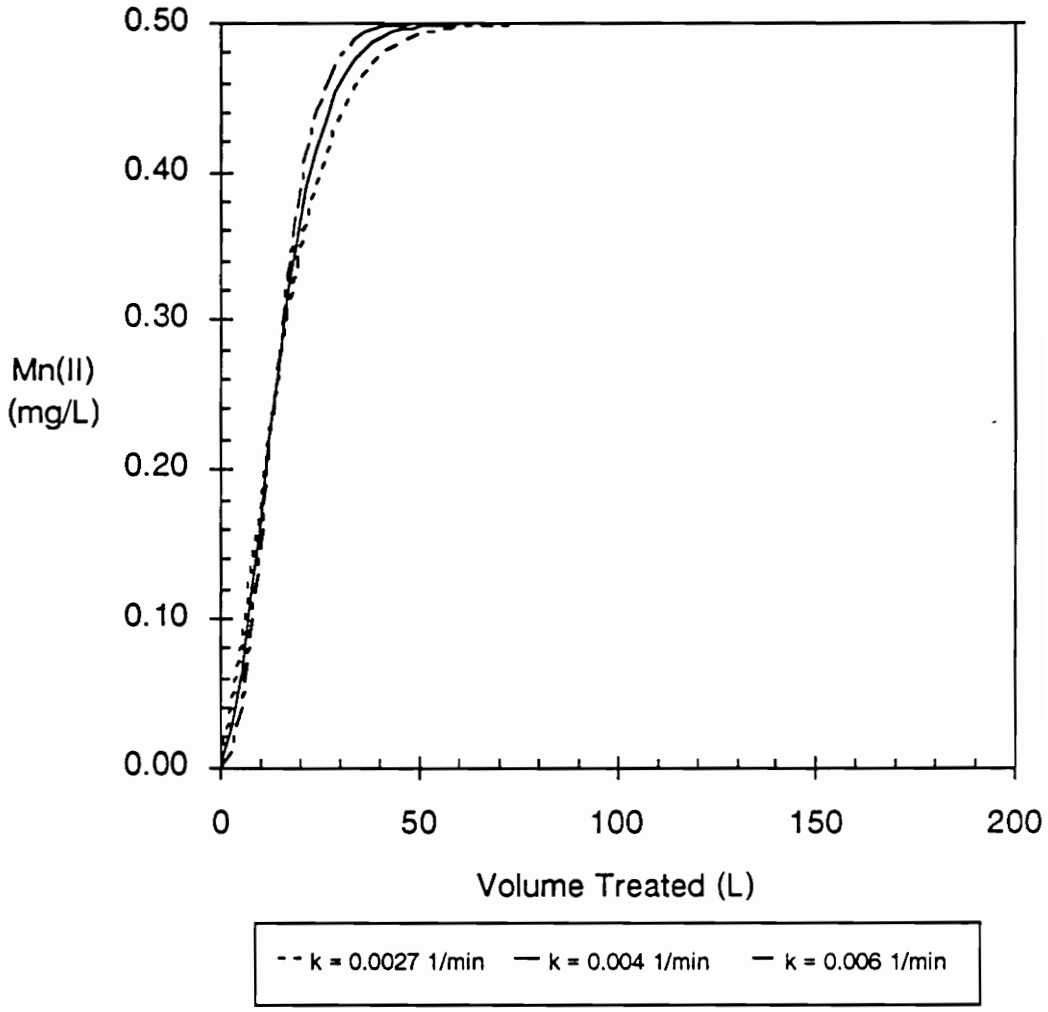

Figure 24. Effect of Reaction Constant k on Theoretical Breakthrough (effluent depth = 5.75", HLR = 3.0 $^{gpm}/_{ft^2}$, influent Mn(II) = 0.5 $^{mg}/_{L}$, pH = 7.0, no chlorine)

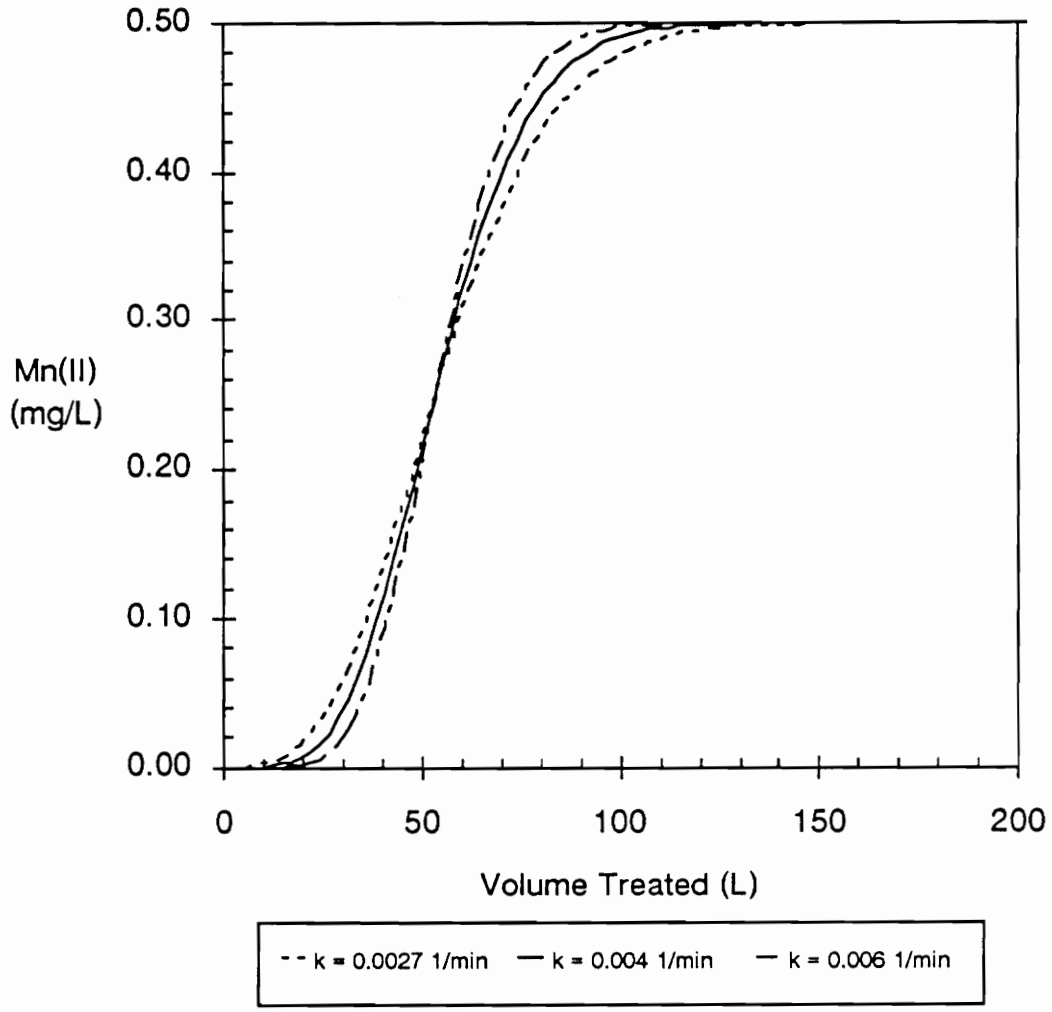

Figure 25. Effect of Reaction Constant k on Theoretical Breakthrough (effluent depth = 23", HLR = 3.0 $^{gpm}/_{ft^2}$, influent Mn(II) = 0.5 $^{mg}/_{L}$, pH = 7.0, no chlorine)

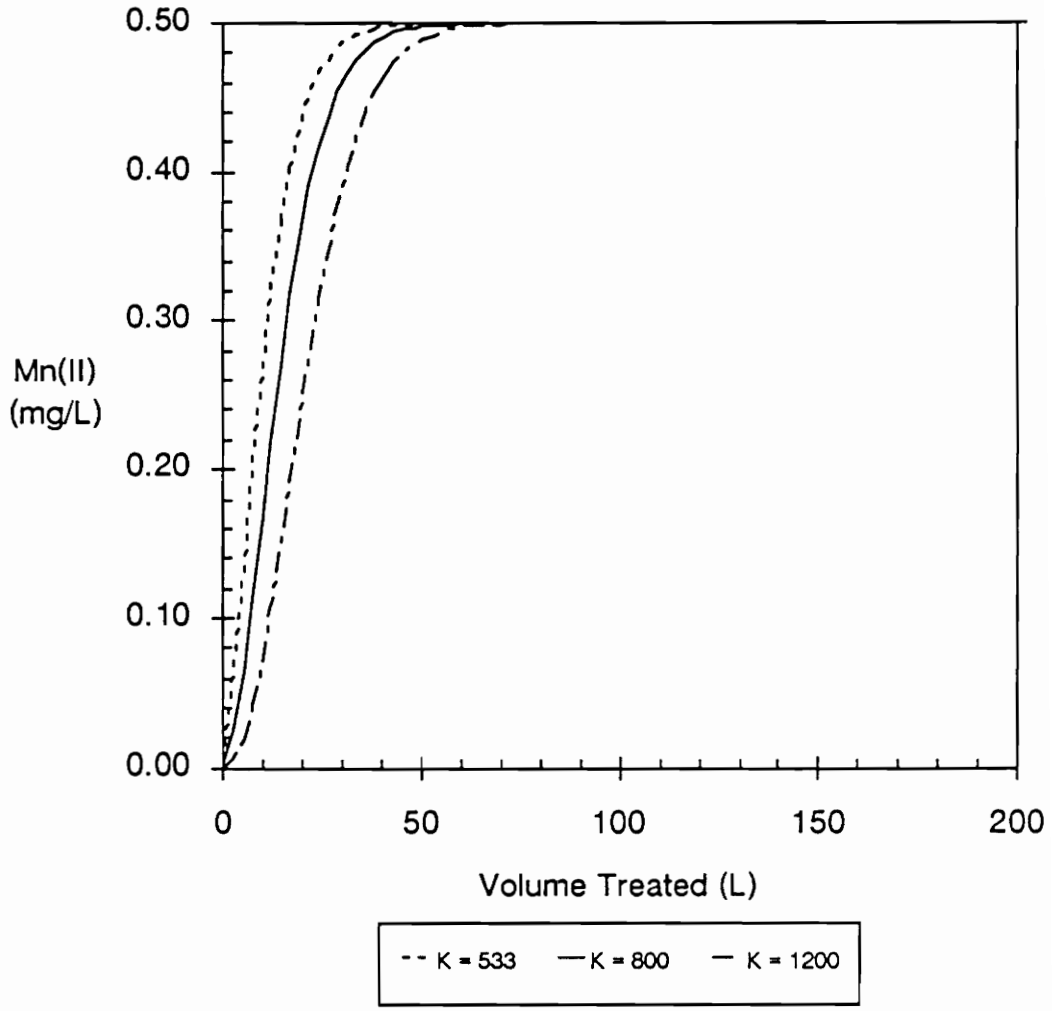

Figure 26. Effect of Reaction Constant K on Theoretical Breakthrough (effluent depth = 5.75", HLR = 3.0 $^{gpm}/_{ft^2}$, influent Mn(II) = 0.5 $^{mg}/_{L}$, pH = 7.0, no chlorine)

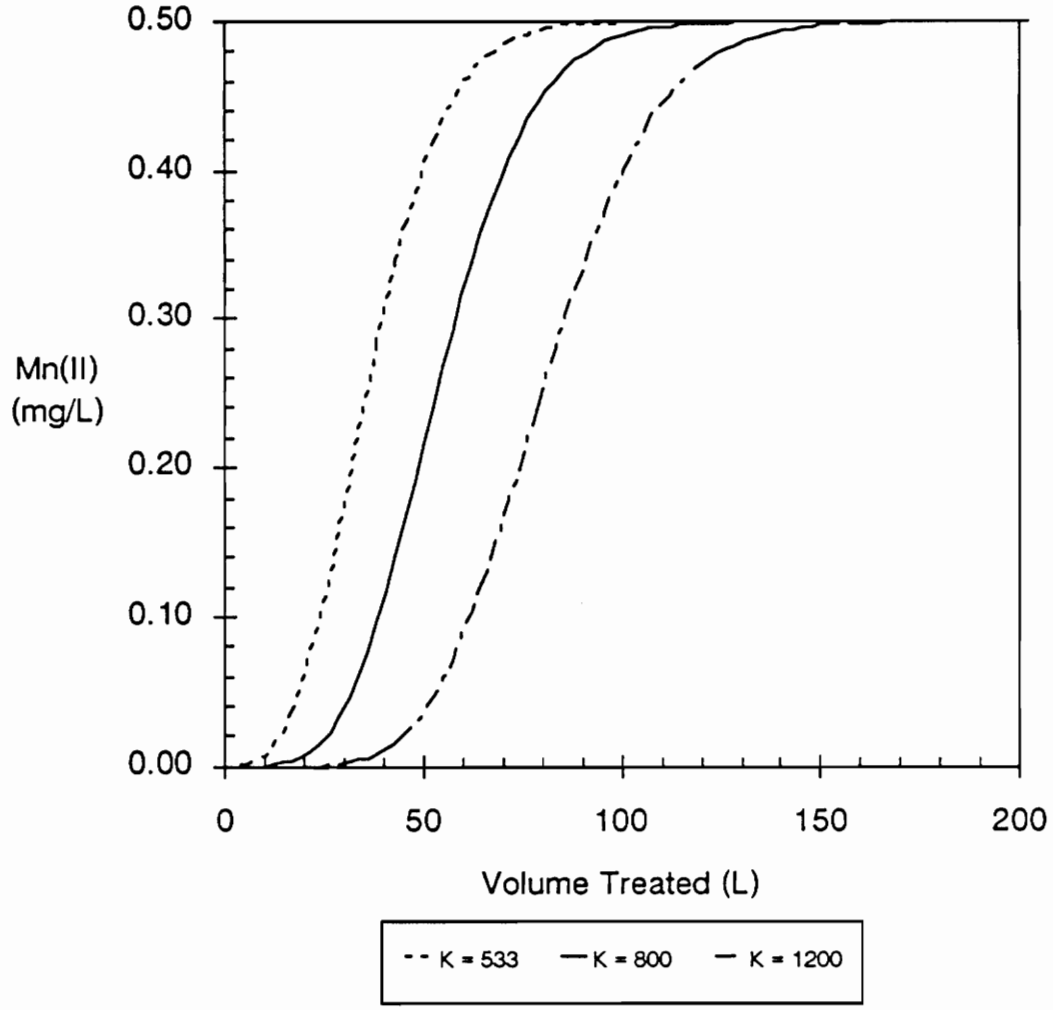

Figure 27. Effect of Reaction Constant K on Theoretical Breakthrough (effluent depth = 23", HLR = 3.0 $^{gpm/ft^2}$, influent Mn(II) = 0.5 $^{mg/L}$, pH = 7.0, no chlorine)

Model Parameter Estimation

The next task in the modeling process, after a sensitivity analysis, was parameter estimation. Because of the theoretical basis for the continuous regeneration model, it should contain parameters applicable to many waters. In contrast, the intermittent regeneration parameters must be determined for each specific raw water. This results from the incorporation of pH effects into the parameters k and K.

Continuous Regeneration Model Parameter Estimation

Nakanishi determined the parameters k_1, k_2, and k_3 for the continuous regeneration model using a least-squares parameter estimation technique. However, Nakanishi expressed some doubt regarding the accuracy of his parameters. One particular concern with Nakanishi's parameters resulted from the limited range of experimental conditions to calculate the values.

In addition to this concern, the sensitivity analysis demonstrated that the parameter k_1 exerts a moderate effect on the manganese removal profile, but the parameters k_2 and k_3 exert only a minimal effect. For this reason, the results of independent research were used to validate the parameter k_1, and Nakanishi's predictions of k_2 and k_3 remained uncontested.

Two different sources were used to evaluate the parameter k_1. The first source was from results presented by Pankow and Morgan (1981). Pankow and Morgan modeled autocatalytic oxidation of manganese from solution using oxygen. The reaction proposed earlier by Morgan (1964) was

$$\frac{d[Mn^{2+}]}{dt} = -k_2 [Mn^{2+}] - k_3 [Mn^{2+}] [MnO_x] \qquad (24)$$

where the second term represents soluble manganese removal from solution through adsorption onto precipitated manganese oxides. Therefore, the term k_3 physically represents the same parameter as Nakanishi's k_1 (Eq. 5). Sung (1980) reexamined the data obtained by Morgan (1964) at a pH of 9.5 and a partial pressure of oxygen of 1.0 atm. His analysis, as summarized by Pankow and Morgan, suggested a value for k_3 of 260 M^{-1} min^{-1}. This value was more than twice that estimated by Nakanishi of 110 M^{-1} min^{-1}.

A second independent estimate of the parameter was needed then to resolve this discrepancy. Hungate (1988) conducted kinetic studies to describe the sorption of soluble manganese on an $MnO_{x(s)}$ surface during filtration. From five experiments at varying influent soluble manganese concentrations, he determined uptake rate constants. Table 8 shows the results of these kinetic experiments. Hungate then assumed first-order kinetics according to the following model:

$$[Mn^{2+}]_t = [Mn^{2+}]_o e^{-kt} \qquad (18)$$

where

$[Mn^{2+}]_t$ = effluent manganese concentration ($^{mg}/_{L}$) at time t

$[Mn^{2+}]_o$ = influent manganese concentration ($^{mg}/_{L}$)

k = uptake rate constant, (min^{-1})

t = solution detention time in column (min)

The uptake rate constants determined at various influent manganese concentrations were then averaged to obtain one reaction rate, k, equal to 4.9 min^{-1}. The experiments were performed at pH 7.1, with a surface oxide coating on the media of 3.90 $^{mg\ Mn}/_{g\ media}$.

Table 8. Uptake Rate Constants Determined at Various Influent Manganese Concentrations (pH = 7.1, Surface Oxide Coating = 3.9 $^{mg\ Mn}/_{g\ media}$), from Hungate (1988)

Influent Mn ($^{mg}/_{L}$)	Residence Time of Solution in Column (min)	Effluent Mn ($^{mg}/_{L}$)	Uptake Rate Constant, k (min^{-1})
0.20	0.05 0.08 0.09 0.10 0.11 0.14 0.22 0.22	0.19 0.18 0.16 0.15 0.15 0.12 0.10 0.08	4.8
0.30	0.12 0.18 0.22 0.23 0.25 0.33 0.52	0.19 0.18 0.16 0.15 0.15 0.12 0.10	4.8
0.45	0.11 0.15 0.18 0.19 0.21 0.47	0.31 0.28 0.21 0.19 0.19 0.10	4.1
0.80	0.09 0.12 0.17 0.19 0.24 0.32	0.59 0.50 0.28 0.31 0.21 0.13	5.7
1.20	0.08 0.11 0.18 0.19 0.23 0.26 0.63	0.90 0.84 0.41 0.43 0.39 0.38 0.09	5.0

Hungate's model contains subtle differences from the models proposed by Nakanishi and Morgan. For Hungate's model, he essentially incorporated the oxide coating concentration into the parameter k. Therefore, Hungate's model could be rewritten as

$$[Mn^{2+}]_t = [Mn^{2+}]_o \, e^{-k_1 s_o t}$$

where k from Hungate is equivalent to $(k_1)(s_o)$ from Nakanishi or $(k_3)(MnO_{x(s)})$ from Morgan.

Hungate's surface oxide coating extraction can be reformulated as a total adsorption capacity through the following conversion:

$$s_o = [\,3.9 \tfrac{\text{mg Mn}}{\text{g media}}]\,[\,840 \tfrac{\text{g media}}{\text{L media}}]\,[\tfrac{\text{1 mol Mn}}{\text{54.94 g Mn}}]\,[\tfrac{\text{1 g}}{\text{1000 mg}}] = 0.060 \tfrac{\text{mol Mn}}{\text{L media}}$$

This amount of oxide coating then can adsorb, according to Morgan (1964), approximately 0.35 mol of soluble Mn per mol of oxide surface at pH 7.1. This corresponds to a total adsorption capacity of 0.021 $^{\text{mol Mn(II) sorbed}}/_{\text{L media}}$.

Finally, a parameter comparable to Nakanishi and Morgan is calculated by

$$k_1 = \frac{k}{s_o} = \frac{4.9 \text{ min}^{-1}}{0.021 \frac{\text{mol}}{\text{L}}} = 230 \text{ M}^{-1} \text{ min}^{-1}$$

Table 9 presents the results of the parameter estimation from the three sources. Since the parameters obtained independently from Hungate (1988) and from Pankow and Morgan (1981) are very similar, an average of these two values was used as the parameter for operating the model and Nakanishi's estimate was discarded. Also, since nearly the same parameter was obtained using experiments at different pH conditions (pH 9.5 versus pH 7.1), it was assumed that pH does not effect the reaction rate constants k_1, k_2, and k_3.

Table 9. Comparison of Reaction Rate Constants for Soluble Manganese Sorption onto Oxide-Coatings.

Source for k_1	Magnitude (M^{-1} min^{-1})
Nakanishi (1967)	110
Pankow and Morgan (1981)	260
Hungate (1988)	230

Intermittent Regeneration Model Parameter Estimation

The parameter estimation for the intermittent regeneration model was more straightforward than the parameter estimation for the continuous regeneration model. However, since the parameters incorporate more of the raw water characteristics, a separate estimation is required for different pH conditions. Because there are only two parameters and the model is fairly sensitive to both of them, the parameter estimation lends itself easily to a method of trial and error.

A trial and error parameter estimation is essentially a manual curve-fitting exercise. For the parameter estimation, data from an experiment by Hungate (1988) was utilized. Hungate operated four small 5.75 inch long columns in series. Soluble manganese concentrations were monitored at the effluent of each column to determine the breakthrough profile. Using the operating conditions of the experiment, the parameters k and K could then be manually adjusted until the model breakthrough profile closely fit the experimental results. Results from the sensitivity analysis indicated that the parameter K impacts the manganese profile more than the parameter k; this provides qualitative information on relative changes in the parameters needed.

Important to the utility of the model, the parameters were determined only using the first column breakthrough profile. Therefore, the effluent manganese profile for the remaining three columns in series could be used as a verification of the model. Figure 28 shows the breakthrough profile and modeled response for the effluent from the first column at a depth of 5.75 inches. Table 10 shows the parameters obtained and operating conditions for this experiment.

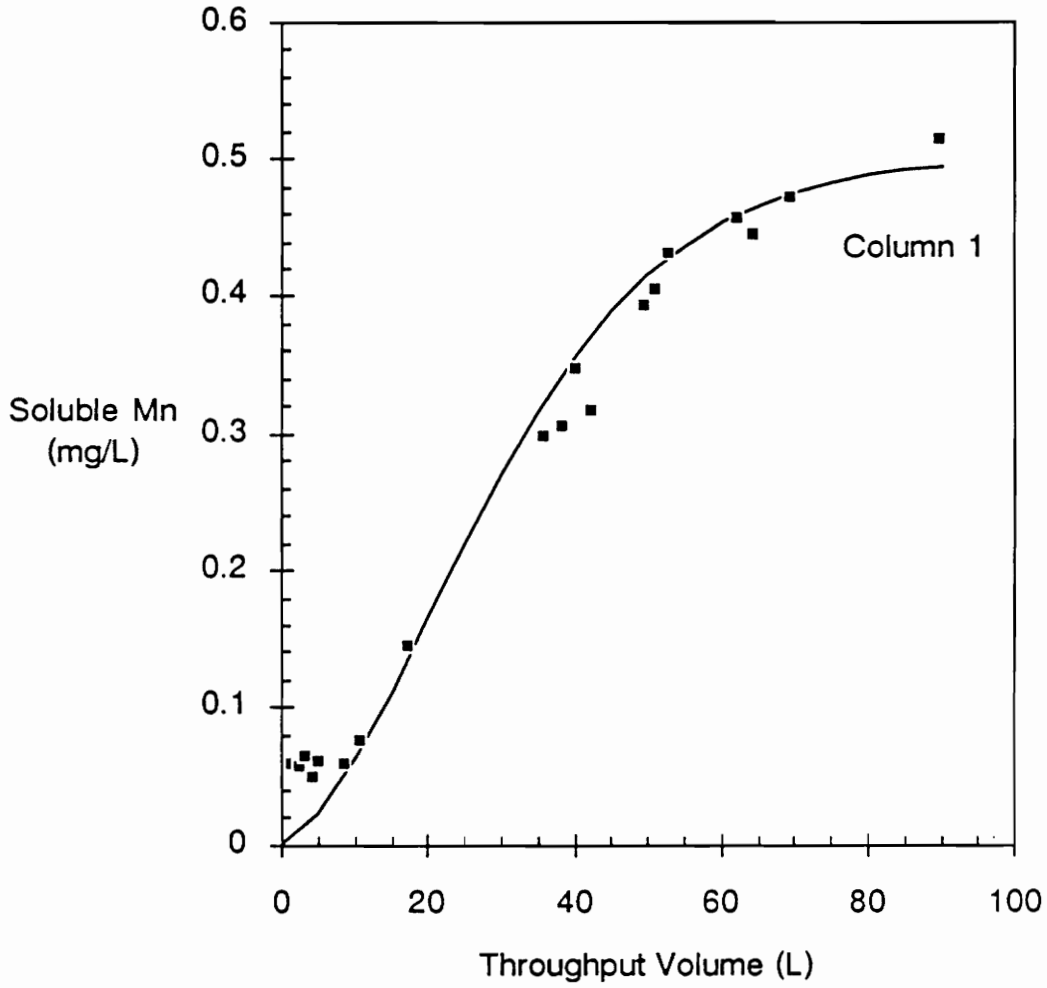

Figure 28. Breakthrough Profile and Modeled Effluent for Parameter Estimation of Intermittent Regeneration Model (effluent depth = 5.75", HLR = 3.0 $^{gpm}/_{ft^2}$, influent Mn(II) = 0.5 $^{mg}/_{L}$, pH = 7.0, no chlorine; experimental data from Hungate (1988))

Table 10. Estimated Parameters and Operating Conditions for Intermittent Regeneration Model

Operating Conditions and Parameters	Value
PARAMETERS	
k	0.0040 min^{-1}
K	800
OPERATING CONDITIONS	
hydraulic loading rate	3.0 gpm/ft^2
porosity	0.42
pH	7.0
Influent Mn(II) conc.	0.5 mg/L
Influent Cl_2 conc.	0.0 mg/L
Depth of column	5.75 in

CHAPTER 6
DISCUSSION

This chapter presents a discussion of the pilot-plant experimental results and applications of the two manganese removal models. The pilot-plant results are discussed in two major sections: (1) an evaluation of the filter media configurations when operated in the standard mode adding both chlorine and permanganate; and, (2) an evaluation of combined adsorption/oxidation as a treatment method for Columbus City Utilities. The modeling results are also subdivided into two major categories, one addressing the continuous regeneration model and the other addressing the intermittent regeneration model.

Filter Media Configurations

Two primary characteristics were investigated to evaluate the filter media configurations: (1) effluent quality with respect to total and soluble iron and manganese and (2) the rate of head loss buildup. Secondary characteristics included filter backwashing and clean bed head loss.

Head Loss and Metals Breakthrough

The breakthrough patterns shown in Figures 9 and 10 indicate that the anthracite-greensand filter and the anthracite-sand-garnet filters treated more water before metals breakthrough than the other filters. However, head loss increased more quickly in the anthracite-greensand filter than in any other configuration tested. Figure 11 shows this effect. Using linear regression, the

head loss accumulation rate was determined. Filter I, the uncoated, anthracite-sand filter, had a rate of 5.1 inches of head loss accumulated per 100 gallons of water treated. Filter II, the anthracite-greensand filter, had a rate of 7.4 inches of head loss accumulated per 100 gallons of water treated, an increase of forty-five percent. In contrast to the anthracite-greensand filter, the tri-media filter developed significantly less head loss. Metals breakthrough, however, occurred after similar volumes of water were treated.

Since the physical configuration of Columbus City Utilities Water Plant No. 1 was head loss limited, the use of greensand could shorten the filter operation times. The limited operation would not result from iron or manganese breakthrough but from the amount of head loss generated. In summary, the greensand filter can treat a larger volume of water before breakthrough; however, the filter operation time might be limited by the head available at the plant and not by solids breakthrough.

Clean Bed Head Loss

The clean bed head loss results (Figure 12) show that Filter II exhibited a much higher head loss due to frictional losses within the filter. This result was expected, as greensand has a smaller effective size than anthracite or sand.

Impact of Oxidants Used

When chlorine and $KMnO_4$ are added in sufficient amounts to completely oxidize the iron and manganese in the groundwater, iron and manganese removal becomes a suspended solids collection problem and not a metal ion oxidation problem. Thus, the removal of the iron and manganese requires only

the removal of turbidity or suspended solids created by the oxidation. Figure 29 shows this result. At the effluent of the reaction chamber (a chemical reaction time of between 2.8 and 11 minutes depending on the total flow rate), an average of 97 percent of the iron and 74 percent of the manganese was oxidized. In addition to the above results, Knocke, *et al.* (1990) showed that, at pH 7.0 - 7.3, rapid Fe^{2+} oxidation by HOCl (less than three seconds) and Mn^{2+} by $KMnO_4$ (less than ten seconds) occurred.

Figure 29 shows another effect of using $KMnO_4$ to oxidize manganese. For every 1.0 mg of $KMnO_4$ added to the raw water, 0.55 mg of $MnO_2(s)$ are formed and must be removed by the filter. These solids result entirely from permanganate reduction, not soluble manganese oxidation. For the Columbus raw water with a reduced manganese concentration of approximately 0.25 mg/L and a reduced iron concentration of approximately 1.7 mg/L, the solids addition from permanganate contributes a relatively small portion. However, even this small amount can impact the head loss accumulation in a filter. Figure 30 shows how the addition of permanganate increased the total head loss through the filter. Figure 31 shows that solids breakthrough occurred earlier when both permanganate and chlorine were added than when chlorine alone was added. If the raw water contained a greater amount of soluble manganese, the comparison between adding HOCl only and adding both oxidants would be more dramatic.

Combined Adsorption/Oxidation

Three topics were investigated to determine the suitability of manganese removal by combined adsorption/oxidation onto surface oxide-coated media.

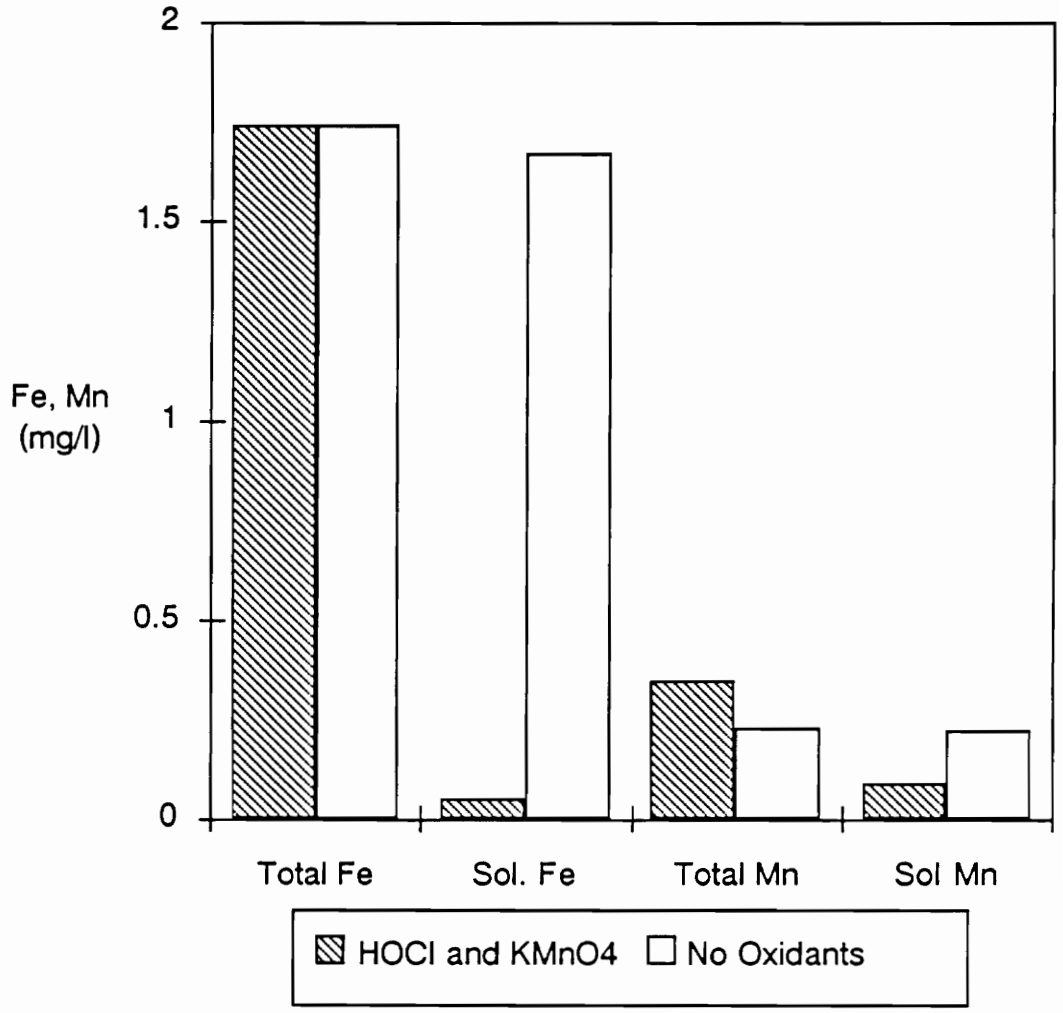

Figure 29. Oxidation of Iron and Manganese in the Baffled Reaction Chamber

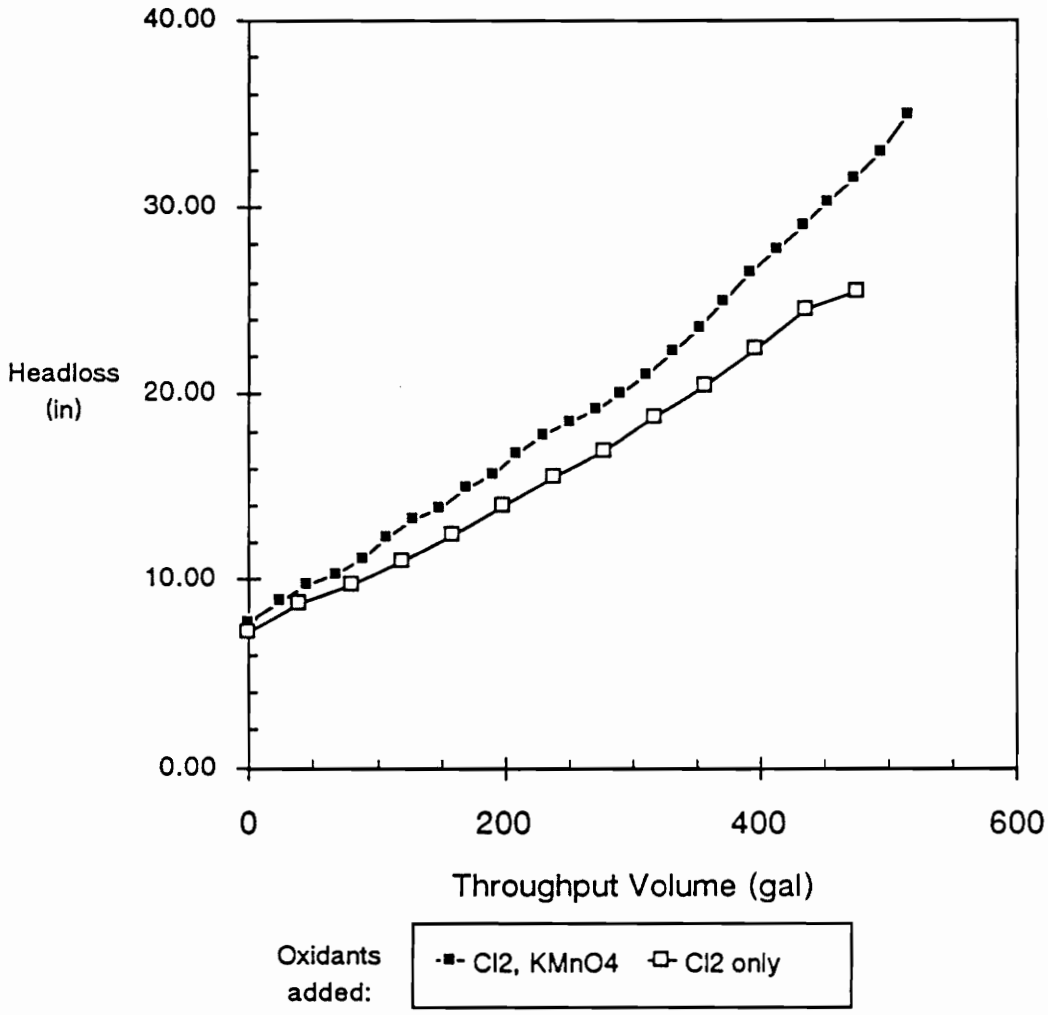

Figure 30. Impact of Permanganate Addition on Head Loss Accumulation (Filter I (anthracite-sand), HLR = 4 gpm/ft^2, HOCl = 3.0 mg/L, KMnO4 = 0.5 mg/L)

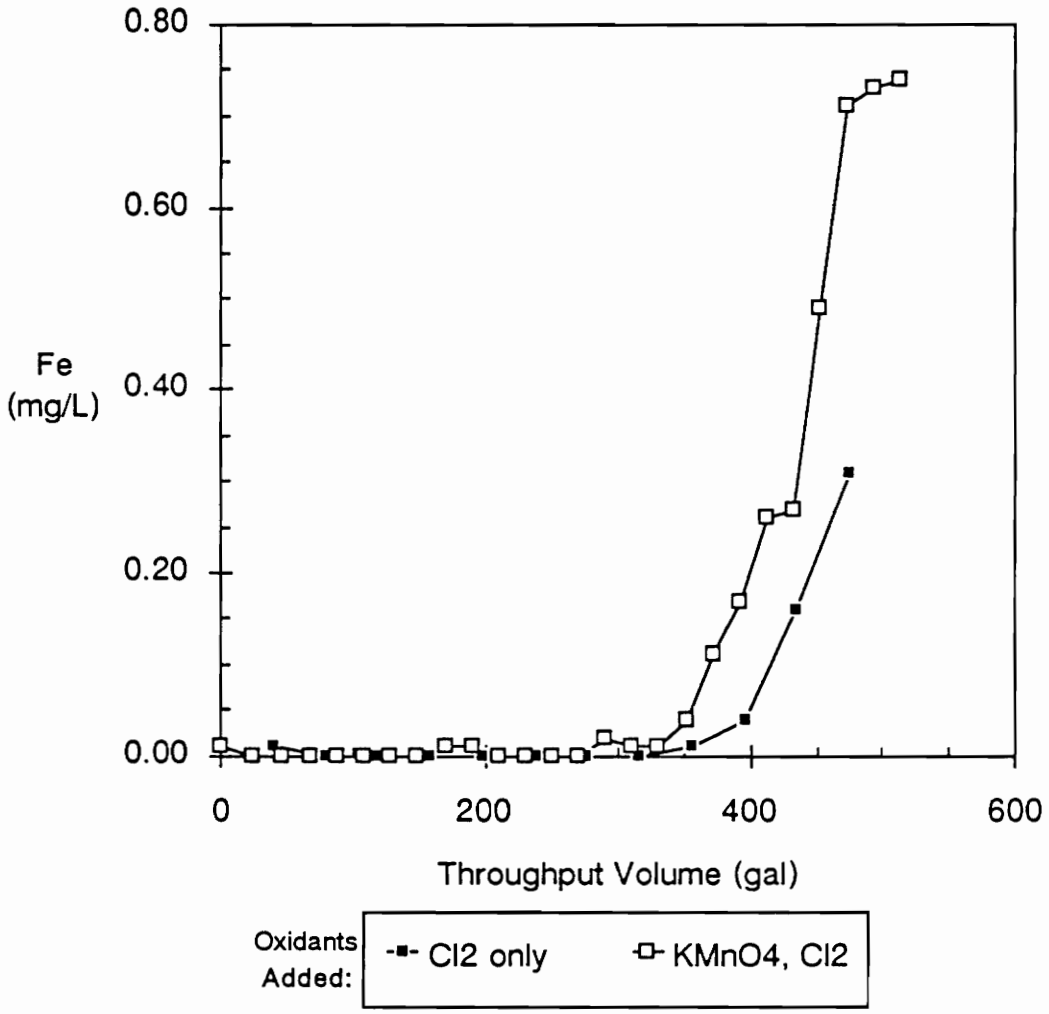

Figure 31. Impact of Permanganate Addition on Iron Breakthrough (Filter I (anthracite-sand), HLR = 4 $^{gpm/ft^2}$, HOCl = 3.0 $^{mg/L}$, KMnO4 = 0.5 $^{mg/L}$)

These topics were (1) amount of media surface oxide coatings present, (2) removal of Mn^{2+} in the absence of an applied oxidant, and (3) effects of chlorine addition on Mn^{2+} removal. A secondary purpose was to determine the effectiveness of pre-coated media versus naturally-occurring, oxide-coated media for soluble Mn removal.

Media Surface Oxide Coatings

Very little surface oxide was present on either the sample from Filter III (tri-media filter) or on the pre-coated media. The media from Water Plant No. 2 had an oxide coating more than five times greater than the extractable coating on greensand and several hundred times greater than the extractable coating on the pre-coated anthracite. This oxide coating probably accounted for a portion of the manganese removal currently being realized at Plant No. 2 and possibly at Plant No. 1. In addition, the oxide coating also acts as an oxidation "buffer" for permanganate. For example, if too much permanganate is added to the raw water, the surface coating on the media will be oxidized and no permanganate laden water (purple water) will enter the distribution system. Conversely, if too little permanganate is added for soluble manganese oxidation, the remaining soluble portion will be adsorbed by the filter media.

Removal of Mn^{2+} in the Absence of an Applied Oxidant

Filters II (anthracite-greensand), IV (precoated anthracite-sand), and V (Water Plant #2 anthracite-sand) were tested for their ability to remove soluble manganese from solution without oxidant addition. Media with very small amounts of surface oxide present (e.g., the anthracite in Filter II) exhibited a

significant degree of Mn^{2+} removal capacity. Secondly, media with more surface oxide exhibited even greater Mn^{2+} removal capacity.

Figures 13 - 15 demonstrate the highly variable adsorption capacity of different media. The naturally oxide coated media removed many times more soluble manganese than either of the other filters. In addition, these results showed that both the filters containing anthracite-greensand and Water Plant No. 2 media possessed significantly greater manganese removal capacity than the pre-coated filter media. The amount of oxide coating on the filter media, when operated in the intermittent regeneration mode without the use of an oxidant in the unfiltered water, greatly impacted the amount of soluble manganese removed. The amount of soluble manganese removed was related to the total number of $MnO_{x(s)}$ adsorption sites present. These sites were not regenerated without the addition of an oxidant; eventually all became occupied with Mn(II), and the filter Mn removal capacity was exhausted.

Effect of Oxidant Addition on Mn^{2+} Removal

Data presented in Figure 16 showed that in the anthracite-greensand filter, essentially all the manganese was removed in the anthracite layer. Ninety-six percent of the manganese was removed in the anthracite layer (upper eighteen inches) with only four percent removed in the greensand layer (remaining twelve inches). Therefore, when the filter was operated in the adsorption/oxidation mode, even in the presence of minimal oxide coating, greensand was not necessary for effective soluble manganese removal.

Samples taken over a 29-hour period indicated that the removal profiles remained nearly constant and that a steady-state adsorption/oxidation reaction

was established in the upper depths of the filter. Therefore, it is hypothesized that this experiment could have continued indefinitely with the same manganese and chlorine loadings and not have yielded significant manganese breakthrough.

In contrast to the previous column exhaustion experiments, the amount of surface oxide coating had only a minimal effect on the adsorption/oxidation profile. This demonstrates that the operation of columns in a continuous regeneration mode would efficiently remove manganese even in the presence of a very small amount of oxide coating. Evidently, in the operation of the columns in the continuous regeneration mode, the number of available sites for adsorption and oxidation reached a limiting value based on the surface area of the media. Nakanishi (1967) also noticed this effect and showed that the total adsorption capacity did not increase linearly with a corresponding increase in the media surface $MnO_{2(s)}$ coating concentration.

Modeling

Continuous Regeneration Model

To evaluate this model, a Mn(II) removal profile from Columbus pilot-plant data was compared to predictions from Nakanishi's model. Filter V, containing Water Plant No. 2 media with an oxide coating of 16 $^{mg\ Mn}/_{g\ media}$, was used for the comparison. Table 11 shows the operating conditions and parameters used in the model. Figure 32 shows the predicted and experimental results. A reasonable agreement between predicted removal and experiment was obtained. Figure 33 shows the effect of uncertainties in the parameter k_1 on the model. Variation of k_1 by as much as 50 percent did not

Table 11. Operating conditions and parameters for continuous regeneration model validation.

Operating Conditions and Parameters	Value
hydraulic loading rate	4.0 gpm/ft^2
surface oxide coating	16 mg Mn/g media
Mn(II) adsortion capacity	0.086 mol/L-bed
porosity	0.42
pH	7.4
Influent Mn(II) conc.	1.0 mg/L
Influent Cl_2 conc.	2.0 mg/L
k_1	245 L/(mol*min)
k_2	5.84E9 $L^2/(mol^2*min)$
k_3	62.6 L/(mol*min)

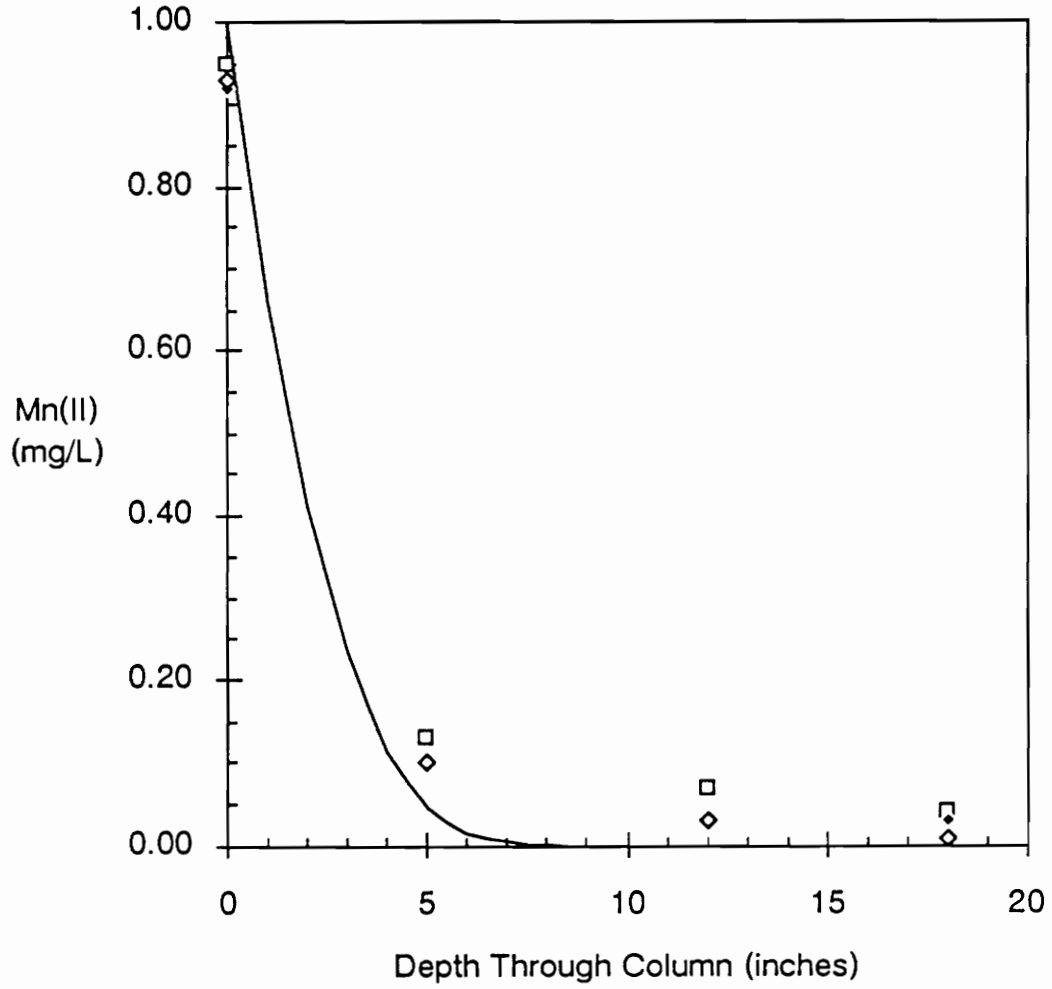

Figure 32. Comparison of Theoretical and Experimental Data for Filter V (Water Plant #2 anthracite-sand) (HLR = 4.0 $^{gpm}/_{ft^2}$, total adsorption capacity = 0.086 $^{mol}/_{L}$-bed, influent Mn(II) = 1.0 $^{mg}/_{L}$, HOCl = 1.5 $^{mg}/_{L}$)

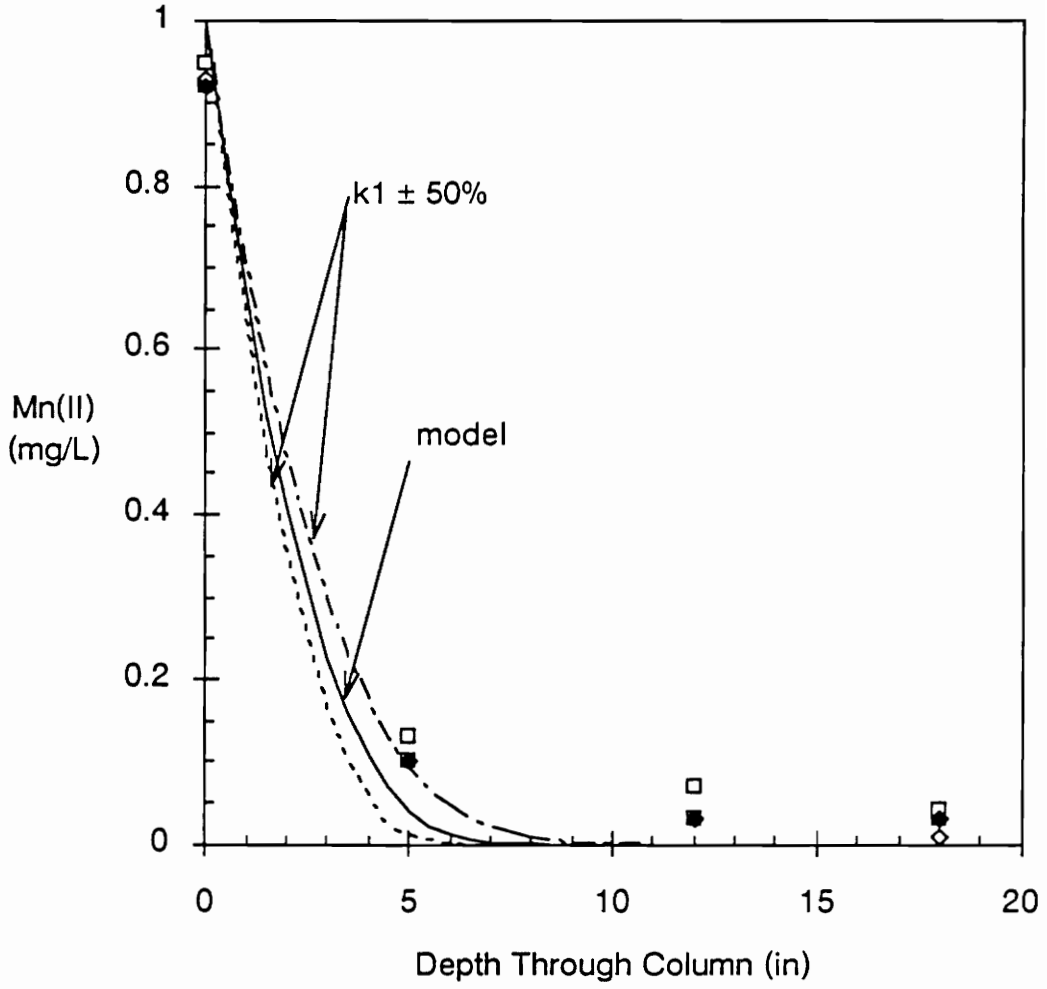

Figure 33. Effect of Uncertainty of k1 on Model Results for Filter V (Water Plant #2 anthracite-sand) (HLR = 4.0 $^{gpm}/_{ft^2}$, total adsorption capacity = 0/086 ^{mol}/L-bed volume, influent Mn(II) = 1.0 ^{mg}/L, HOCl = 1.5 ^{mg}/L, k1 = 245 L/(mol*min))

greatly change the model predictions. This experiment provided only limited experimental validation of the model; therefore, results from Occiano (1988) were also used as a validation step.

Three of Occiano's experiments were used to compare with model predictions. The operating conditions for the experiments are shown in Table 12. The only difference between these experiments was that the filter applied water pH was adjusted to 6.0-6.2, 7.8, or 8.8. The parameters were obtained from the parameter estimation in Chapter 5. The surface oxide coating, in Occiano's data, was expressed as $^{mg\ Mn}/_{g\ media}$. This value was first converted to moles of $MnO_{x(s)}$ present per liter of media as derived in Chapter 5. Using Figure 1 and the pH defined by Nakanishi (pH 7.5), the total adsorption capacity could then be expressed as the moles of Mn(II) sorbed per liter of media.

Figures 34 through 36 show the results obtained by Occiano for the continuous regeneration experiments at different pH. The manganese concentrations predicted by the model are overlaid on the figures also. Note that the removal for pH 7.8 and 8.8 was very similar. The model predicted this response because at pH 7 and above, the model remained insensitive to changes in pH. However, the higher effluent Mn(II) concentration obtained at pH 6-6.2 was also well predicted by the model. This agreement provides more evidence that pH effects are acceptably incorporated into the Nakanishi model, and that the reaction rate constants k_1, k_2, and k_3 are not strong functions of pH.

Figure 37 shows the predicted effect of changing the influent chlorine concentration. There exists a minimum amount of chlorine which can be added before steady state no longer exists. Alternately, as the chlorine concentration

Table 12. Operating conditions and parameters for continuous regeneration model comparison to data from Occiano (1988)

Operating Conditions and Parameters	Value
hydraulic loading rate	2.5 gpm/ft^2
surface oxide coating	4 mg Mn/g media
Mn(II) adsortion capacity	0.031 mol/L-bed
porosity	0.42
pH	6.0, 7.8, 8.8
Influent Mn(II) conc.	1.0 mg/L
Influent Cl_2 conc.	2.0 mg/L as HOCl
effluent depth	6.5 inches
k_1	245 L/(mol*min)
k_2	5.84E9 $L^2/(mol^2*min)$
k_3	62.6 L/(mol*min)

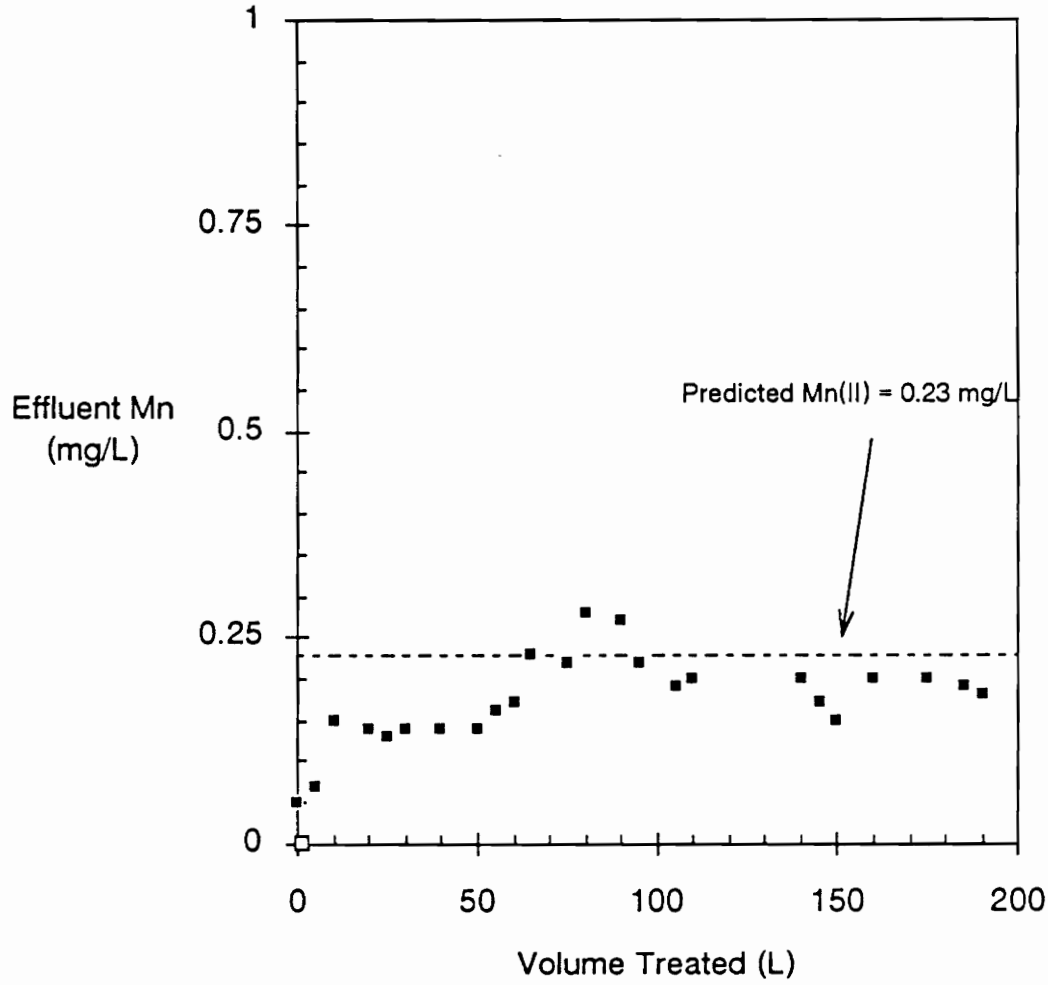

Figure 34. Predicted and Experimental Mn(II) Uptake at pH 6-6.2 (influent Mn(II) = 1.0 mg/L, HOCl = 2.0 mg/L, HLR = 2.5 gpm/ft^2, pH = 6.2, total adsorption capacity = 0.031 mol/L-bed, effluent depth = 6.5"; experimental data from Occiano (1988))

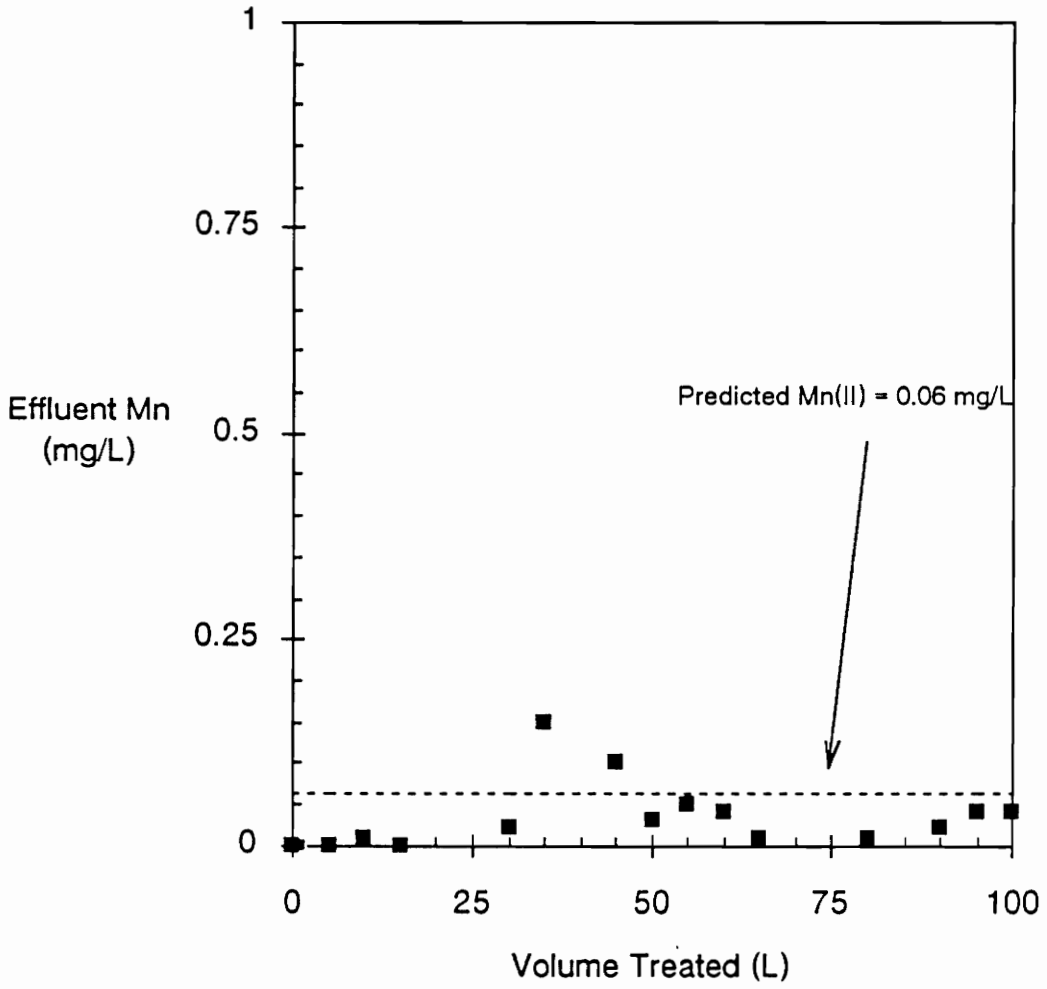

Figure 35. Predicted and Experimental Mn(II) Uptake at pH 7.8 (influent Mn(II) = 1.0 mg/L, HOCl = 2.0 mg/L, HLR = 2.5 gpm/ft^2, pH = 7.8, total adsorption capacity = 0.031 mol/L-bed, effluent depth = 6.5"; experimental data from Occiano (1988))

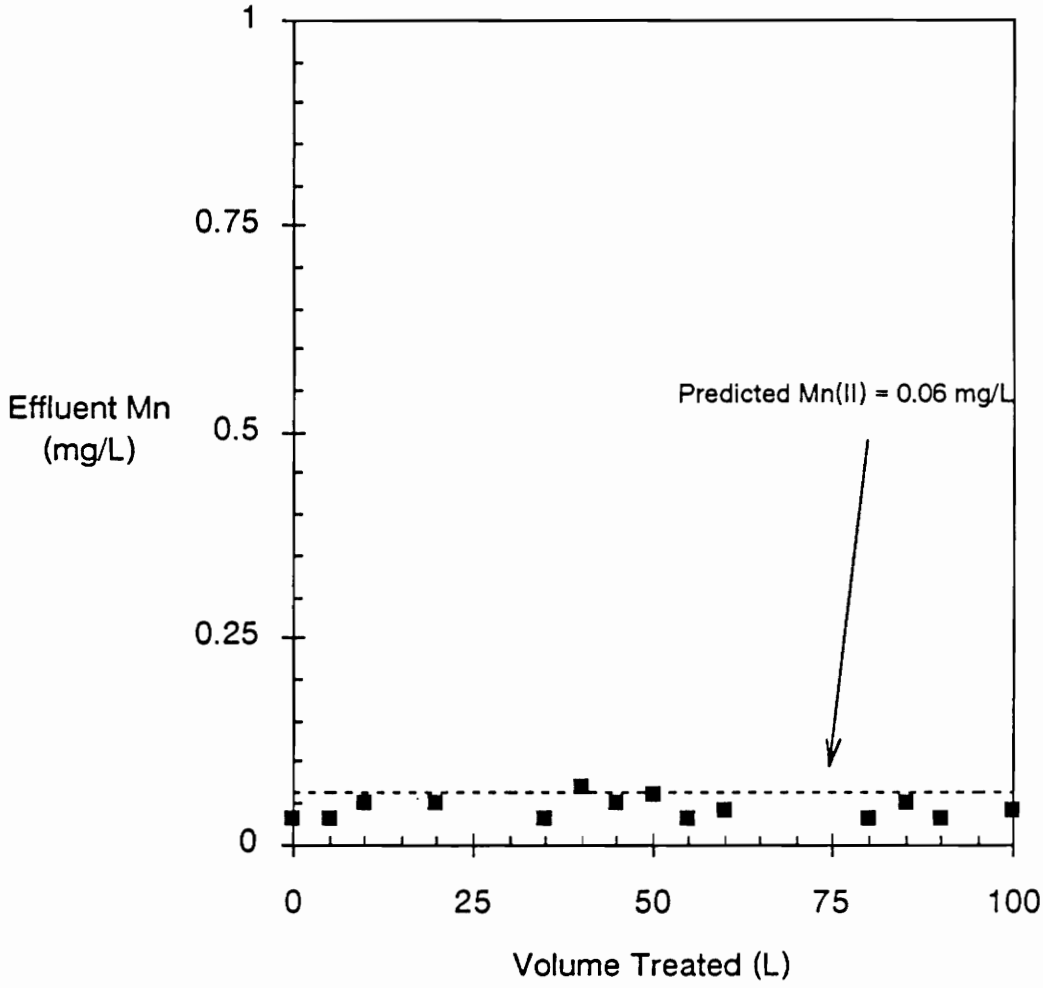

Figure 36. Predicted and Experimental Mn(II) Uptake at pH 8.8 (influent Mn(II) = 1.0 mg/L, HOCl = 2.0 mg/L, HLR = 2.5 gpm/ft^2, pH = 8.8, total adsorption capacity = 0.031 mol/L-bed, effluent depth = 6.5"; experimental data from Occiano (1988))

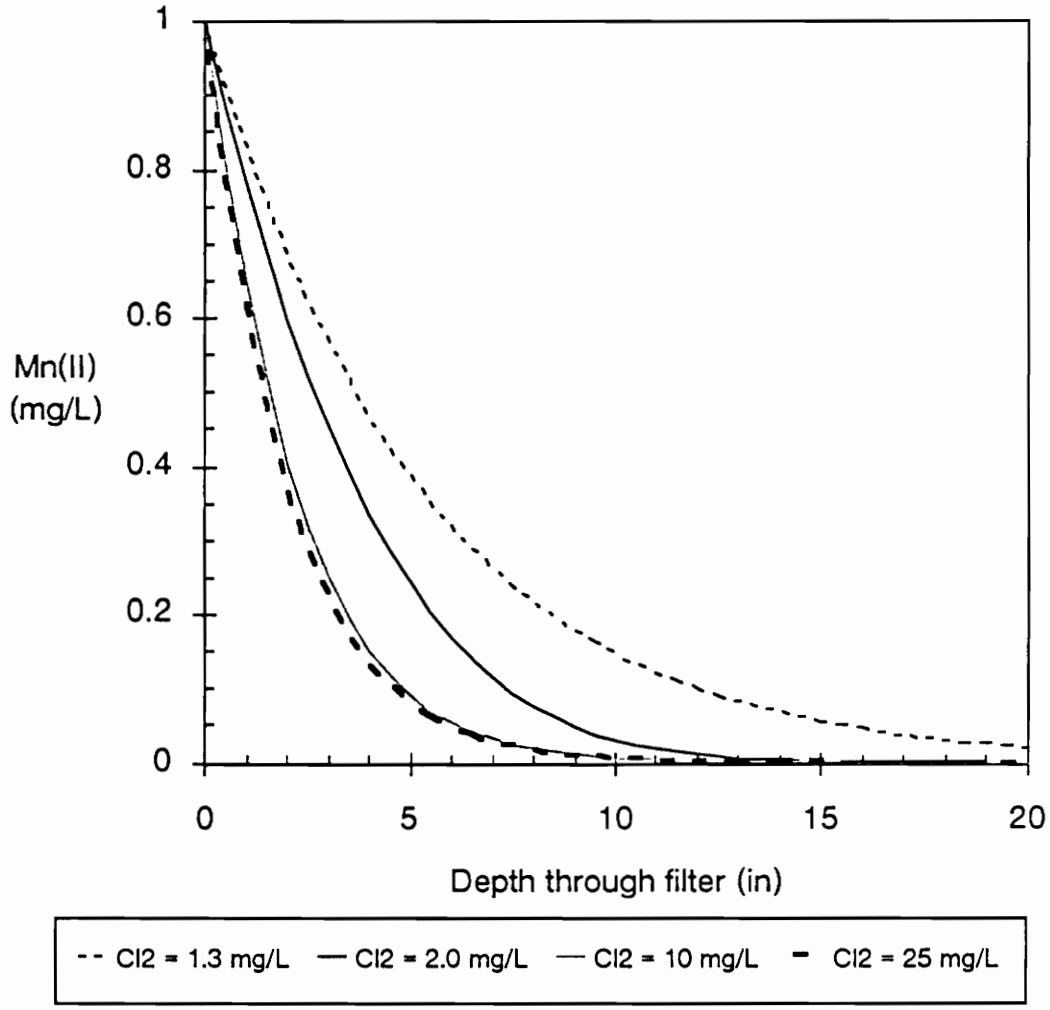

Figure 37. Effect of Influent Chlorine Concentration on Theoretical Removal Pattern (influent Mn(II) = 1.0 $^{mg}/_{L}$, HLR = 3.8 $^{gpm}/_{ft^2}$, total adsorption capacity = 0.09 $^{mol}/_{L}$-bed)

increases, fewer sites are available to be oxidized and the removal profile no longer changes significantly.

By using Eq. 15 (repeated below) standards for design and operation of a plant for continuous removal of Mn(II) can be obtained.

$$\frac{z\, s_o}{u} = \frac{1}{k_1} \ln \frac{[Mn^{2+}]_o}{[Mn^{2+}]} + \frac{1}{k_3} \ln \frac{[HOCl]_o}{[HOCl]_o - \{[Mn^{2+}]_o - [Mn^{2+}]\}}$$

$$+ \frac{k_2 [H^+]^2}{k_1 k_3 \{[HOCl]_o - [Mn^{2+}]_o\}} \left(\ln \frac{[Mn^{2+}]_o}{[Mn^{2+}]} - \ln \frac{[HOCl]_o}{[HOCl]_o - \{[Mn^{2+}]_o - [Mn^{2+}]\}} \right) \quad (15)$$

First, the Mn(II) concentration and pH of the raw water would be measured. Then the desired effluent Mn(II) concentration is specified. Subsequently, the amount of HOCl to be added to the unfiltered water is calculated as the summation of the HOCl requirement of the raw water (chlorine demand for oxidation of organics, iron, etc.), the amount for Mn(II) surface oxidation, and the desired residual HOCl concentration. When these values are substituted into the right hand side of Eq. 15, the left hand side (z^*s_o/u) is obtained. If the total capacity of manganese adsorption onto the media is measured separately, the relationship between the hydraulic loading rate and thickness of the media is obtained.

The continuous regeneration model, after the parameter estimation and verification, can be used to predict manganese removal through oxide coated media for varying treatment conditions. Figures 38 - 41 show four different treatment scenarios. The scenarios represent soluble manganese removal at two concentrations (0.5 and 0.2 mg Mn/L) and at two different chlorine dosages (1.0 and 3.0 mg HOCl/L). The two different chlorine dosages were included

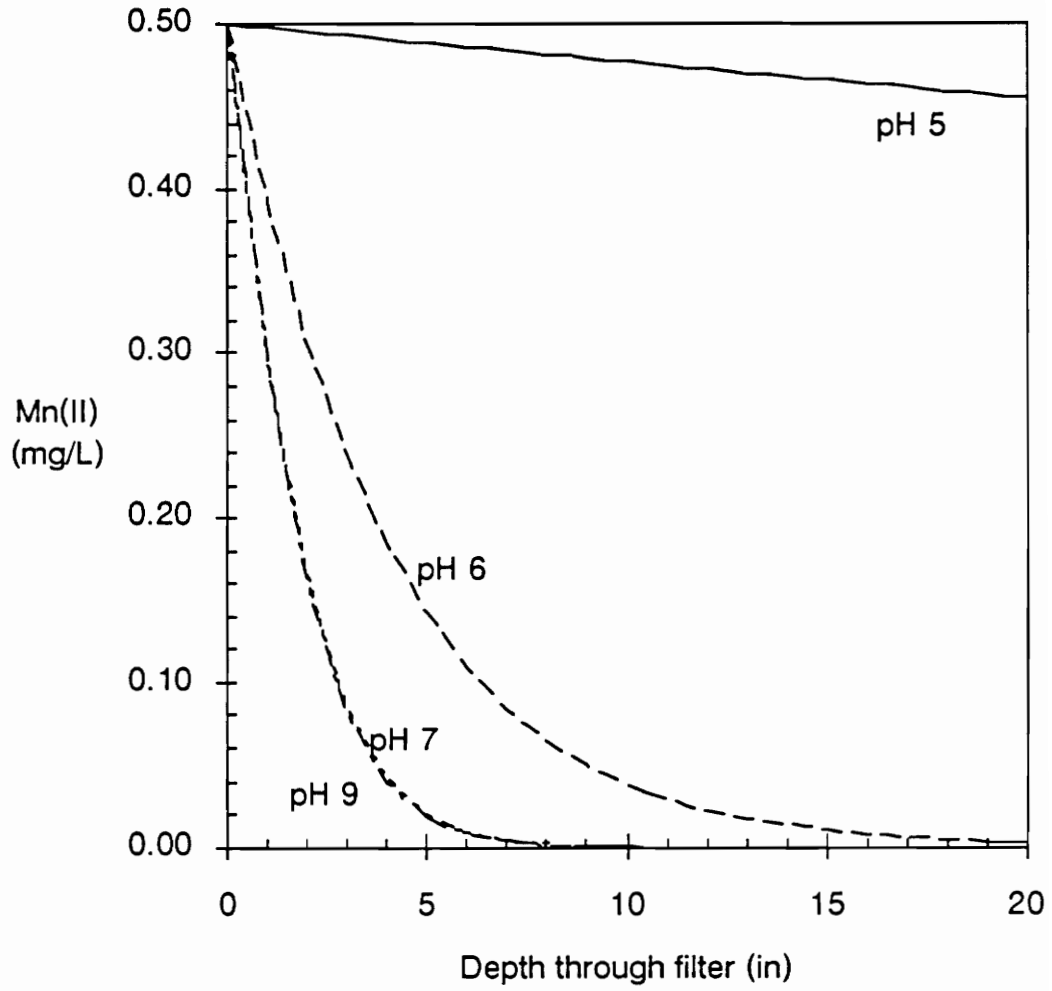

Figure 38. Predicted Manganese Removal for Low TOC Treatment Conditions (HOCl = 3.0 mg/L, HLR = 2.5 gpm/ft^2, surface oxide coating =4 mg Mn/g media, influent Mn(II)=0.5 mg/L)

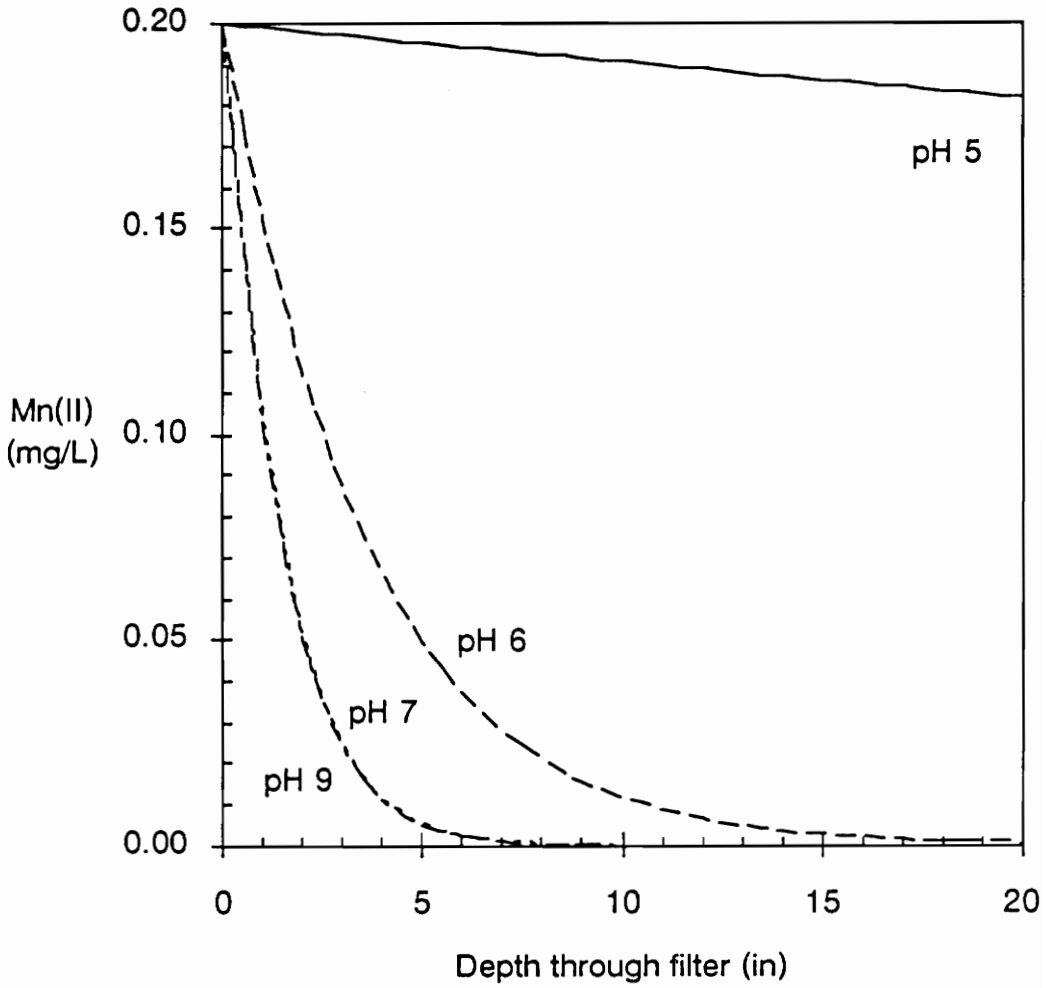

Figure 39. Predicted Manganese Removal for Low TOC Treatment Conditions (HOCl = 3.0 mg/L, HLR = 2.5 gpm/ft^2, surface oxide coating =4 mg Mn/g media, influent Mn(II)=0.2 mg/L)

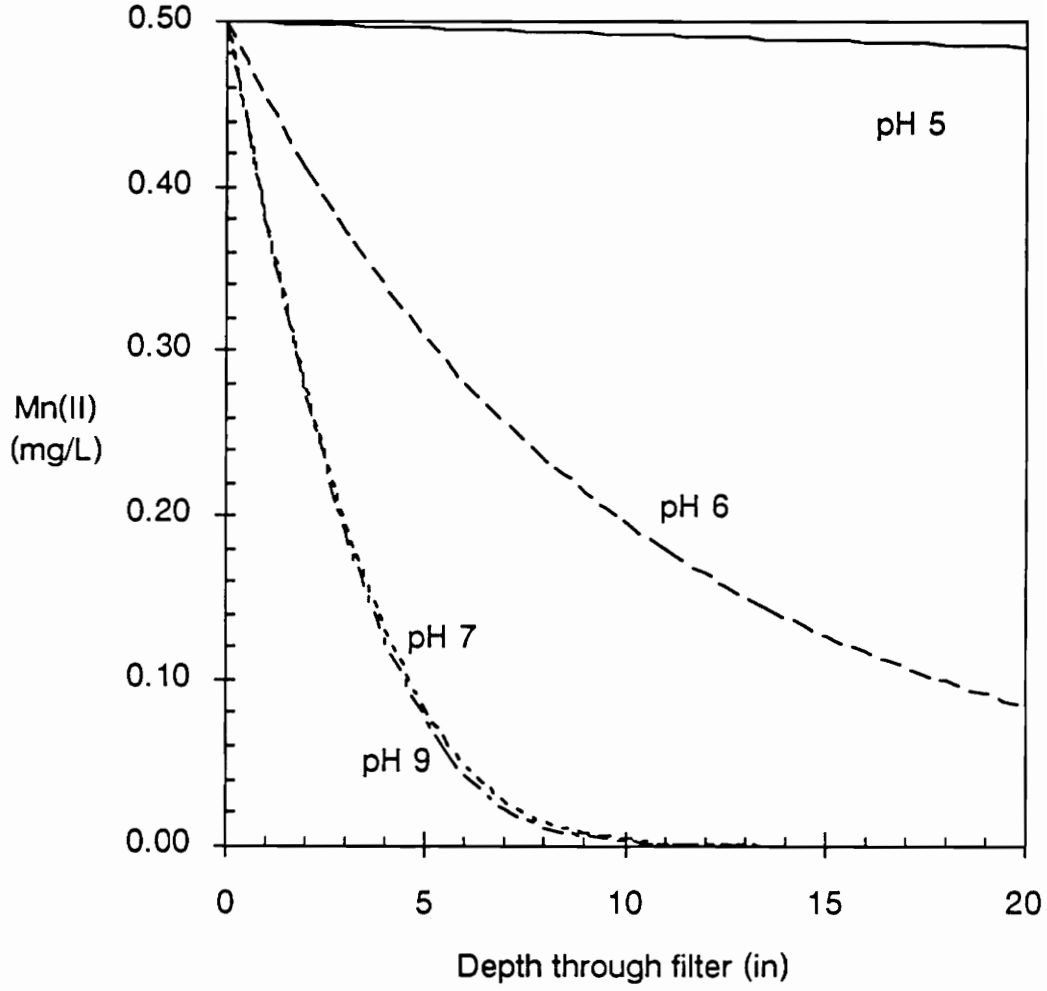

Figure 40. Predicted Manganese Removal for High TOC Treatment Conditions (HOCl = 1.0 mg/L, HLR = 2.5 gpm/ft^2, surface oxide coating =4 mg Mn/g media, influent Mn(II)=0.5 mg/L)

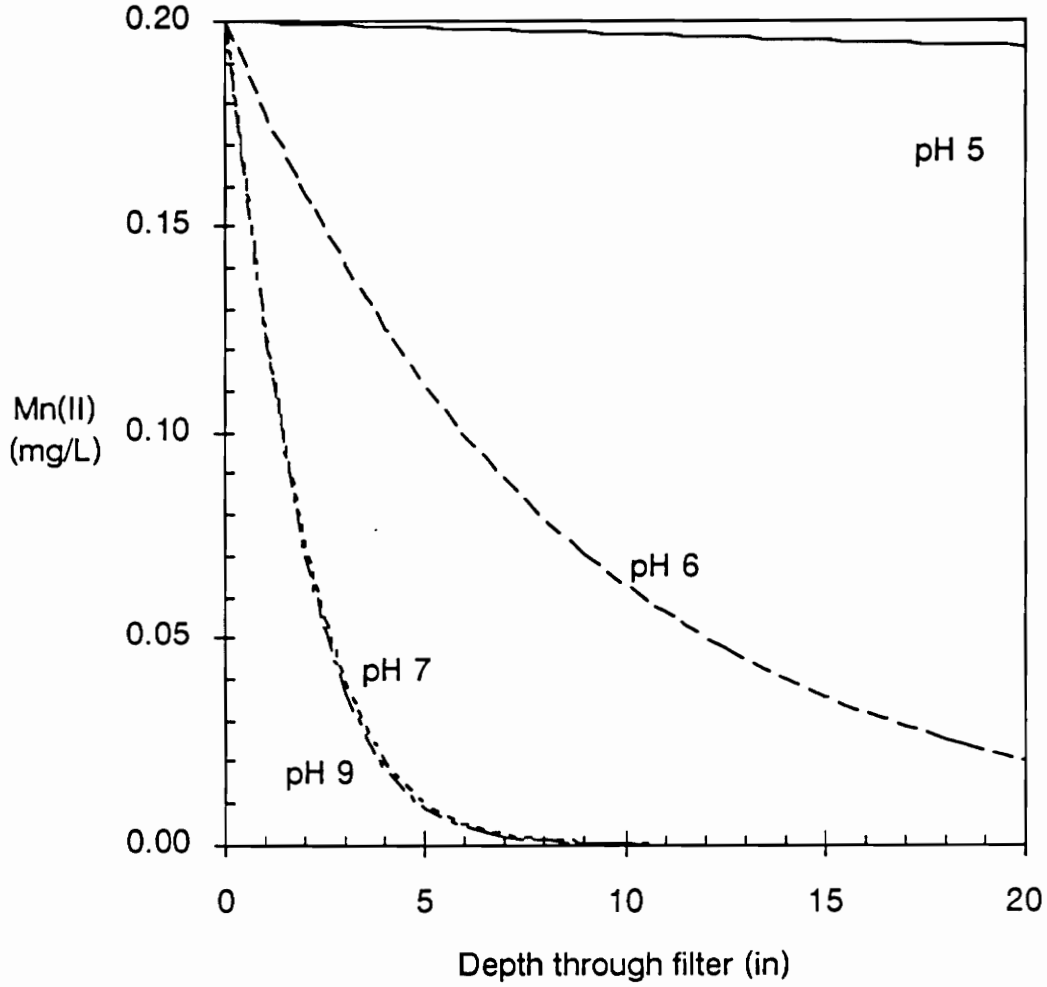

Figure 41. Predicted Manganese Removal for High TOC Treatment Conditions (HOCl = 1.0 mg/L, HLR = 2.5 gpm/ft^2, surface oxide coating =4 mg Mn/g media, influent Mn(II)=0.2 mg/L)

because many utilities must reduce the chlorine added to raw water to limit the formation of trihalomethanes (THMs).

Figures 38 and 39 show that the manganese was removed below the maximum contaminant level (0.05 mg Mn/L) within 10 inches if the pH was greater than 6.0 and the free chlorine concentration in the filter applied water was above 3.0 mg/L. However, below pH 6.0, the adsorption capacity of the oxide coated media was essentially eliminated. When chlorine addition to the filter applied water was limited (Figures 40 and 41), the Mn(II) removal through the oxide-coated media markedly decreased. These results show general treatment conditions under which continuous Mn(II) removal with free chlorine might be utilized. However, even if no chlorine can be added to the filter applied water, the intermittent regeneration treatment method can remove significant quantities of Mn(II), especially if the pH is greater than about 6.5.

Unfortunately, the continuous regeneration model contains certain limitations. First, at either very high or very low values of oxide coating on the media, the model does not accurately predict the removal profile. For example, Figures 16 - 18 show the manganese removal profile for three separate columns with media surface oxide coatings of 16, 0.071, and 0.064 $^{mg\ Mn}/_{g\ media}$. The three columns contain similar manganese removal patterns. However, the model would predict widely different removal patterns, especially with such light coatings.

A second limitation is inherent in the steady state assumptions required for a closed form solution of the equations presented in Chapter 3. For example, in Figure 37, the reducing the influent chlorine concentration only changes the manganese removal profile. At some point, steady state no longer

exists and a wavefront begins propagating through the column. The Nakanishi model cannot predict this changing wavefront. When chlorine addition to the filter applied water is limited, however, the intermittent regeneration model can predict the Mn(II) removal and the required media regeneration time.

Intermittent Regeneration Model

The intermittent regeneration model validation used two sources of data: (1) Mn(II) breakthrough data from Hungate (1988); and, (2) Mn(II) breakthrough data from Occiano (1988) at experimental conditions similar to Hungate.

The parameters for the intermittent regeneration model were estimated from the breakthrough profile of Hungate's first column in series. Therefore, the model predictions of the effluent from the next three columns in series provides a verification of the parameters and the model. Figure 42 shows the theoretical and experimental breakthrough profile at the effluent of each 5.75 inch depth column. Excellent agreement between the experimental results and theoretical predictions was obtained. In addition, Figure 43 shows the predicted and experimental wavefront propagation through the column, which is simply a different perspective on the same data. These comparisons show the linear adsorption isotherm used in the intermittent regeneration model provides a good characterization of the broadening Mn(II) mass transfer zone. These results indicate a bench scale experiment could be used to predict when the intermittent regeneration of a full-scale plant is needed.

A second verification of the model was desired to provide independent confirmation of the breakthrough profiles. However, the operating pH and amount of oxide coating must be similar to the experiments used in the

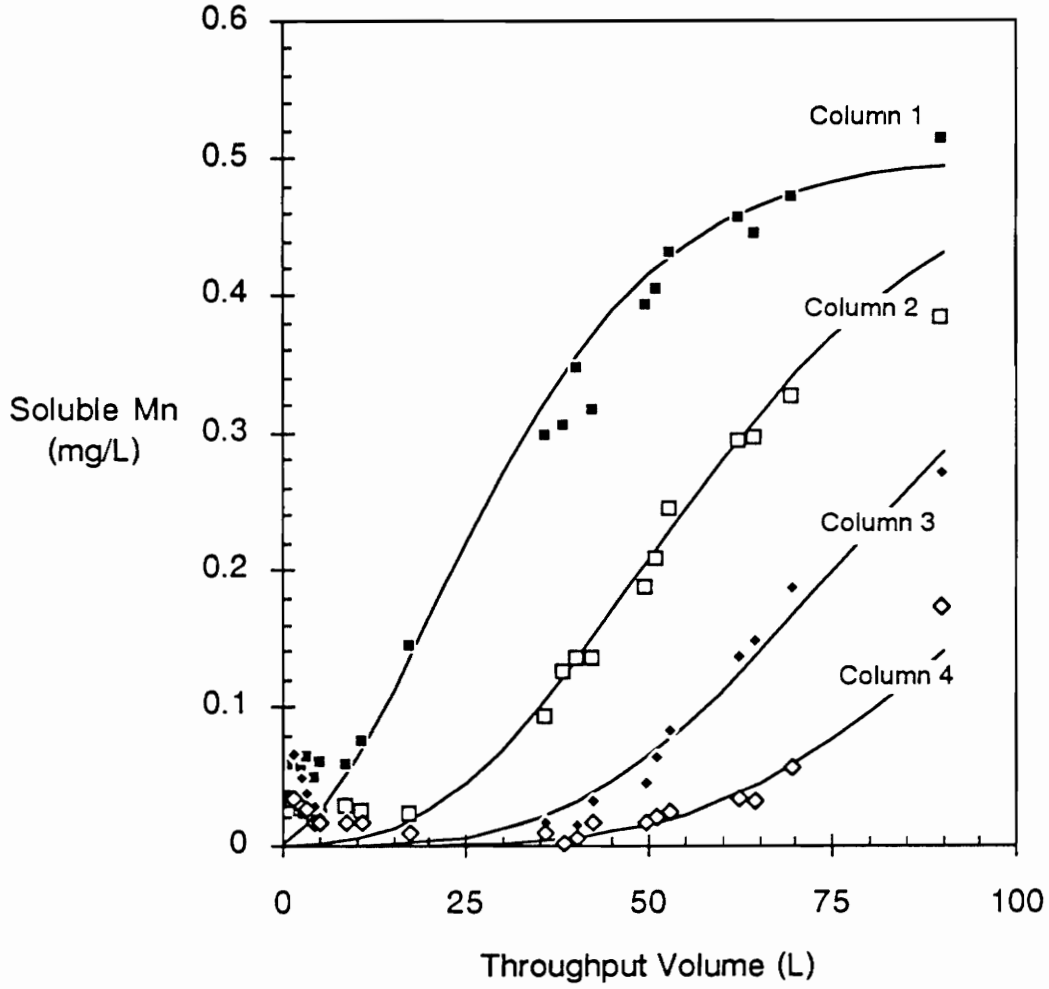

Figure 42. Comparison of Experimental and Predicted Mn(II) Breakthrough Patterns for Intermittent Regeneration Model (influent Mn(II) = 0.5 mg/L, HLR = 3.0 gpm/ft^2, depth of each column = 5.75", pH = 7.0; experimental results from Hungate (1988))

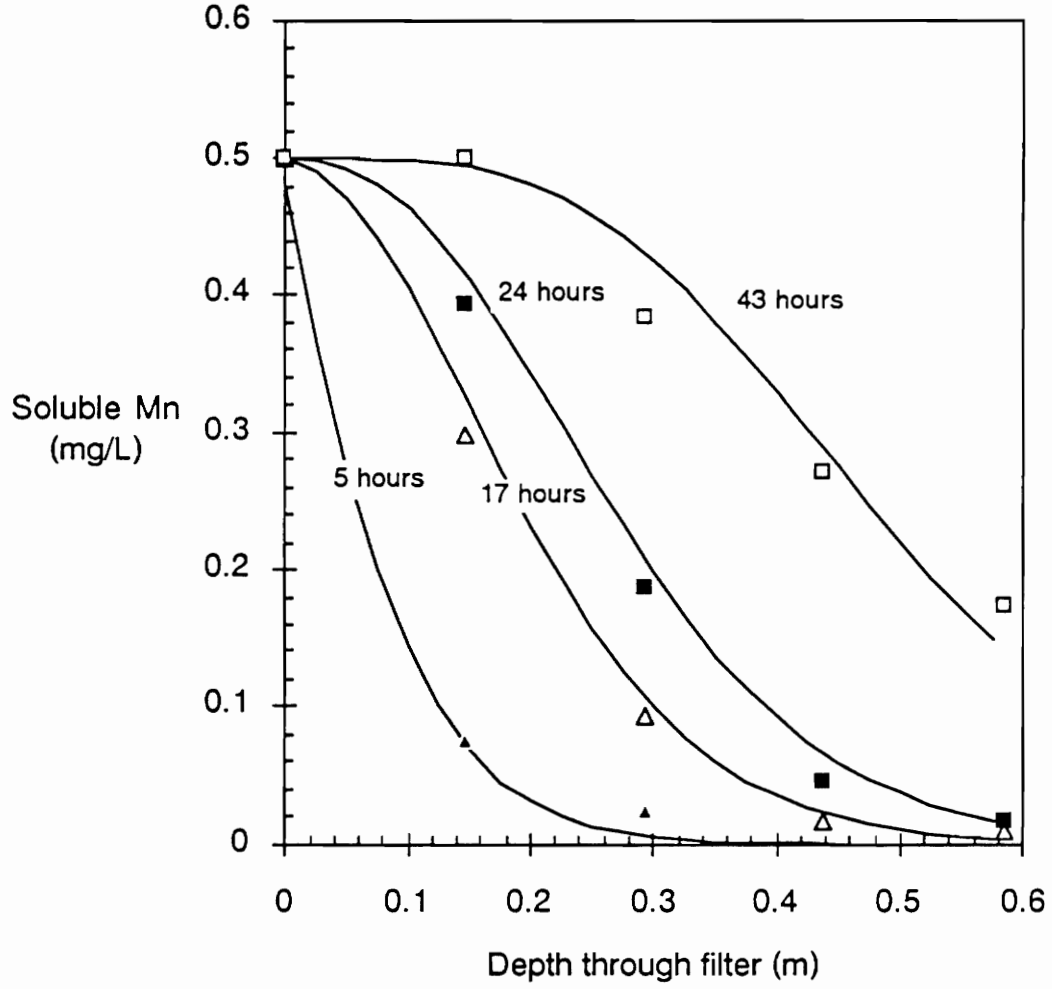

Figure 43. Comparison of Experimental and Predicted Mn(II) Wavefront Patterns for Intermittent Regeneration Model (influent Mn(II) = 0.5 mg/L, HLR = 3.0 gpm/ft^2, pH = 7.0, experimental results from Hungate (1988))

parameter estimation. Occiano performed experiments with a pH of 6.0-6.2, 7.8, and 8.8 for an anthracite media with a surface oxide coating of 4 $^{mg\ Mn}/_{g\ media}$. Therefore, the predicted breakthrough profile should occur between the breakthrough profiles at pH 6.2 and pH 7.8. Figure 44 shows the comparison of these results. The agreement obtained is reasonable. Note that Occiano's experiments used an influent soluble manganese concentration of 1.0 $^{mg}/_{L}$, whereas Hungate (1988) used a 0.5 $^{mg}/_{L}$ influent manganese concentration.

The intermittent regeneration model also can be used to predict the time until soluble manganese breakthrough for varying influent manganese concentrations. Figure 45 shows the breakthrough patterns for Hungate's operating conditions, but also shows predicted breakthrough patterns for lesser influent manganese loadings. Note that the time until breakthrough is a nonlinear function of the influent manganese concentration. For example, at an influent concentration of 0.5 $^{mg}/_{L}$, the effluent from the column reaches the secondary maximum contaminant level after approximately 30 hours of operation at 4 $^{gpm}/_{ft^2}$. If the influent concentration is lowered to 0.2 $^{mg}/_{L}$ the breakthrough time is 40 hours; if the concentration is lowered to 0.1 $^{mg}/_{L}$, the breakthrough time is about 50 hours. Without the intermittent regeneration model, the breakthrough time would be very difficult to predict. At an influent concentration of 0.5 $^{mg}/_{L}$, the total mass of manganese removed before breakthrough is 2 times greater than if the influent concentration were 0.2 $^{mg}/_{L}$ and almost four times greater than if the influent concentration was 0.1 $^{mg}/_{L}$.

Therefore, the intermittent regeneration model is well suited for the scale-up from bench scale Mn(II) adsorption experiments to full-scale treatment plants. This option of manganese removal would be useful at treatment plants

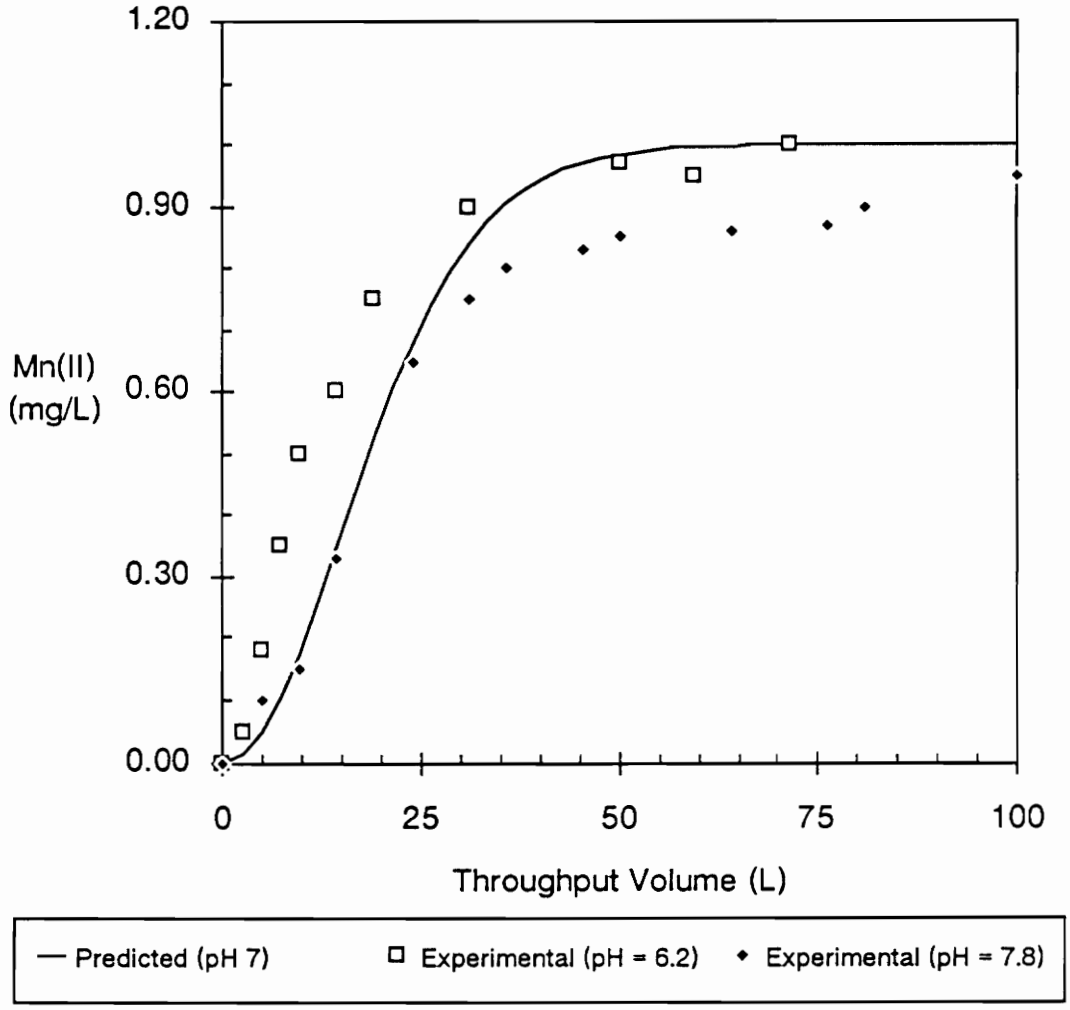

Figure 44. Comparison of Predicted and Experimental Breakthrough Under Different pH Conditions (HLR = 2.5 gpm/ft^2, influent Mn(II) = 1.0 mg/L, experimental results from Occiano (1988))

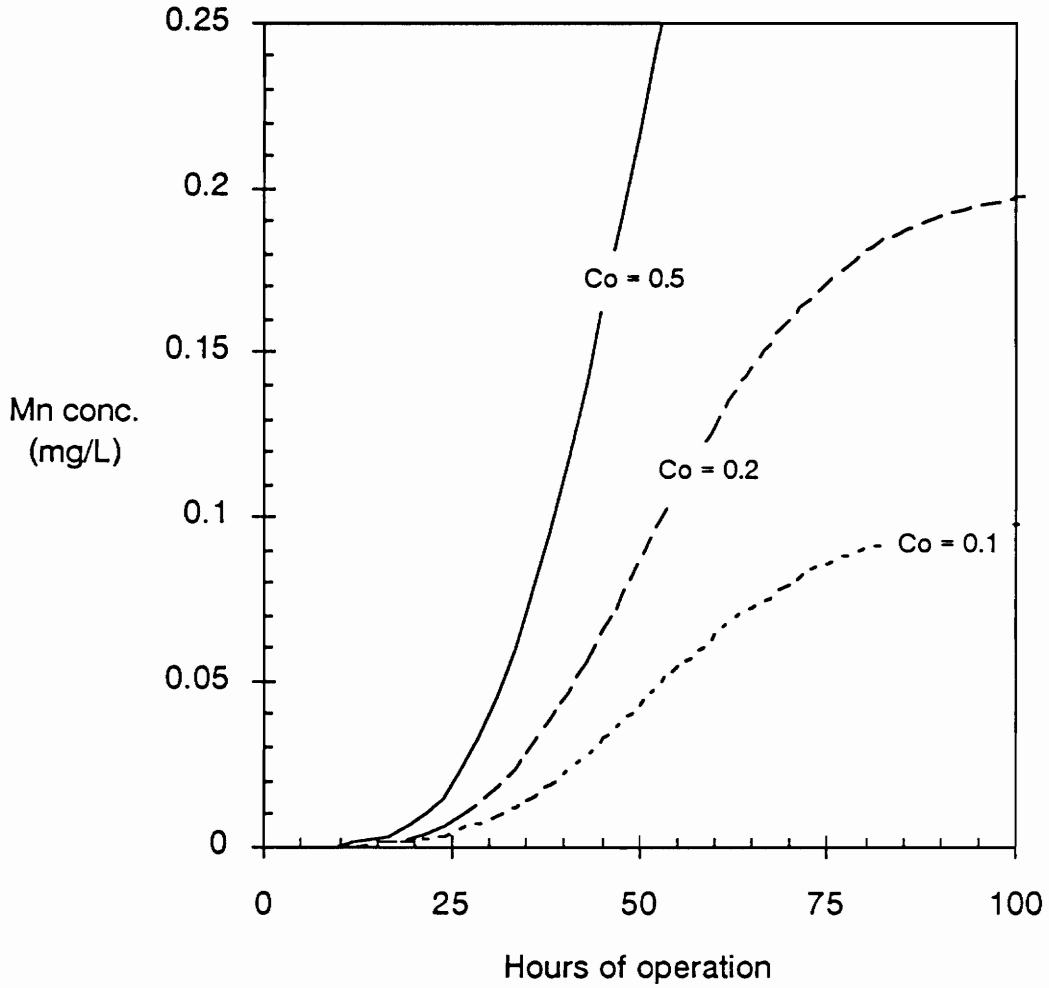

Figure 45. Manganese Breakthrough Patterns for Varying Influent Concentrations (effluent depth = 23", pH = 7.0, HLR = 3.0 gpm/ft^2)

where chlorine addition is not practical because of the formation of trihalomethanes (THMs), such as in the treatment of raw water from reservoirs with a high total organic carbon (TOC) concentration.

CHAPTER 7

CONCLUSIONS AND RECOMMENDATIONS

Based on the experimental and modeling results in this study, the following conclusions were formulated:

- When the filters were operated in a conventional oxidant addition mode (i.e., with the addition of HOCl and $KMnO_4$) the dual-media and tri-media configurations both provided efficient treatment because of the reduced rate of head loss buildup.
- Even though the anthracite-greensand filter treated a larger volume of water before breakthrough than the dual-media filter, the high head loss may limit the filter run time.
- Utilizing the natural oxide coatings on filter media can eliminate $KMnO_4$ addition and reduce head loss buildup within the filter.
- The removal of manganese by adsorption and oxidation on the surface of oxide-coated media is a viable, functional treatment mechanism.
- Pre-coated media did not offer soluble manganese removal advantages over the naturally oxide-coated media which rapidly developed during normal filter operation.
- The Nakanishi model can help predict the removal of soluble manganese by adsorption and oxidation on the surface of oxide-coated media and is useful in the design of filters for continuous Mn(II) removal.
- A linear adsorption isotherm effectively predicts the performance of filters operating in an intermittent regeneration mode and is useful for treatment plants which cannot apply chlorine continuously to their filter applied water.

Additional research should examine the linear isotherm behavior for Mn(II) removal using intermittent regeneration. By more closely investigating the adsorption process of Mn(II) onto the oxide-coating, a less empirical model might be utilized. Ideally, one unified mathematical model would predict Mn(II) removal both in a continuous regeneration mode with the addition of Cl_2 and also predict the breakthrough profile when an insufficient amount of chlorine (or none) was added to regenerate the adsorption sites. At this time, two separate models are necessary to satisfy these conditions. Through relaxing some of the steady state assumptions of Nakanishi's model, this unified model might be attained.

BIBLIOGRAPHY

Adams, R. B., "Manganese Removal by Oxidation with Potassium Permanganate," *Journal of the American Water Works Association*, *52* (2), 219-228 (1960).

Cleasby, J. L., "Iron and Manganese Removal - A Case Study," *Journal of the American Water Works Association*, *67* (3), 147-149 (1975).

Edwards, S. E., and McCall, G. B., "Manganese Removal by Break-Point Chlorination," *Water and Sewage Works*, *93* (8), 303-305 (1946).

Griffin, A. E., "Significance and Removal of Manganese in Water Supplies," *Journal of the American Water Works Association*, *52* (10), 1326-1334 (1960).

Hem, J. D., "Redox Coprecipitation Mechanisms of Manganese Oxides," in *Particulates in Water: Characterization, Fate, Effects, and Removal*, Edited by Kavanaugh and Leckie, American Chemical Society, 45-72 (1980).

Hungate, R. W., "Adsorption Kinetics for the Removal of Soluble Manganese by Oxide-Coated Filter Media," Masters Thesis, Virginia Polytechnic Institute and State University, Blacksburg, Virginia (1988).

Jobin, R., and Ghosh, M. M., "Effect of Buffer Intensity and Organic Matter on the Oxygenation of Ferrous Iron," *Journal of the American Water Works Association*, *64* (9), 590-595 (1972).

Kessick, J. A., and Morgan, J. J., "Mechanism of Autooxidation of Manganese in Aqueous Solution," *Environmental Science and Technology*, *9* (2), 157-159 (1975).

Knocke, W. R., Hoehn, R. C., and Sinsabaugh, R. L., "Using Alternative Oxidants to Remove Dissolved Manganese from Waters Laden with Organics," *Journal of the American Water Works Association*, *79* (3), 75-79 (1987).

Knocke, W. R., Hamon, J. R., and Thompson, C. P., "Soluble Manganese Removal on Oxide-Coated Filter Media," *Journal of the American Water Works Association*, *80* (12), 65-70 (1988).

Knocke, W. R., Van Benschoten, J. E., Kearney, M., Soborski, A., and Reckhow, D. A., "Alternative Oxidants for the Removal of Soluble Iron and Manganese," American Water Works Association Research Foundation Report, Denver, Colorado (March 1990).

Lloyd, A., Grzeskowiak, R., and Mendham, J., "The Removal of Manganese in Water Treatment Clarification Processes," *Water Research*, *17* (11), 1517-1523 (1983).

Montgomery, J. M., "Iron and Manganese Removal," in *Water Treatment Principles and Design*, John Wiley & Sons, Inc., New York, 339-342 (1985).

Morgan, J. J., "Chemistry of Aqueous Manganese II and IV," Doctoral Dissertation, Harvard University, Cambridge, Massachusetts (1964).

Morgan, J. J., "Chemical Equilibria and Kinetic Properties of Manganese in Natural Waters," in *Principles and Applications of Water Chemistry*, Edited by S. D. Faust and J. V. Hunter, John Wiley & Sons, Inc., New York, 561-624 (1967).

Morgan, J. J., and Stumm. W., "Colloid-Chemical Properties of Manganese Dioxide," *Journal of Colloid Science*, *19*, 347-359 (1964).

Nakanishi, H., "Kinetics of Continuous Removal of Manganese in a MnO_2-Coated Sand Bed," *Kogyo Kagaku Zasshi*, *70* (4), Translated by Toshi Umezawa, 407-410 (1967).

Nordell, E., *Water Treatment for Industrial and Other Uses*, 2nd ed., Reinhold Publishing Corporation, New York, 390-410 (1961).

O'Conner, J. T., "Iron and Manganese," in *Water Quality and Treatment*, 3rd ed., Edited by H. B. Crawford and D. N. Fischel, McGraw-Hill Book Company, New York, 380-396 (1971).

Occiano, S. C., "The Mechanisms for Free Chlorine Oxidation of Reduced Manganese in Mixed-Media Filters," Masters Thesis, Virginia Polytechnic Institute and State University, Blacksburg, Virginia (1988).

Pankow, J. F., and Morgan, J. J., "Kinetics for the Aquatic Environment," *Environmental Science & Technology*, *15* (11), 1306-1313 (1981).

Robinson, L. J., Jr., and Breland, E. D., "Removal of Iron and Manganese from Low Alkalinity Waters," *Public Works*, *99* (2), 72-76 (1968).

Ruthven, D. M., *Principles of Adsorption and Adsorption Processes*, John Wiley & Sons, Inc., New York (1984).

Sayell, K. M., and Davis, R. R., "Removal of Iron and Manganese from Raw Water Supplies Using Manganese Greensand Zeolite," *Industrial Water Engineering*, *12* (5), 20-23 (1975).

Standard Methods for the Examination of Water and Wastewater, 16th edition, APHA-AWWA-WPCF (1985).

Stiles, J. F., III, "Survey of the Iron and Manganese Problems in USA," *Proceedings of the American Water Works Association 1978 Annual Conference*, Denver, Colorado (1979).

Stone, A. T., and Morgan, J. J., "Reduction and Dissolution of Manganese (III) and Manganese (IV) Oxides by Organics. 1. Reaction with Hydroquinone," *Environmental Science & Technology*, *18* (6), 450-456 (1984).

Stumm, W., and Lee, G. F., "Oxygenation of Ferrous Iron," *Industrial and Engineering Chemistry*, *53* (2), 143-146 (1961).

Stumm, W., and Morgan, J. J., *Aquatic Chemistry*, 2nd ed., New York, John Wiley & Sons, Inc. (1981).

Theis, T. L., and Singer, P. C., "Complexation of Iron (II) by Organic Matter and Its Effect on Iron (II) Oxygenation," *Environmental Science & Technology*, *8* (6), 569-573 (1974).

Thomas, H. C., "Heterogeneous Ion Exchange in a Flowing System," *Journal of the American Chemical Society*, *66* (10), 1664-1666 (1944).

Trace Inorganic Substances Committee, "Committee Report: Research Needs for the Treatment of Iron and Manganese," *Journal of the American Water Works Association*, *79* (9), 119-122 (1987).

Waite, T. D., Wrigley, I. C., and Szymczak, R., "Photoassisted Dissolution of a Colloidal Manganese Oxide in the Presence of Fulvic Acid," *Environmental Science & Technology*, *22* (7), 778-785 (1988).

Weng, C., Hoven, D. L., and Schwartz, B. J., "Ozonation: An Economic Choice for Water Treatment," *Journal of the American Water Works Association*, *78* (11), 83-89 (1986).

Wilmarth, W. A., "Removal of Iron, Manganese, and Sulfides," *Water Wastes Engineering*, *5* (8), 52-54 (1968).

Wong, J. M., "Chlorination-Filtration for Iron and Manganese Removal," *Journal of the American Water Works Association*, *76* (1), 76-79 (1984).

VITA

Bradley Martin Coffey was born in Lima, Peru, on July 13, 1964. After living in Peru and several locations in California and Virginia, he graduated from Monacan High School in Richmond, Virginia, in the Spring of 1982.

In the fall of 1982, Brad entered Virginia Tech in the College of Arts and Sciences. Later, he transferred into the College of Engineering and obtained both Bachelor and Master of Science degrees in Mechanical Engineering in 1986 and 1988, respectively.

In the fall of 1988, Brad continued graduate studies at Virginia Tech, this time in the Civil Engineering department's environmental engineering program. As part of his thesis research, he spent three months operating a pilot-plant in Columbus, Indiana. Following this research project, he was employed as Laboratory Coordinator for the Virginia Student Environmental Health Project (STEHP) at Virginia Tech for one year. He completed the requirements for a Master of Science Degree in August of 1990.

In October of 1990, he begins work for the Metropolitan Water District of Southern California in Los Angeles as a process research engineer. Hopefully, he will endure a better fate than the Chief Engineer in the motion-picture *Chinatown*.